DISSERTATION

Engineered Nanoparticles in the Environment:

Sorption Behavior of Carbon Nanotubes in Aquatic Systems

Xiaoran Zhang, M.Sc.

angestrebter akademischer Grad

Doktor der Naturwissenschaften (Dr. rer. nat.)

Wien, September 2012

Studienkennzahl It. Studienblatt: A 091426
Dissertationsgebiet It. Studienblatt: Dr.-Studium der Naturwissenschaften Erdwissenschaften
Betreuer: Univ. Prof. Dr. Thilo Hofmann

A little body often harbors a great soul.

Mencius

Table of Contents

Acknowledgments

First and foremost I would like to express my sincerest gratitude to my supervisor, *Prof. Dr. Thilo Hofmann*, who has provided me with the opportunity to study my PhD in his excellent group. His guidance and encouragements always supported me and helped me maintain confidence and motivation throughout my PhD study. I particularly appreciated the many opportunities he offered to develop my network and establish collaborations with outstanding scientists.

I owe my deepest gratitude to *Dr. Mélanie Kah*, my co-supervisor, for her careful and patient guidance. She always imparted knowledge and explained in details. My presentation, writing and organization skills have greatly improved after three years of her guidance. She was always helpful and guided me to find solutions to the problems I faced. I particularly appreciated her careful and detailed revision on my manuscripts and thesis. Always available, she was very efficient and came back to me promptly, which greatly facilitated my work. Her dedication and hard working give me an excellent example in my future career.

I am thankful to *Dr. Michiel T. O. Jonker* (Utrecht University, the Netherland) for an enjoyable and fruitful collaboration. His splendid support at all times was much appreciated. He provided me with numerous valuable ideas and suggestions that put forward the progress of my papers and thesis.

I am grateful to *Mrs. Petra Körner* for her invaluable support in the laboratory. Her efficient guidance made my experimental work possible. She was always very nice to me and cared about my daily life. I am also thankful to *Dr. Vesna Micic* for her guidance in the laboratory when I start my PhD.

Thanks to *Dr. Frank von der Kammer* for answering my questions and provided me with creative ideas. Thanks to *Mr. Wolfgang Obermaier* for solving my computer problems. Thanks to our secretary *Miss. Sabine Kranzl* for the assistance in the daily administration issue.

Thanks to *Dr. Gerlinde Habler* and *Dr. Eugen Libowitzky* for their support on the electron microscopy imaging and Fourier transform infrared spectroscopy, respectively. Thanks to *Bayer* for supplying the carbon nanotubes.

I would like to thank all the members of the Environmental Geosciences Group. Thanks to *Dr. Stephan Wagner, Dr. Andreas Gondikas, Dr. Walter Schenkeveld, Dr. Wilfried Körner* and our former group members *Dr. Stephanie Ottofülling, Dr. Samuel Legros, Dr. Yi Yang* and *Dr.*

Xinyao Yang, you set good examples to me to be excellent researchers. *Elisabeth Neubauer*, *Susanne Laumann*, *Christian Müllegger*, *Boris Meisterjahn*, *Andrea Bichler*, *Cherdphong Seedao* and *Huichao Sun*, my PhD mates, thanks to all of you for giving a hand in the laboratory, discussing scientific problems as well as bringing me a lot of fun during my PhD study. I will cherish all the memories I have been working in this group.

I would like to express my deep gratitude to my parents for their support and wishing. I would like to express my special thanks to *Junfeng Liu*, not only my PhD mate but also my life partner. Thank you for your support and considerate care during these years.

I would like to thank all of my friends in Vienna. *Kongzhao Li, Hua Zhou, Boyu Zhang, Lina Liu, Pengfei Wang, Xiaoyan Meng, Zhiquan Li, Hui Xue* and *Minjian Zhou*, my Chinese friends studied in Vienna, you made my life and work more enjoyable.

Last but not least, I am grateful for the three years scholarship provided by *China Scholarship Council*.

Xiaoran Zhang

16. 08. 2012

List of Abbreviations

Abbreviation	Meaning
NPs	Nanoparticles
ENPs	Engineered nanoparticles
CNPs	Carbonaceous engineered nanoparticles
CNTs	Carbon nanotubes
SWCNTs	Singlewalled carbon nanotubes
MWCNTs	Multiwalled carbon nanotubes
NOM	Natural organic matter
HA	Humic acids
HOCs	Hydrophobic organic compounds
PAHs	Polycyclic aromatic hydrocarbons
POM-SPE	Polyoxymethylene-solid phase extraction
SPME	Solid phase microextraction
FTIR	Fourier transform infrared spectroscopy
XPS	X-ray photoelectron spectroscopy
EDX	Energy-dispersive X-ray spectroscopy
SEM	Scanning electron microscope
DLS	Dynamic light scattering
TOT	Time-of-transition, TOT is a laser-based analyser
CCC	Critical coagulation concentration
PZC	Point of zero charge
FM	Freundlich model
LM	Langmuir model
DLM	Dual Langmuir model
BETM	Brunauer-Emmett-Teller model
DMM	Dual-mode model
DAM	Dubinin–Ashtakhov model
TM	Toth model
AIC	Akaike's Information Criterion
MWSE	Mean weighted square errors
EDA	Electron donor-accepter interactions
K_{CNT}	CNT-water distribution coefficients
K_{HA}	Sorption coefficient of pyrene by HA
K_{OW}	Octanol-water partitioning coefficient
Si	Solubility of subcooled liquid
Bulk/CNTs	CNTs pretreated by hand shaking for 1 min
So/CNTs	CNTs pretreated by 2 h sonication
So-Sh/CNTs	CNTs pretreated by 2 h sonication followed by 6 d shaking

Abstract

With the fast development of nanotechnology, the production of engineered nanoparticles (ENPs) increases rapidly. ENPs will inevitably be released into the environment and may become important emerging pollutants. Interactions between organic contaminants and ENPs can alter the environmental fate of both materials (e.g., ENP-bound cotransport of contaminants). Carbon nanotubes (CNTs) are one type of widely produced ENPs. CNTs have a very strong affinity toward organic contaminants and have been proposed as superior sorbents for environmental remediation as well as for analytical applications. Understanding the interactions between organic contaminants and CNTs is therefore essential for evaluating the materials' potential environmental impact as well as the potential efficiency as superior sorbent.

The objective of this PhD thesis is to advance the understanding of interactions between CNTs and organic compounds, polycyclic aromatic hydrocarbons (PAHs) in particular. The sorption behavior of CNTs was investigated over a range of conditions that have never been investigated before, using a suitable alternative to the classical sorption experimental set up (i.e., passive sampling method). Sorption data were combined to extensive CNTs characterization and data analysis to better understand sorption behavior in the low concentration range, for very hydrophobic compounds and in conditions where CNTs are dispersed. The main findings can be summarized below:

- Conversely to previous studies carried out at unrealistic high concentration ranges, sorption isotherms in the low concentration range (pg–ng/L) indicate that sorption can be described using single sorption coefficients.
- Sorption coefficients for 13 PAHs (11 of which have never been reported before) showed that no competition occurred in the low concentration range and sorption affinity was directly related to the solubility of the subcooled liquid of the compounds.
- Conversely to previous observations restricted to large aggregates, our study highlights the importance of considering both the size and structure of sorbent aggregates.
- To date, limited published data generally suggested that the presence of functional groups on the CNTs decrease the sorption of nonpolar compounds. We here analyzed differences due to the nature of the functionalization and demonstrated that the impact on sorption behavior greatly depends on the CNT dispersion status. The suppression of sorption by natural dispersants greatly depends on the CNTs surface chemistry.

- Aggregation/dispersion significantly affects the sorption behavior of CNTs. Both the nature (e.g., sonication, presence of dispersants or functionalization) and the chronological sequence of the dispersion events are essential in determining the extent and irreversibility of the effects on sorption behavior of CNTs.

Our results show that a number of factors that were not thoroughly considered to date are essential when evaluating the interactions between organic contaminants and carbonaceous nano-sorbents. The sorption behavior of ENPs is a complex process, especially when accounting for colloidal behavior, and many research questions remain unanswered. The use of more suitable and robust methods, such as that develop in the present work, opens up a way to study sorption for a wider range of compounds and ENPs, and over a wide range of relevant conditions. The data generated will be vital for evaluating the materials' potential environmental impact as well as the potential future applications.

1. Introduction

Nanotechnology has become one of the most fantastic technologies in the recent years and has been applied in many areas, such as chemistry, physics, medicine, engineering, and environmental sciences.[1-4] Nanotechnology developed based on the unique properties of nanoparticles, often defined as material having one dimension smaller than 100 nm.[5] As particle size decreases, the reactivity of the surface atoms can increase dramatically. These unique properties make nano-sized particles valuable engineering materials due to their extraordinary strength, chemical reactivity, electrical conductivity, or other characteristics that the same materials do not possess at the micro or macro scales.[6]

With the fast development of nanotechnology, production of engineered nanoparticles (ENPs) increased rapidly during the last decade.[7] ENPs will inevitably enter the environment during their synthesis, purification, application, and disposal.[8] The possible toxicity of ENPs has been widely reported, bringing public concerns and making ENPs to become important potential emerging pollutants.[9, 10]

Sorption is an important process affecting the transport, fate, bioavailability and persistence of environmental contaminants. The fate of toxic compounds may be influenced by ENPs due to the very strong affinity of some ENPs towards organic and inorganic contaminants. For example, carbonaceous ENPs (e.g., carbon nanotubes and fullerenes) and metal based ENPs (e.g., Al_2O_3, ZnO, CuO, Fe_3O_4 and TiO_2) were reported to strongly sorb organic compounds and heavy metals.[11-16] Due to exceptional sorption potential sometimes observed, some researchers even proposed ENPs as superior sorbent to be applied in wastewater treatment[17] and trace analysis.[18] Therefore, understanding the interactions between toxic compounds and ENPs is not only essential to assess their behavior and potential risks in the environment, but also important to evaluate their potential efficiency for remediation applications.

Carbonaceous ENPs (CNPs) have attracted a particular attention for their sorption properties due to their unique structures and hydrophobic surfaces. Sorption potential is known to depend on the CNP properties, such as particle size, size distribution, structure, shape, surface chemistry and surface charge. These properties can control and/or be affected by the CNP colloidal behavior, namely aggregation and dispersion. CNPs tend to form large aggregates in water because of attractive interactions (mostly Van der Waals force) between particles in the nanoscale.[6] The CNP large aggregates may be partly/fully dispersed when they are transported in the environment due to the presence of natural dispersants (e.g., natural organic matter) or oxidants. CNP dispersions can also be intentionally produced in the industry

through mechanical treatment[19, 20] and chemical modification.[21-23]

Although a great deal of work on the interactions between compounds and CNPs has been published in the past years, most studies only refer to aggregated CNPs rather than partially/fully dispersed systems. CNPs have theoretical large surface area due to their very small size. However, the aggregation of CNPs in water may limit the availability of sorption sites for compounds. The lack of data on the possible interactions between compounds and dispersed CNPs is mainly due to the difficulties in phase separation. Generally-applied batch sorption set ups (e.g., centrifugation and filtration) may not allow full separation of the nano-scaled sorbent and aqueous phase. In addition, even though the separation can be fully achieved using advanced technique (e.g., ultra centrifugation), the high sorption capacity of CNPs results in extremely low concentrations of sorbates remaining in the aqueous phase and bring difficulties for analysis. This explains the lack of sorption data for compounds with very low solubility but high environmental risk.

The aim of this PhD is to advance the understanding of interactions between organic compounds and CNPs over a range of conditions that have never been investigated before by establishing an adequate sorption experimental set up, and combining to extensive CNPs characterization and data analysis. The main objectives of this work are:

i) to investigate sorption over a wide sorbate concentration range, representative of both environmental and waste water conditions
ii) to study the effect of CNP aggregation/dispersion status on their sorption behavior
iii) to evaluate the effects of changes in CNP surface chemistry on their sorption behavior.

Carbon nanotubes (CNTs) as one of the important types of CNPs have gained increasing attention due to their unique properties, such as electrical conductivity, optical activity, and mechanical strength.[24] CNTs exhibit very strong affinity towards organic contaminants, and they were proposed as superior sorbent in waste water treatment[25] and solid phase extraction cartridges.[26-28] The structures of CNTs are well defined and their surfaces are relatively uniform. CNTs can thus be considered as a good model sorbent to study adsorption mechanisms. A great deal of work on the CNT sorption behavior has been done in the past years.[29-33] However, there is a lack of knowledge regarding conditions expected to occur in the environment such as the coexistence of low concentration of contaminants or natural dispersants.

Polycyclic aromatic hydrocarbons (PAHs) are produced as byproducts of fuel burning and have been identified as carcinogenic, mutagenic, and teratogenic. PAHs consist of fused

aromatic rings and do not contain heteroatoms or carry substituents.[34] PAHs were selected as model sorbates not only because of their high environmental risks, but also due to their well distributed structure. Sorption of CNTs and PAHs is mainly driven by π–π interactions.[30] Therefore, the influence of CNT aggregation/dispersion status and surface chemistry on sorption can be clearly identified and distinguished. In addition, existing data only considered low molecular weight PAHs.[30] Information for more hydrophobic PAHs, which generally have higher toxicity, are needed.

The present thesis consists of six chapters including a short review of the state of knowledge (Chapter 2), three experimental studies prepared as stand-alone papers for submission to international peer-reviewed journal (Chapter 3–5) and overall conclusions and outlook (Chapter 6). Chapter 3[35] and 4[36] were published in the journal "Environmental Science & Technology". The submission of the results presented in Chapter 5 is planned is the near future.

Chapter 2 presents the state of knowledge on the sorption properties of CNTs as well as background information on passive sampling and characterization techniques used in this work.

Chapter 3 presents an alternative method to study sorption to CNTs (the method was also applied in the studies of Chapter 4 and 5). First, a passive sampling method was evaluated to tackle the issue of phase separation. Subsequently, sorption isotherms were measured for two PAHs in a wide concentration range. Sorption mechanisms were proposed, based on the selected isotherms, selected using statistical testing. Finally, the influence of PAHs properties was examined by measuring sorption coefficients for 13 PAHs in the low concentration range.

Chapter 4 shows the effects of CNT dispersion status on pyrene sorption. The influence of pre-treatments (i.e. shaking and sonication) and natural dispersants was examined by measuring single sorption coefficients as well as full isotherms. Sorption mechanisms were inferred based on a combination of sorption data and extensive characterization of the system.

Chapter 5 focuses on the effects of CNT surface chemistry on pyrene sorption. Gas-functionalized CNTs were selected as model sorbents. First, the influence of the nature of the CNT functionalization (i.e., OH, COOH and NH_2) on the CNT dispersion and sorption behavior is presented. The functionalization effect is then combined with that of pre-treatment (i.e. shaking and sonication) and natural dispersants, previously presented in Chapter 4. The results allow a discussion about the relative contribution of surface chemistry and dispersion effects on the overall sorption behavior.

Chapter 6 summarizes the main conclusions and assesses the importance of the results reported. Future work is addressed based on the past and present study.

Literature Cited

(1) Sanchez, F.; Sobolev, K. Nanotechnology in concrete - A review. *Constr Build Mater* **2010**, *24*, (11), 2060-2071.

(2) Guo, K. W. Green nanotechnology of trends in future energy: a review. *Int J Energ Res* **2012**, *36*, (1), 1-17.

(3) Baruah, S.; Dutta, J. Nanotechnology applications in pollution sensing and degradation in agriculture: a review. *Environ Chem Lett* **2009**, *7*, (3), 191-204.

(4) Karn, B.; Kuiken, T.; Otto, M. Nanotechnology and in Situ Remediation: A review of the benefits and potential risks. *Environ. Health Perspect.* **2009**, *117*, (12), 1823-1831.

(5) Lövestam, G.; Rauscher, H.; Roebben, G.; Klüttgen, B. S.; Gibson, N.; Putaud, J. P.; Stamm, H. Considerations on a definition of nanomaterial for regulatory purposes. *JRC Reference Reports* **2010**.

(6) Pan, B.; Xing, B. S. Chapter Three – Manufactured nanoparticles and their sorption of organic chemicals. *Advances in Agronomy* **2010**, *108*, 137-181.

(7) Ju-Nam, Y.; Lead, J. R. Manufactured nanoparticles: An overview of their chemistry, interactions and potential environmental implications. *Sci. Total Environ.* **2008**, *400*, (1-3), 396-414.

(8) Petersen, E. J.; Zhang, L. W.; Mattison, N. T.; O'Carroll, D. M.; Whelton, A. J.; Uddin, N.; Nguyen, T.; Huang, Q. G.; Henry, T. B.; Holbrook, R. D.; Chen, K. L. Potential Release Pathways, Environmental Fate, And Ecological Risks of Carbon Nanotubes. *Environ. Sci. Technol.* **2011**, *45*, (23), 9837-9856.

(9) Tiede, K.; Hassellov, M.; Breitbarth, E.; Chaudhry, Q.; Boxall, A. B. A. Considerations for environmental fate and ecotoxicity testing to support environmental risk assessments for engineered nanoparticles. *J. Chromatogr. A* **2009**, *1216*, (3), 503-509.

(10) Nowack, B.; Bucheli, T. D. Occurrence, behavior and effects of nanoparticles in the environment. *Environ. Pollut.* **2007**, *150*, (1), 5-22.

(11) Pyrzynska, K.; Bystrzejewski, M. Comparative study of heavy metal ions sorption onto activated carbon, carbon nanotubes, and carbon-encapsulated magnetic nanoparticles. *Colloids and Surfaces a-Physicochemical and Engineering Aspects* **2010**, *362*, (1-3), 102-109.

(12) Cho, H. H.; Wepasnick, K.; Smith, B. A.; Bangash, F. K.; Fairbrother, D. H.; Ball, W. P. Sorption of Aqueous Zn[II] and Cd[II] by Multiwall Carbon Nanotubes: The Relative Roles of Oxygen-Containing Functional Groups and Graphenic Carbon. *Langmuir* **2010**, *26*, (2), 967-981.

(13) Nassar, N. N. Rapid removal and recovery of Pb(II) from wastewater by magnetic nanoadsorbents. *J. Hazard. Mater.* **2010**, *184*, (1-3), 538-546.

(14) Shipley, H. J.; Engates, K. Heavy metal and arsenic sorption to nano-iron oxides. *Abstracts of Papers of the American Chemical Society* **2009**, *237*.

(15) Tan, Y. Q.; Chen, M.; Hao, Y. M. High efficient removal of Pb (II) by amino-functionalized Fe_3O_4 magnetic nano-particles. *Chem. Eng. J.* **2012**, *191*, 104-111.

(16) Ahmadi, S. J.; Sadjadi, S.; Hosseinpour, M. Adsorption behavior of toxic metal ions on nano-structured CuO granules. *Sep. Sci. Technol.* **2012**, *47*, (7), 1063-1069.

(17) Aditya, D.; Rohan, P.; Suresh, G. Nano-adsorbents for wastewater treatment: A Review. *Res J Chem Environ* **2011**, *15*, (2), 1033-1040.

(18) Pierce. D. T. , Zhao, X. J. Trace analysis with nanoparticles. *Wiley-VCH* **2011**.

(19) Huang, W. J.; Lin, Y.; Taylor, S.; Gaillard, J.; Rao, A. M.; Sun, Y. P. Sonication-assisted functionalization and solubilization of carbon nanotubes. *Nano Lett.* **2002**, *2*, (3), 231-234.

(20) Cheng, Q. H.; Debnath, S.; Gregan, E.; Byrne, H. J. Ultrasound-assisted SWNTs dispersion: effects of sonication parameters and solvent properties. *J. Phy. Chem. C* **2010**, *114*, (19), 8821-8827.

(21) Park, H. J.; Heo, H. Y.; Lee, S. C.; Park, M.; Lee, S. S.; Kim, J.; Chang, J. Y. Dispersion of single-walled carbon nanotubes in water with polyphosphazene polyelectrolyte. *Journal of Inorganic and Organometallic Polymers and Materials* **2006**, *16*, (4), 359-364.

(22) Potschke, P.; Bhattacharyya, A. R.; Janke, A.; Pegel, S.; Leonhardt, A.; Taschner, C.; Ritschel, M.; Roth, S.; Hornbostel, B.; Cech, J. Melt mixing as method to disperse carbon nanotubes into thermoplastic polymers. *Fuller Nanotub Car N* **2005**, *13*, 211-224.

(23) Wang, X.; Fan, H. Q.; Ren, P. R.; Yu, H. W.; Li, J. A simple route to disperse silver nanoparticles on the surfaces of silica nanofibers with excellent photocatalytic properties. *Mater. Res. Bull.* **2012**, *47*, (7), 1734-1739.

(24) Lan, Y. C.; Wang, Y.; Ren, Z. F. Physics and applications of aligned carbon nanotubes. *Adv Phys* **2011**, *60*, (4), 553-678.

(25) Mauter, M. S.; Elimelech, M. Environmental applications of carbon-based nanomaterials. *Environ Sci Technol* **2008**, *42*, (16), 5843-5859.

(26) Cai, Y. Q.; Jiang, G. B.; Liu, J. F.; Zhou, Q. X. Multi-walled carbon nanotubes packed cartridge for the solid-phase extraction of several phthalate esters from water samples and their determination by high performance liquid chromatography. *Anal. Chim. Acta* **2003**, *494*, (1-2), 149-156.

(27) Wu, H.; Wang, X. C.; Liu, B.; Lu, J.; Du, B. X.; Zhang, L. X.; Ji, J. J.; Yue, Q. Y.; Han, B. P. Flow injection solid-phase extraction using multi-walled carbon nanotubes packed micro-column for the determination of polycyclic aromatic hydrocarbons in water by gas chromatography-mass spectrometry. *Journal of Chromatography A* **2010**, *1217*, (17), 2911-2917.

(28) Ma, J. P.; Xiao, R. H.; Li, J. H.; Yu, J. B.; Zhang, Y. Q.; Chen, L. X. Determination of 16 polycyclic aromatic hydrocarbons in environmental water samples by solid-phase extraction using multi-walled carbon nanotubes as adsorbent coupled with gas chromatography-mass spectrometry. *Journal of Chromatography A* **2010**, *1217*, (34), 5462-5469.

(29) Zhang, S. J.; Shao, T.; Bekaroglu, S. S. K.; Karanfil, T. The impacts of aggregation and surface chemistry of carbon nanotubes on the adsorption of synthetic organic compounds. *Environ. Sci. Technol.* **2009**, *43*, (15), 5719-5725.

(30) Yang, K.; Zhu, L. Z.; Xing, B. S. Adsorption of polycyclic aromatic hydrocarbons by carbon nanomaterials. *Environ. Sci. Technol.* **2006**, *40*, (6), 1855-1861.

(31) Chen, J. Y.; Chen, W.; Zhu, D. Adsorption of nonionic aromatic compounds to single-walled carbon nanotubes: effects of aqueous solution chemistry. *Environ. Sci. Technol.* **2008**, *42*, (19), 7225-7230.

(32) Wang, L. L.; Zhu, D. Q.; Duan, L.; Chen, W. Adsorption of single-ringed N- and S-heterocyclic aromatics on carbon nanotubes. *Carbon* **2010**, *48*, (13), 3906-3915.

(33) Lin, D. H.; Xing, B. S. Adsorption of phenolic compounds by carbon nanotubes: Role of aromaticity and substitution of hydroxyl groups. *Environ. Sci. Technol.* **2008**, *42*, (19), 7254-7259.

(34) Fetzer, J. C. The chemistry and analysis of the large polycyclic aromatic hydrocarbons. *Polycyclic Aromat. Compd.* **2000**, *27*, (2), 143.

(35) Kah, M.; Zhang, X. R.; Jonker, M. T. O.; Hofmann, T. Measuring and modelling adsorption of PAHs to carbon nanotubes over a six order of magnitude wide concentration range. *Environ. Sci. Technol.* **2011**, *45*, (14), 6011-6017.

(36) Zhang, X. R.; Kah, M.; Jonker, M. T. O.; Hofmann, T. Dispersion state and humic acids concentration-dependent sorption of pyrene to carbon nanotubes. *Environ. Sci. Technol.* **2012**, *46*, (13), 7166–7173.

2. State of Knowledge

2.1 Introduction

The present chapter presents an overview of the state of knowledge and provides background information that is useful when studying the sorption of polycyclic aromatic hydrocarbons (PAHs) to carbon nanotubes (CNTs). Further information can be found in recently published literature reviews (ref 1-5).

The definition and classification of nanoparticles are first introduced. The main features of CNTs are then presented, with a special focus on colloidal behavior and available characterization methods. Sorption behavior of CNTs is then addressed, including sorption mechanisms, isotherms models, and experimental setups. In particular, the past studies on sorption of PAHs to CNTs are summarized. To conclude, the research gaps are identified.

2.2 Nanoparticles

2.2.1 Classification

Nanoparticles (NPs) are particles most often defined as having a size smaller than 100 nm in more than one dimension.[6] Relative to bulk particles, the atoms in NPs have two features: (1) lower coordination number and (2) more exposed reactive species in the environment.[7] According to their source, NPs can be divided into two categories: natural NPs and anthropogenic NPs. Figure 2.1 shows a classification of NPs. We focus on one category of anthropogenic NPs, as introduced in the below section.

Figure 2.1. *Classification of nanoparticles (NPs) as adapted from Pan and Xing.*[3]

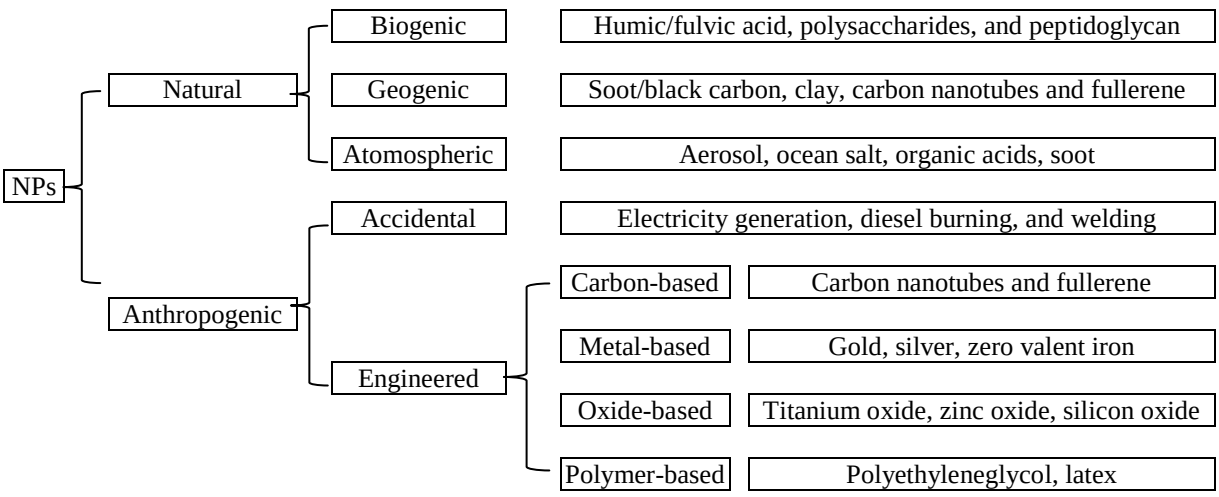

2.2.2 Engineered Nanoparticles

The synthesis of engineered nanoparticles (ENPs) was initiated in the 1970s[3] and now represents the major part of anthropogenic NPs. According to their matrix materials, ENPs can be divided into the following four categories: carbon-based, metal-based, oxide-based, and polymer-based NPs, as illustrated in Figure 2.1. ENPs have been applied in many areas including physics, chemistry, biology, medicine, material science, engineering, and environmental sciences. For example, CNTs reinforced polymers composites are promising new sensing materials for biosensors.[8] Silver NPs have antibacterial properties and can be applied in a range of consumer products such as cooking tools, cloth, personal care products and sports instruments.[3] TiO_2 NPs are used in paints, paper, plastics, sunscreens, and even food due to their inert properties.[9] Zero-valent iron NPs has been already used for ground water remediation.[10, 11]

During their production, ENPs may be accidentally released into the environment. The toxicity of ENPs has been widely reported.[12-17] The widely production and application of ENPs will bring public concern due to their environmental risks.[3] ENPs are reported to strongly interact with heavy metals[18-23] and organic contaminants.[24-28] Some ENPs such as CNTs and zero-valent iron NPs were proposed as materials for water remediation.[11, 29, 30] A great deal of work has therefore been performed to investigate interactions between toxic chemical and ENPs in order to gain a better understanding of their fate and potential applications.

2.3 CNTs and their Characterization

2.3.1 Introduction of CNTs

CNTs were first discovered by Iijima in 1991.[31] There are two types of CNTs: singlewalled CNTs (SWCNTs) and multiwalled CNTs (MWCNTs). SWCNTs consist of a single graphene layer rolled up into a seamless cylinder. MWCNTs consist of two or more graphene layers coaxially arranged around a central hollow core (Figure 2.2). SWCNTs have diameters in the order of a few nanometers, and MWCNTs contain between 2 and 30 graphene layers with outer diameters commonly between 10 and 50 nm. CNTs lengths vary substantially and often range from 100 nm to 10 or more mm.[5]

Both SWCNTs and MWCNTs have attracted considerable attention because of their unique properties including electrical conductivity, optical activity, and mechanical strength. Those

properties offer CNTs great potential for a wide range of applications in the fields of physics, biology, medicine, chemistry, material sciences and environmental sciences.[32-36] MWCNTs present several complementary attractive features with respect to SWCNTs, both for basic science and for applications.[37]

***Figure 2.2**. Singlewalled carbon nanotubes (SWCNTs) and multiwalled carbon nanotubes (MWCNTs)*

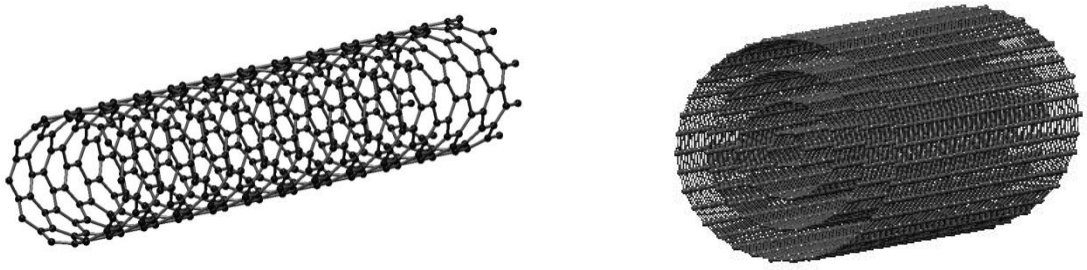

SWCNTs MWCNTs

The worldwide production of CNTs was about 500 tons in 2008.[38] Due to their wide production, CNTs will inevitability be released into the environment. Petersen et al.[39] reviewed the potential release pathways, environmental fate, and ecological risks of CNTs. CNTs can be released during the production of nanocomposite, combustion (incineration or accidental fires) and wastewater treatment plant.[39] Once CNTs are released into the environment, they may exert toxic effect to organisms[14, 40-42] and may have potential impacts to human beings.[43, 44]

2.3.2 Characterization Techniques

The properties of CNTs such as aspects, shape, size, structure, porosity and surface charge are essential to understand the colloidal and sorption behavior of CNTs. A great number of techniques have been applied to characterize CNTs. However, all techniques have limitations mainly due to the design of the devices and sample preparation. Detailed information on the principle, operation and limitations of each approaches are available in a number of recently published reviews.[45-48] The characterization techniques used in this thesis are presented in Table 2.1. Each technique having some limitations, the approach followed in this thesis was to combine a range of characterization techniques to complement one another.

***Table 2.1**. Characterization techniques used in this thesis and their main limitations.*

Techniques/devices	Information acquired	Limitations
UV-Vis spectroscopy	Concentrations in suspensions	Limited to simple matrix (e.g., water), potential interference from other components.
Fourier transform infrared spectroscopy (FTIR)	Functional groups	Not quantitative, some IR modes are too weak to be observed
Raman spectroscopy	Defects or damages can be reflected by I_D:I_G band ratio	Not quantitative, I_D:I_G band ratios can be misinterpreted
X-ray photoelectron spectroscopy (XPS)	Surface chemistry and elemental composition (1 to 10 nm)	Peaks are likely to be over interpreted
Energy-dispersive X-ray spectroscopy (EDX)	Surface elemental composition	Only a small fraction of sample can be measured
Elemental analyser	% of C, H, S, N and O	Only bulk composition is measured
Scanning electron microscope (SEM)	Image in nano-scale, diameter, length, and dispersion state can be evaluated	Sample preparation (e.g. drying) can lead to ambiguous analysis.
Dynamic latter scattering (DLS)	Size, size distribution and surface charge (3–1000 nm)	Large uncertainties for aggregates > 1 μm
Particle size analyser based on a laser time-of-transition principle	Size and size distribution (0.6 –150 μm)	Difficulty in maintaining large particles in suspension during measurement
Mastersizer	Size distribution 100 nm–1 mm	Requires high concentration (100 mg/L). CNTs attached to the plastic tubing, which may cause large uncertainties of the measurement
Surface area analyser	BET surface area, micropore and mesopore volume	Smallest pores cannot be assessed due to slow kinetic of diffusion (linked to the size of size of N_2 and low temperature)

2.4 Colloidal Behavior of CNTs

2.4.1 Influence of Ionic Strength and pH

Both ionic strength and solution pH impact colloids' stability and this applies to ENPs.

At low electrolyte concentrations, the diffusion layer of ENPs is extended and ENPs cannot come into contact. As electrolyte concentration increases, the electrical double layer of ENPs will be compressed and aggregation occurs. At an electrolyte concentration above a certain point, the double layer can be fully compressed, and aggregation goes into favourable condition. This concentration is called the critical coagulation concentration (CCC).[49] The CCC values for MWCNTs were estimated to be 25 mM for NaCl, 2.6 mM for $CaCl_2$, and 1.5 mM for $MgCl_2$.[50]

Adjusting solution pH is another way to influence the stability of ENPs in aqueous systems.

The point of zero charge (PZC) is the pH where the colloid surface exhibits zero net charge. At this pH, ENPs show minimum stability or maximum coagulation/aggregation rate. At pH values below the PZC, the substrate becomes protonated and exhibits a positive net charge. Conversely, the net surface charge turns negative at pH values above the PZC.[51]

For MWCNTs, an increase in solution pH from acidic (pH 3) to basic (pH 11) conditions resulted in a substantial (over 2 orders of magnitude) decrease in MWNT aggregation kinetics, suggesting the presence of ionizable functional groups on the MWCNT carbon scaffold.[50] PZC of MWCNTs treated using different functionalization method can be varied from 2.2–11.8.[52]

2.4.2 Influence of Mechanical Treatments

A large number of mechanical treatments can be applied in the presence of dispersants (e.g., polymer, surfactant) in order to produce stable CNT dispersions. In this section, the most commonly used mechanical methods are introduced and summarized in Table 2.2. Further information is available in the recent review by Ma et al.[5]

Sonication is the most frequently applied technique to disperse CNTs, either using a sonication bath or a horn.[53, 54] When ultrasound propagates via a series of compression, attenuated waves are induced in the molecules of the medium through which it passes. The production of these shock waves promotes the "peeling off" of individual nanoparticles located at the outer part of the nanoparticle bundles, or agglomerates, and thus results in the separation of individualized nanoparticles from the bundles.

A *calender* is a machine tool that employs the shear force created by rollers to mix, disperse or homogenize viscous materials. Using a calender to disperse CNTs in the presence dispersants is a promising approach to achieve a relatively good CNT dispersion.[55, 56] A high shear stress is required to disentangle CNT bundles and distribute the dispersed CNT into dispersant matrix, while a short residence time will likely limit the breakage of individual nanotubes.

Ball milling is a type of grinding method used to grind materials into extremely fine powder for use in paints, pyrotechnics and ceramics.[57, 58] During milling, a high pressure is generated locally due to the collision between the tiny, rigid balls in a concealed container. An internal cascading effect of balls reduces the material to fine powder.

Stir and extrusion is a common technique to disperse particles in liquid systems.[59, 60] Size and shape of the propeller and the mixing speed control the dispersion results.[5]

***Table 2.2**. Comparison of various mechanical pretreatment methods compiled from Ma et al.*[5]

Technique	Damage to CNTs	Governing factors	Availability
Sonication	Yes	Power, mode, time	Commonly used in laboratory, easy operation and cleaning after use
Calendaring	No	Rotation speed, distance between adjacent rolls	Operation training is necessary, hard to clean after use
Ball milling	Yes	Milling time, rotation speed, size of balls, balls/CNT ratio	Easy operation, need to clean after use
Shear mixing	No	Size and shape of the propeller, mixing speed and time	Commonly used in laboratory, easy operation and clean after use
Extrusion	No	Temperature, configuration and rotation speed of the screw	Large-scale production, operation training is necessary, hard to clean after use

2.4.3 Influence of Chemical Modification

2.4.3.1 Functionalization

Functionalization of CNTs changes the wettability of CNT surfaces, and consequently makes CNTs more hydrophilic. For example, highly oxidized CNT suspensions are more dispersed than CNTs without oxidation.[61] Wet chemical oxidation and plasma functionalization are two widely used methods. Wet chemical functionalization is a conventional approach and easily processed. [61, 62 53, 54] CNTs are exposed to oxidants such as H_2SO_4, HNO_3, $KMnO_4$ or their mixture to introduce oxidation groups on CNT surfaces.[53, 54] However, this method is not environmental friendly due to the large amount of chemicals used in the process. Plasma functionalization treatment is a dry chemistry approaches that is more environmental friendly. The CNTs are functionalized using gases such as O_2 and N_2 in the plasma reactor.[63, 64]

2.4.3.2 Natural dispersants

Natural organic matter (NOM) is ubiquitous in the environment and has been shown to disperse CNTs. It is believed that the adsorption of NOM molecules onto CNTs result in a decrease in zeta potential that increases the repulsion between CNTs. Therefore, CNT aggregates can be dispersed in the presence of NOM[65, 66] due to steric repulsion forces rising from the adsorption of NOM and the reduced surface hydrophobicity. Different properties of NOM determine the extent of CNT dispersion. NOM with higher content of surfactant-related component results in better dispersion.[67] The concentration of suspended CNTs can be increased by increasing the concentration of NOM.[65]

Even though the dispersion of CNTs by NOM has been widely reported, the sorption of NOM to CNTs was only rarely studied and existing data are restricted to the sorption to large CNTs

aggregates.[68, 69] This can probably be explained by the challenging phase separation when working with well dispersed systems.

2.4.3.3 Manufactured dispersants

When applied alone, mechanical treatments of CNTs often result in short-term dispersion only. CNTs tend to re-aggregate quickly after the energy input stops. Therefore, the stabilising effect of dispersants is generally combined with mechanical treatments to prepare stable CNT dispersions. Dispersants include various surfactants[51, 70, 71] and polymers.[72-75] Two main dispersion mechanisms were proposed to date. One group of researchers stated that CNTs could be solubilized inside columnar micelles in aqueous solution as a result of energetic sonication of the mixture.[76] Another group of researchers believe that CNTs cannot be dissolved in micelles, but that surfactant molecules adsorbed on the CNT surface form one layer coating that keeps CNTs apart.[51] The main evidence for this mechanism is that CNTs cannot be dispersed unless violent disturbance is involved (e.g., sonication).[51, 77, 78] The spaces between CNT aggregates can be enlarged by the violent disturbance force, while surfactant molecules adsorb and diffuse into internal spaces, overall maintaining CNT dispersed.[79]

2.5 Sorption Behavior of CNTs

CNT surfaces are hydrophobic and are thus expected to interact strongly with hydrophobic compounds. Some researchers suggested CNTs as superior sorbents for solid phase extraction and water treatment applications.[30, 80] The structures of CNTs are well defined and their surfaces are relatively uniform in contrast to activated carbon. CNTs are therefore considered to be a good model to study adsorption mechanisms.[1] Studying the interactions between organic compounds and CNTs is not only essential to assess their behavior and potential risks in the environment, but also important to evaluate their potential efficiency for remediation applications.

Research on the sorption properties of CNTs has been very intensive over the past decades and the state of knowledge was regularly analysed in a number of literature reviews. Pan and Xing[1] focused on sorption mechanisms whereas Yang and Xing[2] focused on the application of the Polanyi theory. The two above mentioned reviews concentrate on organic compounds whereas Ren et al. [4] covered both organic and inorganic pollutants from a water remediation point of view. CNTs have strong sorption potential to both organic and inorganic compounds such as heavy metals and radionuclides from nuclear waste. This section summarizes the

information based on two reviews (ref 1 and 2) and introduce two tools used to study sorption in the following chapters: model fitting and experimental set-ups.

2.5.1 Sorption Mechanisms

2.5.1.1 Influence of sorbate properties

Molecular size, structure, hydrophobicity, functional groups, and ionizability of the sorbates can all affect their sorption to CNTs. Larger molecules were found to have lower sorption capacity to CNT aggregates than smaller molecules.[81] This can be explained by a higher accessibility of pores between CNT aggregates to small molecules, relative to larger molecules (molecular sieving effect). The properties of sorbates will influence the type of possible interactions with CNTs that was further discussed in section 2.5.1.3.

2.5.1.2 Influence of CNTs properties

Sorption of organic compounds was shown to depend on the CNT types (i.e., single-walled or multi-walled), outer diameter and morphology. It was often reported that sorption is stronger for SWCNTs than MWCNTs, and sorption decreases with increasing CNT outer diameter (e.g., ref 24).

The adsorption spaces of CNTs are mainly composed of external surfaces, groove areas, and pores, both between CNT aggregates and between CNT layers (i.e., the space between each CNT layers).[2] The pores between CNT layers are not available for sorption of organic compounds due to the too narrow space.[82, 83] External surface and groove areas are believed to be always available for adsorption, but the pores between CNTs aggregates are not always available especially for large organic molecules.[84]

Thus, the availability of pores between CNT aggregates for organic compounds adsorption is highly dependent on CNT aggregation/dispersion status. The theoretically calculated surface area of CNTs is as high as 3000 m^2/g.[85] However, the measured surface area is much lower. The N_2 BET surface area of CNTs is hundreds of m^2/g.[86, 87] Therefore, the aggregation of CNTs can decrease their effective surface for sorption. Dispersion of large CNT aggregates to small aggregates or individual tubes is expected to enhance sorption of organic compounds. However, no direct experiments have been done due to the difficulties in separating solid and liquid phase when dealing with dispersed systems.

2.5.1.3 Sorption interactions

Five types of interactions are recognized to be responsible for the adsorption of organic chemicals on CNTs: hydrophobic effect, π–π bonds, hydrogen bonds, covalent and

electrostatic interactions. The CNT surface is hydrophobic and preferentially adsorb hydrocarbons relative to alcohols.[88] However, *hydrophobic interaction* alone is not enough to interpret the observed adsorption by CNTs. This is indicated by the failure in establishing a general relationship between the hydrophobic parameters of organic chemical and their adsorption affinity parameters on CNTs.[83, 89] Organic molecules that contain π electrons can interact with the π electrons of the benzene rings on CNT surface through the π–π electron coupling.[24] The *π–π bond* can be enhanced in the electron donor-acceptor (EDA) system if CNTs are functionalized, where the surface functional groups can act as electron acceptors while organic compounds can act as electron donors.[90, 91] Functional groups on the organic compounds or CNTs (e.g., COOH-, OH-, and NH_2-) can also act as hydrogen-bond donors and can form *hydrogen bond* between each other. However, functional groups of CNTs can also form hydrogen bonds with water molecules, which generally results in a competitive sorption between water and organic sorbates.[92, 93] *Covalent bonds* are much stronger than the three noncovalent bonding interactions mentioned above. Therefore, covalent modification of CNTs through functionalization has been widely utilized to form a variety of nanostructures with excellent physical and chemical properties.[94, 95] *Electrostatic attraction* will occur if CNTs and organic chemicals have opposite charges; otherwise, electrostatic repulsion will occur if both CNPs and organic chemicals have the same sign of charges.[96, 97]

It is generally difficult to distinguish one interaction from another because several interactions generally operate simultaneously. The relative contribution of a mechanism on adsorption of a given organic chemical is difficult to quantify. The strength of each type of interactions is challenging to estimate and depends on the ability of both organic chemicals and CNPs to form these interactions.

2.5.2 Sorption Models

Isotherm fitting with model equations is a key tool to explore sorption mechanisms. Several sorption models have been applied to fit sorption isotherms. Table 2.3 shows seven sorption models used to describe sorption of organic compounds to carbonaceous sorbents and that are used to fit sorption data in this thesis.

Yang and Xing[3] discussed the application of Polanyi theory-based models to describe the sorption of organic compounds to carbonaceous nanomaterial. Based on the data collected in the literature, the authors concluded that the sorption of organic compounds to CNTs (i) is neither monolayer formation on a homogeneous surface (i.e., Langmuir model) nor simple multilayer formation (i.e., BET model), (ii) is not a combination of partition and Langmuir-

type adsorption domains (i.e., partition-adsorption model), and (iii) cannot be limited by two types of adsorption sites (i.e., Dual-Langmuir model). Polanyi theory-based equations are not only applicable for pore filling but also applicable for flat surfaces.[2]

Table 2.3*. Sorption models used in this thesis to fit the sorption isotherms, along with accompanying equations and parameters.*

Model	**Equation and Parameters**	**Description**
Freundlich (FM)	$C_{CNT}=K_f C_W^n$ K_f [(μg/kg)/(μg/L)^n], Freundlich affinity coefficient; n, Freundlich exponential coefficient	Empirical model. Assumes an exponential site energy distribution
Langmuir (LM)	$C_{CNT}=Q^0 C_W/(K_d+C_W)$ K_d [μg/L], affinity coefficient	Formation of a sorbate monolayer on the sorbent until saturation. Considers a finite number of one type of sorption sites
dual Langmuir (DLM)	$C_{CNT}=Q^0_1 C_W/(K_{d1}+C_W)+Q^0_2 C_W/(K_{d2}+C_W)$ Q^0_1 [μg/kg] and Q^0_2 [μg/kg], sorbed capacity of site populations 1 and 2, respectively; K_{d1}[μg/L] and K_{d2} [μg/L], affinity coefficient of site populations 1 and 2, respectively	Formation of a sorbate monolayer on the sorbent until saturation. Considers two types of sorption sites (high and low-energy).
Brunauer-Emmett-Teller (BETM)	$C_{CNT}=(BQ^0 C_W)/[(C_S-C_W)[1+(B-1)(C_W/C_S)]]$ B, BET constant	Monolayer adsorption. Condensation of the sorbate, based on its solubility.
dual-mode (DMM)	$C_{CNT}=K_P C_W+Q^0 C_W/(K_d+C_W)$ K_P [L/kg], partition coefficient; K_d [μg/L] affinity coefficient	Combines linear partitioning and Langmuir modes of sorption.
Dubinin–Ashtakhov (DAM)	$\log C_{CNT} = \log Q^0 - (\varepsilon_{sw}/E)^b$ ε_{sw} [kJ/mol], $\varepsilon_{sw} = -RT\ln(C_w/C_s)$, effective adsoption potential, where R [8.314×10^{-3} kJ/(mol K)] and T [K], are universal gas constant and absolute temperature, respectively; E [kJ/mol], the 'correlating divisor'; b, fitting parameter	Based on Polanyi potential theory. Assumes the existence of an adsorption pace at the sorbent surface, where the adsorption potential depends on the distance of the sorbate to the surface.
Toth (TM)	$C_{CNT}=Q^0 C_W/(1/K_t+C_W{}^t)^{1/t}$ K_t [L/μg], Toth equilibrium constant; t, Toth exponent	Derived from the potential theory. An empirical equation developed to improve Langmuir isotherm fittings.

C_{CNT}: sorbed pyrene concentration on CNTs (μg/kg).
C_W: aqueous pyrene concentration at equilibrium (μg/L).
Q^0: maximum sorption capacity of pyrene (μg/kg).
C_S: pyrene solubility in water (μg/L).

Model selection is important to further investigate sorption mechanisms. The concentration range considered the number of fitting parameters and weighing method all impact model fit and may lead to the selection of different model. Further discussion on model selection is presented in Chapter 3.

2.5.3 Sorption Batch Setup

Suitable sorption setup is necessary to produce accurate and reliable sorption data. A number of methods have been used when performing sorption experiments. The pros and cons of each method as well as examples of their applications are listed in Table 2.4.

Table 2.4*. Techniques used to measure freely dissolved concentrations in sorption experiment.*

Methods	Advantages	Limitations	Applications
Centrifugation	No binding to apparatus	In complete phase separation for some NPs	Widely applied set-ups
Filtration	Simple, fast, inexpensive	NPs may pass through filter	Widely applied set-ups
Equilibrium dialysis	Temperature controlled	Time-consuming, ligand binding to apparatus, possible dilution solution components	HOCs to NOM
Fluorescence quenching	Simple	Only fluorescent compounds, poorly sensitive for low affinity	HOCs to NOM
nd-SPME	Easy analysis	Small volumes lead to detection problems	HOCs to NOM
POM-SPE	Compete phase separation, sensitive	Distribution coefficients of compounds to POM need to be determined separately. Long equilibrium time (about 1 month)	HOCs to Soot and charcoal

Centrifugation and filtration are two widely applied methods to separate solid and liquid phases when studying sorption and have therefore been often applied with CNTs. However, these methods may not be suitable for partially dispersed systems. The determination of distribution coefficients (K_d) is difficult using traditional methods as the nano-scaled CNTs may remain in suspension or pass filter membranes. This may result in an inaccurate phase separation and may lead to an underestimation of actual K_d values. In addition, the extremely high sorption capacity of CNTs for very hydrophobic compounds results in extremely low concentrations of sorbates remaining in the aqueous phase (pg–ng/L). To meet the analytical detection limit, one can increase the volume of solution in order to collect enough mass of sorbate, but this can become very laborious if not technically impossible.

Passive sampling is an alternative to the classical set ups, based on free flow (according to the Fick's first law of diffusion) of analyte molecules from the sampled medium to a collecting

medium. Diffusion driving forces and separation mechanisms depend on the different chemical potentials of trapped and nontrapped (remaining in the sample) analytes.[98] Passive sampling is widely used in monitoring studies in the environment. The method can be used to assess the quantity of organic contaminants in various environmental compartments including air and water. For example, solid phase microextraction (SPME) was applied to analyse free dissolved concentration in complex matrix such as soil and organisms.[99, 100] However, SPME method is not sufficiently sensitive to measure desorbed concentrations of very hydrophobic compounds in some cases, due to the limitation of the sampler weight. Jonker and Koelmans developed a passive sampling method based on polyoxymethylene solid phase extraction (POM-SPE), to determine soot-water partition coefficients.[101] One can increase the amount of POM applied to collect more analytes and match analytical capabilities. This POM-SPE method does not necessarily extract a negligible amount, but it determines the free concentration by application of a three-phase model. In addition to an increased sensitivity, the method provides sample clean-up. The necessary parameters to run the model need to be determined separately. POM-SPE technique was successfully applied to study sorption of hydrophobic organic compounds (HOCs) to soot and charcoal.[102, 103] This technique was also applied in the field to study environmental concentration of HOCs.[104, 105]

2.6 Sorption of PAHs to CNTs

2.6.1 PAHs

PAHs are produced as byproducts of fuel burning and have been identified as carcinogenic, mutagenic, and teratogenic. PAHs consist of fused aromatic rings and do not contain heteroatoms or carry substituents.[106] PAHs were selected as model sorbates in this thesis, not only because of their high environmental risks, but also because of their well distributed structure. The molecular structure and the property parameters of the 13 PAHs studied in this thesis are listed in Figure 2.3 and Table 2.5.

2.6.2 Sorption to CNTs

Sorption of PAHs to CNTs was first reported by Yang and Xing in 2006.[24] Sorption of three low molecular weight PAHs (i.e., naphthalene, phenanthrene and pyrene) was measured across three orders of magnitude aqueous concentration range. A Polanyi theory based model was selected to describe the sorption isotherms. Yang and Xing[24] proposed that the main interaction between PAHs and CNTs is π–π bonding. Since then, researchers further

examined the sorption of PAH to CNTs for a wider range of conditions. Strong competition between these three PAHs was reported at relative high concentrations (mg/L range).[107] Cho et al.[92] studied the influence of acid oxidation of CNT surface on naphthalene sorption, and found that acid oxidation can decrease CNTs sorption capacity but not affinity. Zhang et al.[108] observed a negligible influence of ionic strength and pH on phenanthrene sorption to CNTs. It was also reported that NOM can supress phenanthrene sorption to CNTs.[109] Wang et al. reported that both the NOM competition[110] and coating[111] can decrease naphthalene and phenanthrene sorption.

Figure 2.3. *Molecular structures of the 13 polycyclic aromatic hydrocarbons (PAHs) studied in this thesis*

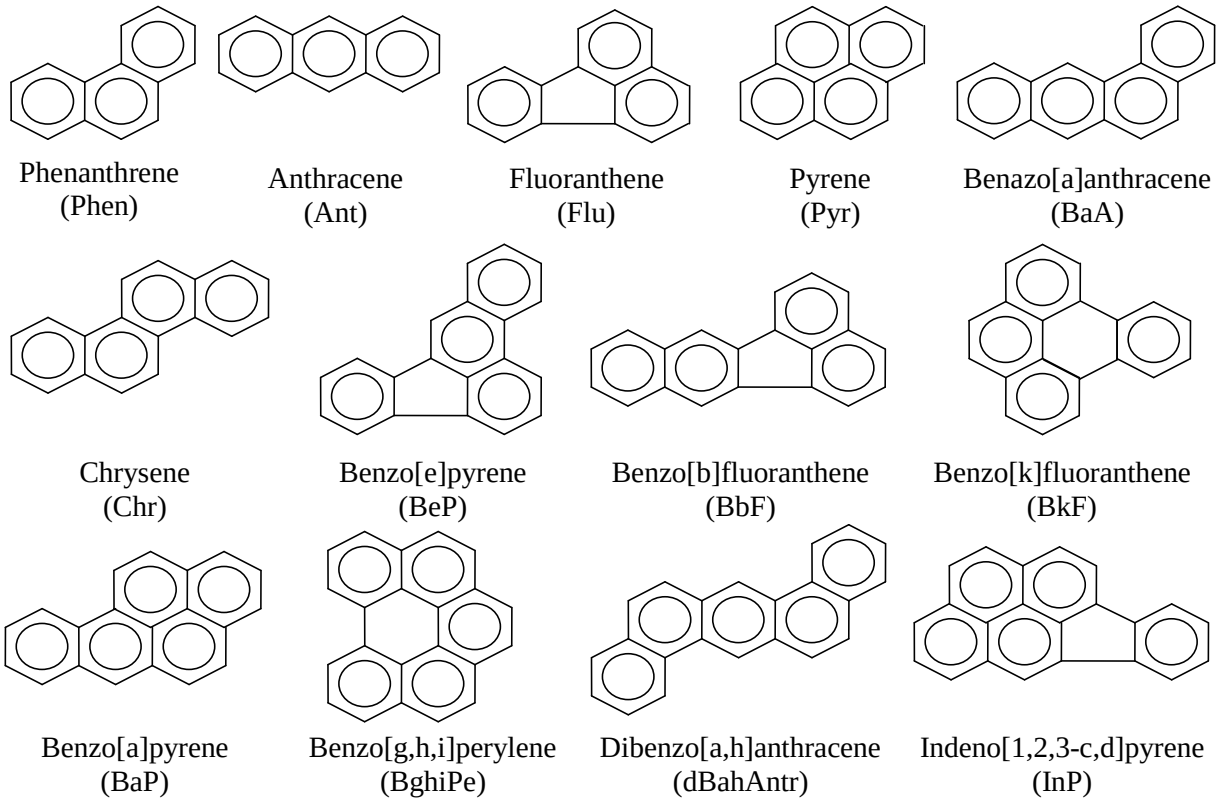

***Table 2.5**. Property parameters of the 13 polycyclic aromatic hydrocarbons (PAHs) studied in this thesis*

Note	Parameters	Phen	Ant	Flu	Pyr	BaA	Chr	BeP	BbF	BkF	BaP	BghiPe	dBahAntr	InP
(a)	MW	178.2	178.2	202.2	202.2	228.3	228.3	239.3	252.3	252.3	252.3	276.3	278.3	276.3
	Molecular V	199	197	217	214	248	251	263	268.9	268.9	263	277	300	200.4
	Total surface area	199.4	200.2	218.6	213.5	244.3	240.2	227.8	260.8	265	255.6	266.9	286.5	-
(b)	log *K*ow literature	4.57	4.68	5.16	5.22	5.91	5.81	6.44	6.20	6.20	6.20	6.90	7.00	7.00
(c)	Log*K*ow EPI	4.35	4.35	4.93	5.54	5.52	5.52	6.11	6.11	6.11	6.11	6.70	6.70	6.70
(d)	Log*K*ow SPARC	4.74	4.69	5.29	5.25	5.85	5.9	6.59	6.58	6.5	6.54	7.04	7.39	7.09
(e)	LogSi comp	-1.64	-1.67	-2.30	-2.35	-3.21	-3.39	-3.67	-4.13	-3.86	-4.21	-4.22	-3.70	-4.88
(f)	molar refraction	2.055	2.290	2.377	2.808	2.992	3.027	3.625	3.194	3.194	3.625	4.073	4.000	3.610
	molar volume	1.454	1.454	1.585	1.585	1.823	1.823	1.954	1.954	1.954	1.954	2.084	2.192	2.084
	edonnor	0.29	0.28	0.2	0.29	0.35	0.36	0.44	0.44	0.44	0.44	0.46	0.46	0.44
	Polarizability	1.29	1.34	1.55	1.71	1.70	1.73	1.99	1.82	1.91	1.98	1.90	2.04	1.90
(g)	Log P hexadecane/water	4.550	4.530	5.219	4.809	5.711	5.637	5.807	5.794	5.649	5.823	6.730	6.934	6.519
	Log P alkane/water	4.312	4.430	5.085	4.666	5.532	5.457	5.589	5.591	5.442	5.606	6.489	6.673	6.285
	Log P cyclohexane/water	4.904	5.058	5.766	5.400	6.379	6.306	6.560	6.503	6.347	6.578	7.588	7.787	7.308
(h)	Polarizability	2.46e-23	2.46e-23	2.87e-23	2.87e-23	3.16e-23	3.16e-23	3.58e-23	3.58e-23	3.58e-23	3.58e-23	4.00e-23	3.87e-23	4.00e-23
(i)	EHOMO	-0.211	-0.192	-0.212	-0.196	-0.196	-0.202	-	-0.210	-0.198	-0.187	-0.191	-0.197	-0.196
	ELUMO	-0.037	-0.060	-0.064	-0.054	-0.057	-0.047	-	-0.063	-0.063	-0.064	-0.061	-0.054	-0.074
	TE	-539.54	-539.53	-615.75	-615.77	-693.18	-693.18	-	-769.40	-769.40	-769.41	-845.65	-846.83	-845.63
	μ	0.042	0.000	0.329	0.000	0.066	0.000	-	0.383	0.285	0.045	0.067	0.000	0.608
	QH+	0.133	0.130	0.134	0.130	0.134	0.134	-	0.134	0.133	0.134	0.133	0.135	0.133
	QC-	-0.207	-0.298	-0.220	-0.226	-0.316	-0.206	-	-0.306	-0.286	-0.336	-0.229	-0.317	-0.314
	LCC	1.458	1.446	1.476	1.438	1.466	1.453	-	1.475	1.474	1.443	1.469	1.461	1.476
	Re	2623.74	2861.02	3194.23	2991.09	4932.22	4779.34	-	5423.88	5863.59	5260.46	5447.81	8010.23	6167.50

(a) Molecular weight (g/mol), volume (cm^3/mole) and surface area ($Å^2$) taken from Mackay[112]; (b) Log K_{OW} collected from the literature[113]; (c) Log K_{OW} derived by EPI Suite[114]; (d) Log K_{OW} derived by SPARC[115]; (e) Solubility of the subcooled liquid[116]; Value for InP was not available and was taken from Ma et al.[117]; (f) Linear free energy relationship parameters[118] (excess molar refraction, molar volume, electron donor capability, polarizability); (g) Hexadecane, alkane, and cyclohexane-water partitioning coefficients[119]; (h) Polarizability predicted by ACD Lab prediction software and available in the Chemspider database[120]; (i) Quantum chemical descriptors[121]: eigenvalues of the highest occupied and lowest unoccupied molecular orbital (EHOMO and ELUMO), molecular total energy (TE), dipole moment (μ), the most negative Mulliken atomic charges on a carbon atom (QC−), the most positive Mulliken atomic charges on a hydrogen atom (QH+), the largest bond length between two aromatic carbon atoms (LCC), and the electronic spatial extent (Re).

2.7 Conclusions

This chapter gave an overview of the CNTs characteristics likely to influence sorption behavior as well as the techniques available to study the subject. CNTs sorption behavior is complex as it can be influenced by many factors. When reviewing the work published in the past years, it appears that sorption data are still limited in terms of compounds, concentrations and conditions investigated, leading to the identification of the following knowledge gaps:

First, there is lack of studies on the very hydrophobic compounds (i.e., large PAHs). Experimental data for very hydrophobic compounds down to lower concentrations are essential to better understand the mechanisms of interaction likely to occur in the environment and how compound properties affect sorption affinity.

Second, sorption isotherms have been restricted to a relatively high concentration range.[24, 122] Isotherm shapes and strengths of sorption relevant to the lower concentration range remain mostly speculative. Isotherms fitting needs to be better examined and statistically tested in a wide concentration range considering both environmental and waste water conditions.

Third, existing studies only refer to large CNT aggregates[24, 122-125] and there is currently very limited data on the sorption potential of partially/fully dispersed CNT systems. On the one hand, dispersion of CNT aggregates can enlarge their effective surface sites for sorption of contaminants and may improve their efficiency on water treatment. On the other hand, depending on the production and release routes, CNTs may be discharged as large aggregates and/or in dispersed forms.[126] Understanding the influence of dispersion/aggregation phenomena on sorption is essential for evaluating the potential environmental impact of CNTs and their application as sorbent.

Fourth, the influence of functionalization of CNTs on sorption has not been systematically studied. Existing studies mainly focus on investigating the sorption of wet chemical oxidized CNTs.[92, 127] There are few studies on investigating the effect of gas functionalization (e.g., plasma treatment) which is widely applied in industry.[128, 129] There are no studies comparing different functional groups and aiming at weighing their contributions on sorption mechanisms. During CNTs production, functionalized CNTs may be directly released to the environment. Released CNTs can later be further oxidized in oxidative environment. Understanding the influence of CNT functionalization on sorption is thus important when evaluating the fate of CNTs.

Fifth, sorption measurements are generally not accompanied by adequate CNTs characterization that can help understanding sorption mechanisms. For example, aggregation and dispersion status can be reflected by the size distribution and zeta potential measured by dynamic light scattering device. The CNT surface heterogeneity can be reflected by the amounts of defects measured by Raman spectrometer. Even though there are a large number of available methods to characterize CNTs, characterization was often limited when performing sorption studies.

The research gaps listed above are addressed in the following three Chapters.

2.8 Literature Cited

(1) Pan, B.; Xing, B. S. Adsorption mechanisms of organic chemicals on carbon nanotubes. *Environ. Sci. Technol.* **2008**, *42*, (24), 9005-9013.

(2) Yang, K.; Xing, B. S. Adsorption of organic compounds by carbon nanomaterials in aqueous phase: Polanyi theory and its application. *Chem. Rev.* **2010**, *110*, (10), 5989-6008.

(3) Pan, B.; Xing, B. S. Chapter Three – Manufactured nanoparticles and their sorption of organic chemicals. *Advances in Agronomy* **2010**, *108*, 137-181.

(4) Ren, X. M.; Chen, C. L.; Nagatsu, M.; Wang, X. K. Carbon nanotubes as adsorbents in environmental pollution management: A review. *Chem. Eng. J.* **2011**, *170*, (2-3), 395-410.

(5) Ma, P. C.; Siddiqui, N. A.; Marom, G.; Kim, J. K. Dispersion and functionalization of carbon nanotubes for polymer-based nanocomposites: A review. *Compos Part a-Appl S* **2010**, *41*, (10), 1345-1367.

(6) Nowack, B.; Bucheli, T. D. Occurrence, behavior and effects of nanoparticles in the environment. *Environ. Pollut.* **2007**, *150*, (1), 5-22.

(7) Jones, C. F.; Grainger, D. W. In vitro assessments of nanomaterial toxicity. *Adv Drug Deliver Rev* **2009**, *61*, (6), 438-456.

(8) Yogeswaran, U.; Chen, S. M. Recent trends in the application of carbon nanotubes-polymer composite modified electrodes for biosensors: A review. *Anal. Lett.* **2008**, *41*, (2), 210-243.

(9) Nohynek, G. J.; Lademann, J.; Ribaud, C.; Roberts, M. S. Grey goo on the skin? Nanotechnology, cosmetic and sunscreen safety. *Crit. Rev. Toxicol.* **2007**, *37*, (3), 251-277.

(10) Calabro, P. S.; Moraci, N.; Suraci, P. Estimate of the optimum weight ratio in Zero-Valent Iron/Pumice granular mixtures used in permeable reactive barriers for the remediation of nickel contaminated groundwater. *J. Hazard. Mater.* **2012**, *207*, 111-116.

(11) Mueller, N. C.; Braun, J.; Bruns, J.; Cernik, M.; Rissing, P.; Rickerby, D.; Nowack, B. Application of nanoscale zero valent iron (NZVI) for groundwater remediation in Europe. *Environ Sci Pollut R* **2012**, *19*, (2), 550-558.

(12) Munoz, A.; Costa, M. Elucidating the mechanisms of nickel compound uptake: A review of particulate and nano-nickel endocytosis and toxicity. *Toxicol. Appl. Pharmacol.* **2012**, *260*, (1), 1-16.

(13) Canas, J. E.; Qi, B. B.; Li, S. B.; Maul, J. D.; Cox, S. B.; Das, S.; Green, M. J. Acute and reproductive toxicity of nano-sized metal oxides (ZnO and TiO2) to earthworms (Eisenia fetida). *J. Environ. Monit.* **2011**, *13*, (12), 3351-3357.

(14) Mwangi, J. N.; Wang, N.; Ingersoll, C. G.; Hardesty, D. K.; Brunson, E. L.; Li, H.; Deng, B. L. Toxicity of carbon nanotubes to freshwater aquatic invertebrates. *Environ. Toxicol. Chem.* **2012**, *31*, (8), 1823-1830.

(15) Song, M. Y.; Yuan, S. P.; Yin, J. F.; Wang, X. L.; Meng, Z. H.; Wang, H. L.; Jiang, G. B. Size-dependent toxicity of nano-C-60 aggregates: more sensitive indication by apoptosis-related bax translocation in cultured human cell. *Environ. Sci. Technol.* **2012**, *46*, (6), 3457-3464.

(16) Sergent, J. A.; Paget, V.; Chevillard, S. Toxicity and genotoxicity of nano-SiO_2 on human epithelial intestinal HT-29 cell line. *Ann Occup Hyg* **2012**, *56*, (5), 622-630.

(17) Smeraldi, J.; Rajagopalan, G.; Hosseini, T.; Khatib, L.; Olson, B. H.; Rosso, D. Evaluation of nano copper removal and toxicity in wastewaters. *Abstracts of Papers of the American Chemical Society* **2010**, *240*.

(18) Pyrzynska, K.; Bystrzejewski, M. Comparative study of heavy metal ions sorption onto activated carbon, carbon nanotubes, and carbon-encapsulated magnetic nanoparticles. *Colloids and Surfaces a-Physicochemical and Engineering Aspects* **2010**, *362*, (1-3), 102-109.

(19) Cho, H. H.; Wepasnick, K.; Smith, B. A.; Bangash, F. K.; Fairbrother, D. H.; Ball, W. P. Sorption of aqueous Zn[II] and Cd[II] by multiwall carbon nanotubes: The relative roles of oxygen-containing functional groups and graphenic carbon. *Langmuir* **2010**, *26*, (2), 967-981.

(20) Nassar, N. N. Rapid removal and recovery of Pb(II) from wastewater by magnetic nanoadsorbents. *J. Hazard. Mater.* **2010**, *184*, (1-3), 538-546.

(21) Shipley, H. J.; Engates, K. Heavy metal and arsenic sorption to nano-iron oxides. *Abstracts of Papers of the American Chemical Society* **2009**, *237*.

(22) Tan, Y. Q.; Chen, M.; Hao, Y. M. High efficient removal of Pb (II) by amino-functionalized Fe3O4 magnetic nano-particles. *Chem. Eng. J.* **2012**, *191*, 104-111.

(23) Ahmadi, S. J.; Sadjadi, S.; Hosseinpour, M. Adsorption behavior of toxic metal ions on nano-structured CuO granules. *Sep. Sci. Technol.* **2012**, *47*, (7), 1063-1069.

(24) Yang, K.; Zhu, L. Z.; Xing, B. S. Adsorption of polycyclic aromatic hydrocarbons by carbon nanomaterials. *Environ. Sci. Technol.* **2006**, *40*, (6), 1855-1861.

(25) Cheng, X. K.; Kan, A. T.; Tomson, M. B. Naphthalene adsorption and desorption from aqueous C60 fullerene. *J. Chem. Eng. Data* **2004**, *49*, (3), 675-683.

(26) Fang, J.; Shan, X. Q.; Wen, B.; Lin, J. M.; Lu, X. C.; Liu, X. D.; Owens, G. Sorption and desorption of phenanthrene onto iron, copper, and silicon dioxide nanoparticles. *Langmuir* **2008**, *24*, (19), 10929-10935.

(27) Yang, K.; Xing, B. S. Sorption of Phenanthrene by Humic Acid-Coated Nanosized TiO2 and ZnO. *Environ. Sci. Technol.* **2009**, *43*, (6), 1845-1851.

(28) Zhang, D.; Pan, B.; Zhang, H.; Ning, P.; Xing, B. S. Contribution of different sulfamethoxazole species to their overall adsorption on functionalized carbon nanotubes. *Environ. Sci. Technol.* **2010**, *44*, (10), 3806-3811.

(29) Cai, Y. Q.; Jiang, G. B.; Liu, J. F.; Zhou, Q. X. Multiwalled carbon nanotubes as a solid-phase extraction adsorbent for the determination of bisphenol a, 4-n-nonylphenol, and 4-tert-octylphenol. *Anal. Chem.* **2003**, *75*, (10), 2517-2521.

(30) Long, R. Q.; Yang, R. T. Carbon nanotubes as superior sorbent for dioxin removal. *J. Am. Chem. Soc.* **2001**, *123*, (9), 2058-2059.

(31) Iijima, S. Helical Microtubules of Graphitic Carbon. *Nature* **1991**, *354*, (6348), 56-58.

(32) Herrera-Herrera, A. V.; Gonzalez-Curbelo, M. A.; Hernandez-Borges, J.; Rodriguez-Delgado, M. A. Carbon nanotubes applications in separation science: A review. *Anal. Chim. Acta* **2012**, *734*, 1-30.

(33) Tan, A.; Yildirimer, L.; Rajadas, J.; De La Pena, H.; Pastorin, G.; Seifalian, A. Quantum dots and carbon nanotubes in oncology: a review on emerging theranostic applications in nanomedicine. *Nanomedicine-Uk* **2011**, *6*, (6), 1101-1114.

(34) Liang, F.; Chen, B. A review on biomedical applications of single-walled carbon nanotubes. *Curr Med Chem* **2010**, *17*, (1), 10-24.

(35) Vairavapandian, D.; Vichchulada, P.; Lay, M. D. Preparation and modification of carbon nanotubes: Review of recent advances and applications in catalysis and sensing. *Anal. Chim. Acta* **2008**, *626*, (2), 119-129.

(36) Gooding, J. J. Nanostructuring electrodes with carbon nanotubes: A review on electrochemistry and applications for sensing. *Electrochim. Acta* **2005**, *50*, (15), 3049-3060.

(37) Dresselhaus, M. S.; Dresselhaus, G.; Avouris, Ph. Carbon nanotubes synthesis, structure, properties, and applications. *Springer* **2001**.

(38) Mueller, N. C.; Nowack, B. Exposure modeling of engineered nanoparticles in the environment. *Environ. Sci. Technol.* **2008**, *42*, (12), 4447-4453.

(39) Petersen, E. J.; Zhang, L. W.; Mattison, N. T.; O'Carroll, D. M.; Whelton, A. J.; Uddin, N.; Nguyen, T.; Huang, Q. G.; Henry, T. B.; Holbrook, R. D.; Chen, K. L. Potential Release Pathways, Environmental Fate, And Ecological Risks of Carbon Nanotubes. *Environ. Sci. Technol.* **2011**, *45*, (23), 9837-9856.

(40) Reddy, A. R. N.; Reddy, Y. N.; Krishna, D. R.; Himabindu, V. Pulmonary toxicity assessment of multiwalled carbon nanotubes in rats following intratracheal instillation. *Environ Toxicol* **2012**, *27*, (4), 211-219.

(41) Zhao, X. C.; Liu, R. T. Recent progress and perspectives on the toxicity of carbon nanotubes at organism, organ, cell, and biomacromolecule levels. *Environ Int* **2012**, *40*, 244-255.

(42) Oleszczuk, P.; Josko, I.; Xing, B. S. The toxicity to plants of the sewage sludges containing multiwalled carbon nanotubes. *J. Hazard. Mater.* **2011**, *186*, (1), 436-442.

(43) Helland, A.; Wick, P.; Koehler, A.; Schmid, K.; Som, C. Reviewing the environmental and human health knowledge base of carbon nanotubes. *Environ. Health Perspect.* **2007**, *115*, (8), 1125-1131.

(44) Poland, C. A.; Duffin, R.; Kinloch, I.; Maynard, A.; Wallace, W. A. H.; Seaton, A.; Stone, V.; Brown, S.; MacNee, W.; Donaldson, K. Carbon nanotubes introduced into the abdominal cavity of mice show asbestos-like pathogenicity in a pilot study. *Nat Nanotechnol* **2008**, *3*, (7), 423-428.

(45) Belin, T.; Epron, F. Characterization methods of carbon nanotubes: a review. *Mat Sci Eng B-Solid* **2005**, *119*, (2), 105-118.

(46) Wepasnick, K. A.; Smith, B. A.; Bitter, J. L.; Fairbrother, D. H. Chemical and structural characterization of carbon nanotube surfaces. *Anal Bioanal Chem* **2010**, *396*, (3), 1003-1014.

(47) Lehman, J. H.; Terrones, M.; Mansfield, E.; Hurst, K. E.; Meunier, V. Evaluating the characteristics of multiwall carbon nanotubes. *Carbon* **2011**, *49*, (8), 2581-2602.

(48) Saito, R.; Hofmann, M.; Dresselhaus, G.; Jorio, A.; Dresselhaus, M. S. Raman spectroscopy of graphene and carbon nanotubes. *Adv Phys* **2011**, *60*, (3), 413-550.

(49) Petosa, A. R.; Jaisi, D. P.; Quevedo, I. R.; Elimelech, M.; Tufenkji, N. Aggregation and deposition of engineered nanomaterials in aquatic environments: role of physicochemical interactions. *Environ. Sci. Technol.* **2010**, *44*, (17), 6532-6549.

(50) Saleh, N. B.; Pfefferle, L. D.; Elimelech, M. Aggregation kinetics of multiwalled carbon nanotubes in aquatic systems: measurements and environmental implications. *Environ. Sci. Technol.* **2008**, *42*, (21), 7963-7969.

(51) Matarredona, O.; Rhoads, H.; Li, Z. R.; Harwell, J. H.; Balzano, L.; Resasco, D. E. Dispersion of single-walled carbon nanotubes in aqueous solutions of the anionic surfactant NaDDBS. *J. Phys. Chem. B* **2003**, *107*, (48), 13357-13367.

(52) Lee, S.; Zhang, Z. T.; Wang, X. M.; Pfefferle, L. D.; Haller, G. L. Characterization of multi-walled carbon nanotubes catalyst supports by point of zero charge. *Catal. Today* **2011**, *164*, (1), 68-73.

(53) Lal, M.; Verma, G.; Dharamvir, K. Better dispersability of un-functionalized multiwalled carbon nanotubes through sonication techniques. *Asian J. Chem.* **2012**, *24*, (8), 3537-3540.

(54) Chew, H. B.; Moon, M. W.; Lee, K. R.; Kim, K. S. Compressive dynamic scission of carbon nanotubes under sonication: fracture by atomic ejection. *P Roy Soc a-Math Phy* **2011**, *467*, (2129), 1270-1289.

(55) Dutta, A. K.; Penumadu, D.; Files, B. Nanoindentation testing for evaluating modulus and hardness of single-walled carbon nanotube-reinforced epoxy composites. *J. Mater. Res.* **2004**, *19*, (1), 158-164.

(56) Thostenson, E. T.; Chou, T. W. Processing-structure-multi-functional property relationship in carbon nanotube/epoxy composites. *Carbon* **2006**, *44*, (14), 3022-3029.

(57) Jhan, Y. R.; Duh, J. G. Synthesis of entanglement structure in nanosized $Li_4Ti_5O_{12}$/multi-walled carbon nanotubes composite anode material for Li-ion batteries by ball-milling-assisted solid-state reaction. *J. Power Sources* **2012**, *198*, 294-297.

(58) Huh, S.; Batmunkh, M.; Kim, Y.; Chung, H.; Jeong, H.; Choi, H. The ball milling with various rotation speeds assisted to dispersion of the multi-walled carbon nanotubes. *Nanosci Nanotech Let* **2012**, *4*, (1), 20-29.

(59) Wang, Z. C.; Fan, X.; Wang, K.; Deng, H.; Chen, F.; Fu, Q. Fabrication of polypropylene/carbon nanotubes composites via a sequential process of (rotating solid-state mixing)-plus-(melt extrusion). *Compos. Sci. Technol.* **2011**, *71*, (11), 1397-1403.

(60) Sulong, A.; Park, J. Alignment of multi-walled carbon nanotubes in a polyethylene matrix by extrusion shear flow: mechanical properties enhancement. *J. Compos. Mater.* **2011**, *45*, (8), 931-941.

(61) Chen, J. L.; Chen, Q. H.; Ma, Q. Influence of surface functionalization via chemical oxidation on the properties of carbon nanotubes. *J. Colloid Interface Sci.* **2012**, *370*, 32-38.

(62) Smith, B.; Wepasnick, K.; Schrote, K. E.; Cho, H. H.; Ball, W. P.; Fairbrother, D. H. Influence of surface oxides on the colloidal stability of nulti-walled carbon nanotubes: A structure-property relationship. *Langmuir* **2009**, *25*, (17), 9767-9776.

(63) Oh, W. K.; Yoon, H.; Jang, J. Characterization of surface modified carbon nanoparticles by low temperature plasma treatment. *Diamond Relat. Mater.* **2009**, *18*, (10), 1316-1320.

(64) Chirila, V.; Marginean, G.; Brandl, W. Effect of the oxygen plasma treatment parameters on the carbon nanotubes surface properties. *Surf Coat Tech* **2005**, *200*, (1-4), 548-551.

(65) Hyung, H.; Fortner, J. D.; Hughes, J. B.; Kim, J. H. Natural organic matter stabilizes carbon nanotubes in the aqueous phase. *Environ. Sci. Technol.* **2007**, *41*, (1), 179-184.

(66) Zhou, X. Z.; Shu, L.; Zhao, H. B.; Guo, X. Y.; Wang, X. L.; Tao, S.; Xing, B. S. Suspending multi-walled carbon nanotubes by humic acids from a peat soil. *Environ. Sci. Technol.* **2012**, *46*, (7), 3891-3897.

(67) Chappell, M. A.; George, A. J.; Dontsova, K. M.; Porter, B. E.; Price, C. L.; Zhou, P. H.; Morikawa, E.; Kennedy, A. J.; Steevens, J. A. Surfactive stabilization of multi-walled carbon nanotube dispersions with dissolved humic substances. *Environ. Pollut.* **2009**, *157*, (4), 1081-1087.

(68) Wang, X. L.; Shu, L.; Wang, Y. Q.; Xu, B. B.; Bai, Y. C.; Tao, S.; Xing, B. S. Sorption of peat humic acids to multi-walled carbon nanotubes. *Environ. Sci. Technol.* **2011**, *45*, (21), 9276-9283.

(69) Wang, S. G.; Liu, X. W.; Gong, W. X.; Nie, W.; Gao, B. Y.; Yue, Q. Y. Adsorption of fulvic acids from aqueous solutions by carbon nanotubes. *J. Chem. Technol. Biotechnol.* **2007**, *82*, (8), 698-704.

(70) Moore, V. C.; Strano, M. S.; Haroz, E. H.; Hauge, R. H.; Smalley, R. E.; Schmidt, J.; Talmon, Y. Individually suspended single-walled carbon nanotubes in various surfactants. *Nano Lett.* **2003**, *3*, (10), 1379-1382.

(71) Blanch, A. J.; Lenehan, C. E.; Quinton, J. S. Optimizing surfactant concentrations for dispersion of single-walled carbon nanotubes in aqueous solution. *J. Phys. Chem. B* **2010**, *114*, (30), 9805-9811.

(72) Piret, J. P.; Detriche, S.; Vigneron, R.; Vankoningsloo, S.; Rolin, S.; Mendoza, J. H. M.; Masereel, B.; Lucas, S.; Delhalle, J.; Luizi, F.; Saout, C.; Toussaint, O. Dispersion of multi-walled carbon nanotubes in biocompatible dispersants. *J. Nanopart. Res.* **2010**, *12*, (1), 75-82.

(73) Vaisman, L.; Marom, G.; Wagner, H. D. Dispersions of surface-modified carbon nanotubes in water-soluble and water-insoluble polymers. *Adv. Funct. Mater.* **2006**, *16*, (3), 357-363.

(74) Didenko, V. V.; Moore, V. C.; Baskin, D. S.; Smalley, R. E. Visualization of individual single-walled carbon nanotubes by fluorescent polymer wrapping. *Nano Lett.* **2005**, *5*, (8), 1563-1567.

(75) Park, H. J.; Heo, H. Y.; Lee, S. C.; Park, M.; Lee, S. S.; Kim, J.; Chang, J. Y. Dispersion of single-walled carbon nanotubes in water with polyphosphazene polyelectrolyte. *Journal of Inorganic and Organometallic Polymers and Materials* **2006**, *16*, (4), 359-364.

(76) O'Connell, M. J.; Bachilo, S. M.; Huffman, C. B.; Moore, V. C.; Strano, M. S.; Haroz, E. H.; Rialon, K. L.; Boul, P. J.; Noon, W. H.; Kittrell, C.; Ma, J. P.; Hauge, R. H.; Weisman, R. B.; Smalley, R. E. Band gap fluorescence from individual single-walled carbon nanotubes. *Science* **2002**, *297*, (5581), 593-596.

(77) Yu, J. R.; Grossiord, N.; Koning, C. E.; Loos, J. Controlling the dispersion of multi-wall carbon nanotubes in aqueous surfactant solution. *Carbon* **2007**, *45*, (3), 618-623.

(78) Schwyzer, I.; Kaegi, R.; Sigg, L.; Magrez, A.; Nowack, B. Influence of the initial state of carbon nanotubes on their colloidal stability under natural conditions. *Environ. Pollut.* **2011**, *159*, (6), 1641-1648.

(79) Bandyopadhyaya, R.; Nativ-Roth, E.; Regev, O.; Yerushalmi-Rozen, R. Stabilization of individual carbon nanotubes in aqueous solutions. *Nano Lett.* **2002**, *2*, (1), 25-28.

(80) Liu, G. H.; Wang, J. L.; Zhu, Y. F.; Zhang, X. R. Application of multiwalled carbon nanotubes as a solid-phase extraction sorbent for chlorobenzenes. *Anal. Lett.* **2004**, *37*, (14), 3085-3104.

(81) Vermisoglou, E. C.; Georgakilas, V.; Kouvelos, E.; Pilatos, G.; Viras, K.; Romanos, G.; Kanellopoulos, N. K. Sorption properties of modified single-walled carbon nanotubes. *Microporous Mesoporous Mater.* **2007**, *99*, (1-2), 98-105.

(82) Yang, K.; Xing, B. S. Desorption of polycyclic aromatic hydrocarbons from carbon nanomaterials in water. *Environ. Pollut.* **2007**, *145*, (2), 529-537.

(83) Pan, B.; Lin, D. H.; Mashayekhi, H.; Xing, B. S. Adsorption and hysteresis of bisphenol A and 17 alpha-ethinyl estradiol on carbon nanomaterials. *Environ. Sci. Technol.* **2008**, *42*, (15), 5480-5485.

(84) Oleszczuk, P.; Pan, B.; Xing, B. S. Adsorption and desorption of oxytetracycline and carbamazepine by multiwalled carbon nanotubes. *Environ. Sci. Technol.* **2009**, *43*, (24), 9167-9173.

(85) Yin, Y. F.; Mays, T.; McEnaney, B. Molecular simulations of hydrogen storage in carbon nanotube arrays. *Langmuir* **2000**, *16*, (26), 10521-10527.

(86) Bacsa, R. R.; Laurent, C.; Peigney, A.; Bacsa, W. S.; Vaugien, T.; Rousset, A. High specific surface area carbon nanotubes from catalytic chemical vapor deposition process. *Chem. Phys. Lett.* **2000**, *323*, (5-6), 566-571.

(87) Eswaramoorthy, M.; Sen, R.; Rao, C. N. R. (19)A study of micropores in single-walled carbon nanotubes by the adsorption of gases and vapors. *Chem. Phys. Lett.* **1999**, *304*, (3-4), 207-210.

(88) Bittner, E. W.; Smith, M. R.; Bockrath, B. C. Characterization of the surfaces of single-walled carbon nanotubes using alcohols and hydrocarbons: a pulse adsorption technique. *Carbon* **2003**, *41*, (6), 1231-1239.

(89) Chen, W.; Duan, L.; Zhu, D. Q. Adsorption of polar and nonpolar organic chemicals to carbon nanotubes. *Environ. Sci. Technol.* **2007**, *41*, (24), 8295-8300.

(90) Gotovac, S.; Yang, C. M.; Hattori, Y.; Takahashi, K.; Kanoh, H.; Kaneko, K. Adsorption of polyaromatic hydrocarbons on single wall carbon nanotubes of different functionalities and diameters. *J. Colloid Interface Sci.* **2007**, *314*, (1), 18-24.

(91) Lu, C.; Su, F.; Hu, S. Surface modification of carbon nanotubes for enhancing BTEX adsorption from aqueous solutions. *Appl. Surf. Sci.* **2008**, *254*, (21), 7035-7041.

(92) Cho, H. H.; Smith, B. A.; Wnuk, J. D.; Fairbrother, D. H.; Ball, W. P. Influence of surface oxides on the adsorption of naphthalene onto multiwalled carbon nanotubes. *Environ. Sci. Technol.* **2008**, *42*, (8), 2899-2905.

(93) Wu, W. H.; Chen, W.; Lin, D. H.; Yang, K. Influence of Surface Oxidation of Multiwalled Carbon Nanotubes on the Adsorption Affinity and Capacity of Polar and Nonpolar Organic Compounds in Aqueous Phase. *Environ. Sci. Technol.* **2012**, *46*, (10), 5446-5454.

(94) Ramanathan, T.; Fisher, F. T.; Ruoff, R. S.; Brinson, L. C. Amino-functionalized carbon nanotubes for binding to polymers and biological systems. *Chem. Mater.* **2005**, *17*, (6), 1290-1295.

(95) Huang, W. J.; Taylor, S.; Fu, K. F.; Lin, Y.; Zhang, D. H.; Hanks, T. W.; Rao, A. M.; Sun, Y. P. Attaching proteins to carbon nanotubes via diimide-activated amidation. *Nano Lett.* **2002**, *2*, (4), 311-314.

(96) Lu, C. Y.; Su, F. S. Adsorption of natural organic matter by carbon nanotubes. *Sep. Purif. Technol.* **2007**, *58*, (1), 113-121.

(97) Yang, K.; Xing, B. S. Adsorption of fulvic acid by carbon nanotubes from water. *Environ. Pollut.* **2009**, *157*, (4), 1095-1100.

(98) Namiesnik, J.; Zabiegala, B.; Kot-Wasik, A.; Partyka, M.; Wasik, A. Passive sampling and/or extraction techniques in environmental analysis: a review. *Anal Bioanal Chem* **2005**, *381*, (2), 279-301.

(99) Fucci, N.; De Giovanni, N.; Chiarotti, M.; Scarlata, S. SPME-GC analysis of THC in saliva samples collected with "EPITOPE" device. *Forensic Science International* **2001**, *119*, (3), 318-321.

(100) Yang, Z. Y.; Maruya, K. A.; Greenstein, D.; Tsukada, D.; Zeng, E. Y. Experimental verification of a model describing solid phase microextraction (SPME) of freely dissolved organic pollutants in sediment porewater. *Chemosphere* **2008**, *72*, (10), 1435-1440.

(101) Jonker, M. T. O.; Koelmans, A. A. Polyoxymethylene solid phase extraction as a partitioning method for hydrophobic organic chemicals in sediment and soot. *Environ. Sci. Technol.* **2001**, *35*, (18), 3742-3748.

(102) Cornelissen, G.; Gustafsson, O. Sorption of phenanthrene to environmental black carbon in sediment with and without organic matter and native sorbates. *Environ. Sci. Technol.* **2004**, *38*, (1), 148-155.

(103) Cornelissen, G.; Kukulska, Z.; Kalaitzidis, S.; Christanis, K.; Gustafsson, O. Relations between environmental black carbon sorption and geochemical sorbent characteristics. *Environ. Sci. Technol.* **2004**, *38*, (13), 3632-3640.

(104) Cornelissen, G.; Pfttersen, A.; Broman, D.; Mayer, P.; Breedveld, G. D. Field testing of equilibrium passive samplers to determine freely dissolved native polycyclic aromatic hydrocarbon concentrations. *Environ. Toxi. Chem.* **2008**, *27*, (3), 499-508.

(105) Cornelissen, G.; Wiberg, K.; Broman, D.; Arp, H. P. H.; Persson, Y.; Sundqvist, K.; Jonsson, P. Freely dissolved goncentrations and sediment-water activity ratios of PCDD/Fs and PCBs in the open baltic sea. *Environ. Sci. Technol.* **2008**, *42*, (23), 8733-8739.

(106) Fetzer, J. C. The chemistry and analysis of the large polycyclic aromatic hydrocarbons. *Polycyclic Aromat. Compd.* **2000**, *27*, (2), 143.

(107) Yang, K.; Wang, X. L.; Zhu, L. Z.; Xing, B. S. Competitive sorption of pyrene, phenanthrene, and naphthalene on multiwalled carbon nanotubes. *Environ. Sci. Technol.* **2006**, *40*, (18), 5804-5810.

(108) Zhang, S. J.; Shao, T.; Bekaroglu, S. S. K.; Karanfil, T. Adsorption of synthetic organic chemicals by carbon nanotubes: Effects of background solution chemistry. *Water Res.* **2010**, *44*, (6), 2067-2074.

(109) Zhang, S. J.; Shao, T.; Karanfil, T. The effects of dissolved natural organic matter on the adsorption of synthetic organic chemicals by activated carbons and carbon nanotubes. *Water Res.* **2011**, *45*, (3), 1378-1386.

(110) Wang, X. L.; Tao, S.; Xing, B. S. Sorption and competition of aromatic compounds and humic acid on multiwalled carbon nanotubes. *Environ. Sci. Technol.* **2009**, *43*, (16), 6214-6219.

(111) Wang, X. L.; Lu, J. L.; Xing, B. S. Sorption of organic contaminants by carbon nanotubes: influence of adsorbed organic matter. *Environ. Sci. Technol.* **2008**, *42*, (9), 3207-3212.

(112) Mackay, D.; Shiu, W. Y.; Ma, K. C., *Illustrated Handbook Of Physical-Chemical Properties And Environmental Fate For Organic Chemicals. Vol. I and II.* Lewis Publishers, Boca Raton, Ann Arbor, London, Tokyo: 1992.

(113) Jonker, M. T. O.; van der Heijden, S. A. Bioconcentration factor hydrophobicity cutoff: An artificial phenomenon reconstructed. *Environ. Sci. Technol.* **2007**, *41*, 7363-7369.

(114) US-EPA EPI Suite Package. Estimation Program Interface from the U.S. Environmental Protection Agency. Available at http://www.epa.gov/oppt/exposure/pubs/episuitedl.htm. Last accessed Nov. 2010. **2000**.

(115) Yang, W. C.; Mang, J.; Zhang, C. D.; Zhu, L. Y.; Chen, W. Sorption and resistant desorption of atrazine in typical chinese soils. *J. Environ.l Qual.* **2009**, *38*, (1), 171-179.

(116) van Noort, P. C. M. Estimation of amorphous organic carbon/water partition coefficients, subcooled aqueous solubilities, and n-octanol/water distribution coefficients of alkylbenzenes and polycyclic aromatic hydrocarbons. *Chemosphere* **2009**, *74*, (8), 1018-1023.

(117) Ma, Y. G.; Lei, Y. D.; Xiao, H.; Wania, F.; Wang, W. H. Critical review and recommended values for the physical-chemical property data of 15 polycyclic aromatic hydrocarbons at 25 degrees C. *J. Chem. Engin. Data* **2010**, *55*, (2), 819-825.

(118) Arp, H. P. H.; Breedveld, G. D.; Cornelissen, G. Estimating the in situ sediment-porewater distribution of PAHs and chlorinated aromatic hydrocarbons in anthropogenic impacted sediments. *Environ. Sci. Technol.* **2009**, *43*, (15), 5576-5585.

(119) Abraham, M. H.; Chadha, H. S.; Whiting, G. S.; Mitchell, R. C. Hydrogen bonding. 32. An anaylsis of water-octanol and water-alkane partitioning and the delta-logP parameter of Seiler. *J. Pharm. Sci.* **1994**, *83*, (8), 1085-1100.

(120) Yu, S. M.; Chen, C. L.; Chang, P. P.; Wang, T. T.; Lu, S. S.; Wang, X. K. Adsorption of Th(IV) onto Al-pillared rectorite: Effect of pH, ionic strength, temperature, soil humic acid and fulvic acid. *Appl Clay Sci* **2008**, *38*, (3-4), 219-226.

(121) Lu, G. N.; Dang, Z.; Tao, X. Q.; Yang, C.; Yi, X. Y. Modeling and prediction of photolysis half-lives of polycyclic aromatic hydrocarbons in aerosols by quantum chemical descriptors. *Science of the Total Environment* **2007**, *373*, (1), 289-296.

(122) Zhang, S. J.; Shao, T.; Bekaroglu, S. S. K.; Karanfil, T. The impacts of aggregation and surface chemistry of carbon nanotubes on the adsorption of synthetic organic compounds. *Environ. Sci. Technol.* **2009**, *43*, (15), 5719-5725.

(123) Chen, J. Y.; Chen, W.; Zhu, D. Adsorption of nonionic aromatic compounds to single-walled carbon nanotubes: effects of aqueous solution chemistry. *Environ. Sci. Technol.* **2008**, *42*, (19), 7225-7230.

(124) Wang, L. L.; Zhu, D. Q.; Duan, L.; Chen, W. Adsorption of single-ringed N- and S-heterocyclic aromatics on carbon nanotubes. *Carbon* **2010**, *48*, (13), 3906-3915.

(125) Lin, D. H.; Xing, B. S. Adsorption of phenolic compounds by carbon nanotubes: Role of aromaticity and substitution of hydroxyl groups. *Environ. Sci. Technol.* **2008**, *42*, (19), 7254-7259.

(126) Kohler, A. R.; Som, C.; Helland, A.; Gottschalk, F. Studying the potential release of carbon nanotubes throughout the application life cycle. *J Clean Prod* **2008**, *16*, (8-9), 927-937.

(127) Wu, W. H.; Chen, W.; Lin, D. H.; Yang, K. Influence of surface oxidation of multiwalled carbon Nanotubes on the adsorption affinity and capacity of polar and nonpolar organic compounds in aqueous Phase. *Environ. Sci. Technol.* **2012**, *46*, (10), 5446-5454.

(128) Scaffaro, R.; Maio, A.; Agnello, S.; Glisenti, A. Plasma functionalization of multiwalled carbon nanotubes and their use in the preparation of nylon 6-based nanohybrids. *Plasma Process Polym* **2012**, *9*, (5), 503-512.

(129) Chen, W.; Liu, X.; Liu, Y.; Bang, Y.; Kim, H. I. Preparation of O/W pickering emulsion with oxygen plasma treated carbon nanotubes as surfactants. *J. Ind. Eng. Chem.* **2011**, *17*, (3), 455-460.

3. Method Development and Influence of Sorbate Properties and Concentration

Measuring and Modeling Adsorption of PAHs to Carbon Nanotubes Over a Six Order of Magnitude Wide Concentration Range

Kah, M.; Zhang, X. R.; Jonker, M. T. O.; Hofmann, T.

Environ. Sci. Technol. **2011**, *45*, (14), 6011-6017.

3.1 Abstract

Understanding the interactions between organic contaminants and carbon nanomaterials is essential for evaluating the materials' potential environmental impact and their application as sorbent. Although a great deal of work has been published in the past years, data are still limited in terms of compounds, concentrations, and conditions investigated. We applied a passive sampling method employing POM-SPE to gain a better understanding of the interactions between PAHs and multi-walled CNTs over a six order of magnitude wide concentration range. In the low concentration range (pg–ng/L) sorption of phenanthrene and pyrene was linear on a non-logarithmic scale. Here, sorption could thus be described using a single sorption coefficient. Isotherm fits over the entire concentration range showed that (i) monolayer sorption models described the data very well, and (ii) the CNTs sorption capacity was directly related to their surface area. Sorption coefficients for 13 PAHs (11 of which have not been reported to date) were also measured at environmentally-relevant low concentrations. No competition seemed to occur in the low concentration range and sorption affinity was directly related to the solubility of the subcooled liquid of the compounds.

3.2 Introduction

Production of CNTs is expected to increase rapidly in the future and the materials' release in the environment is therefore inevitable. CNTs exhibit a high surface area to volume ratio, as well as a strong sorption affinity towards organic contaminants, such as PAHs, chlorobenzenes, and dioxins.[1] CNTs have thus been suggested as superior sorbents for applications such as treatment of contaminated water[2] or solid phase extraction cartridges.[3-5] Understanding the interactions between organic contaminants and CNTs is therefore essential for evaluating the potential environmental impact of CNTs through e.g., facilitated

nanoparticle-bound co-transport of organic contaminants[6], as well as the potential efficiency as superior sorbent in waste water treatment or for groundwater remediation.

Although a great deal of work on organic chemicals has been published in the past years, sorption data are still limited in terms of compounds, concentrations, and conditions investigated (for an overview on the literature, see[7]). This can be mainly explained by limitations associated with the generally-applied batch sorption test set ups. First, the high sorption capacity of CNTs results in extremely low concentrations of sorbates remaining in the aqueous phase. Second, classical separation techniques (e.g., centrifugation or filtration) are not adequate to efficiently separate the CNTs and liquid phase under conditions where CNTs are partially dispersed (e.g., in the presence of natural organic matter[8] or surfactants[9]). Questions thus remain open on the sorption mechanisms occurring over a wide range of concentrations and environmental conditions.

Isotherm fitting with model equations is a key tool to gain information on sorption mechanisms and several models were already tested to fit sorption isotherms to CNTs.[7] However, isotherms have been restricted to a relatively high concentration range. Consequently, isotherm shapes and strengths of sorption relevant to the lower concentration range remain mostly speculative. PAHs sorption to CNTs from aqueous solution has been described for less hydrophobic PAHs (naphthalene, phenanthrene, and pyrene) at the µg/L range.[10, 11] Based on the results, these compounds have been suggested to sorb to CNTs by a combination of hydrophobic and π–π interactions.[7] Experimental data for a larger series of PAHs down to lower concentrations would be needed to better understand the mechanisms of interaction with CNTs likely to occur in the environment and how compound properties affect sorption affinity.

In the present study, we applied a passive sampling method (POM-SPE method[12]) previously developed and validated for sorbents with similar characteristics as CNTs to investigate these aspects of sorption that have not been studied to date. The objectives were (i) to verify the applicability of the POM-SPE method for studying sorption of PAHs to CNTs and to compare the results to those obtained with a traditional batch/centrifugation method, and (ii) to use the POM-SPE method to investigate sorption behavior of very hydrophobic PAHs in the low concentration range and to gain insights into the sorption mechanism by data-fitting a series of sorption isotherm models.

3.3 Materials and Methods

3.3.1 Sorbents and Chemicals

A Polyoxymethylene sheet (POM; thickness 0.5 mm; density: 1.41 g/cm^3) was purchased from Vink Kunststoffen BV, Didam, the Netherlands. The POM sheet was cut into strips and was cold-extracted with hexane (30 min) and methanol (3 times for 30 min) as described in Jonker and Koelmans.[12] Multi-walled CNTs were provided by Baytubes (Luverkusen, Germany; C150HP, synthesized by vapour deposition, >99% purity, Table 3.1).

CNTs (1 g) were first heated to 350 °C for 30 min to remove amorphous carbon.[13] After 20 h of exposure to an acid solution (40 mL H_2SO_4:HNO_3, 1:3[14]), the CNT suspension was poured into a filtration system. Milli-Q water was added continuously until the pH of the CNTs suspension was approximately 7. The suspension was then filtered (0.1 μm cellulose nitrate membrane) by using a vacuum pump. CNTs retained by the filter were collected, dried at 105 °C for 48 h, and then stored in sealed amber glass vials.

Elemental analysis of the bulk CNTs (Elementar Vario MACRO, duplicates) gave an O% of 0.000 and 1.072% (stdev 0.01) before and after pre-treatment, respectively. Energy dispersive X-ray spectroscopy was also performed to assess the degree of oxidation at the surface of the CNTs aggregates (EDX on Quanta 3D FEG, 10 measurements per treatment). Results indicated an O% of 4.78 (± 0.50%) and 5.64 (± 0.73%) before and after pre-treatment, respectively. The purification process resulted in an increase in the overall oxygen content of about 1%, which is comparable to values reported in the literature.[15]

Table 3.1. *Properties of the CNTs used (as provided by the supplier)*

Property	Value	Unit	Method
C-Purity	> 99	%	Elementary analysis
Free amorphous carbon	Not detectable	%	TEM
Number of walls	3-15	-	TEM
Outer mean diameter	13-16	nm	TEM
Outer diameter distribution	5-20	nm	TEM
Inner mean diameter	4	nm	TEM
Inner diameter distribution	2-6	nm	TEM
Length	>1	μm	SEM
Bulk density	140-230	kg m^{-3}	EN ISO 60
BET surface area	200-500	m^2 g^{-1}	BET
Metal catalysts	Co, Mn, Mo, Al, Mg		

Phenanthrene (Phen, 99.0%), pyrene (Pyr, 99.0%), Phen-d10 (99.5%), and Pyr-d10 (99.5%) were purchased from Dr. Ehrenstorfer (Germany). Other PAHs (anthracene, fluoranthene, benz[*a*]anthracene, chrysene, benzo[*e*]pyrene, benzo[*b*]fluoranthene, benzo[*k*]fluoranthene, benzo[*a*]pyrene, benzo[*g,h,i*]perylene, dibenz[*a,h*]anthracene, and indeno[*1,2,3-c,d*]pyrene were obtained from Sigma-Aldrich (Germany). All stock solutions were prepared in methanol. Solvents used were hexane, methanol, acetonitrile (residue analysis grade, Lab Scan, Dublin, Ireland and Acros Organics, Geel, Belgium)

3.3.2 Batch/Centrifugation Method

Sorption isotherms of Phen and Pyr to CNTs were measured by a batch approach using centrifugation, as described in the literature (e.g., ref 10 and 11). All experiments were carried out at 20±1°C and using background solution prepared with 0.01 M $CaCl_2$ and 200 mg/L NaN_3 as biocide (pH 7.0). One mg of aggregated CNTs and 50 mL of background solution were added to 50 mL glass centrifugation tubes. Phen or Pyr in methanol was spiked using a glass microsyringe and keeping the volume of methanol added always below 0.2% (v/v). Yang et al.[10] showed that PAHs equilibrated with CNTs within four days and an equilibration time of five days was therefore applied in the present study. Upon equilibration, the samples were centrifuged (1000*g* for 20 min) and 40 mL of supernatant were carefully collected with a glass pipette. After the addition of internal standard (Phen-d10 or Pyr-d10), the supernatants were extracted three times with hexane (3×5 mL). Extracts were combined, water was removed with anhydrous sodium sulfate, and extracts were concentrated under N_2 down to 0.1–1 mL, prior to GC-MS analysis (Agilent 7890A gas chromatograph coupled to Agilent 5975C mass spectrometer; HP-5MS fused silica column (60 m×250µm×0.25 µm, J&W Scientific); pulsed splitless mode and oven temperature of 55°C for 1 min, then 10°C min^{-1} up to 300°C).

3.3.3 POM-SPE Method

The procedure outlined in Jonker and Koelmans[12] was used to determine sorption isotherms of Phen and Pyr to CNTs over a very wide concentration range (pg–µg/L). The experimental setting was similar to the one described for the centrifugation method; only deviations were (i) the addition of 0.1–1g POM to each sample before shaking and (ii) the extension of the shaking period from 5 to 28 d to ensure equilibration of PAHs with POM. POM strips were then taken out the tubes, rinsed with deionized water and wiped with a wet tissue in order to remove CNTs that may have remained on the surface. Full removal of CNTs from the smooth surface of POM was confirmed by microscopy imaging (Figure 3.1). After the addition of the

internal standard (Phen-d10 or Pyr-d10), POM strips were extracted with methanol by accelerated solvent extraction (ASE 200, Dionex, USA; 1500 psi, 100°C). Extracts were concentrated under N_2 and methanol was exchanged to hexane, after which the extracts were concentrated again and analyzed by GC-MS.

The POM-SPE method was also used to determine sorption coefficients of 13 PAHs (see Sorbents and Chemicals section) spiked simultaneously. This multiple solute experiment was performed at two-three concentration levels in the low concentration range (see details in Table 3.5). Deviations from the protocol described above were (i) the use of 250 mL full glass bottles (instead of 50 mL tubes), (ii) POM strips were Soxhlet-extracted and the extracts were cleaned-up as described in Jonker and Koelmans[12], and (iii) PAHs were analyzed by HPLC as described in Jonker and Van der Heijden.[16]

Figure 3.1. *Microscope image of POM surface before (a) and after (b) wiping with a wet tissue, confirming the removal of CNTs prior to extraction.*

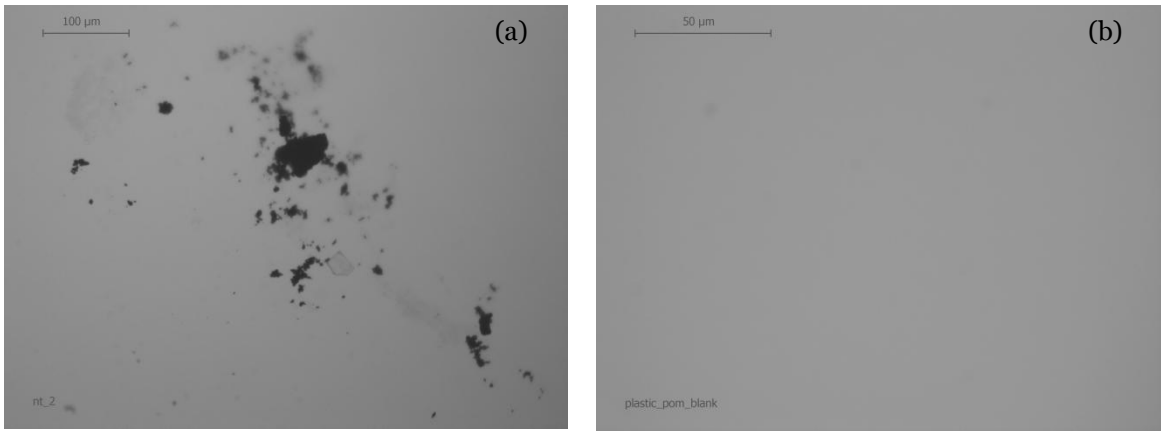

3.3.4 Sorption Models and Statistics

Six sorption models previously applied to describe sorption to CNTs[10] and commonly used for activated carbon[17], soot/coal[18] and geosorbents[19] were fit to the isotherms. The equations and parameters are listed in Table 2.3 of Chapter 2. Detailed descriptions of the models are available in the literature (e.g.,[19]) and here we only present a brief description and remind the abbreviation here. The Freundlich (FM) is an empirical model that assumes an exponential site energy distribution. The Langmuir model describes the formation of a sorbate monolayer on the sorbent until saturation. The single Langmuir model (LM) considers a finite number of one type of sorption sites, whereas the dual Langmuir model (DLM) considers two types of

sorption sites (high and low-energy). The Brunauer-Emmett-Teller model (BETM) describes a monolayer adsorption, followed by condensation of the sorbate, based on its solubility. The Dual-mode model (DMM) combines linear partitioning and Langmuir modes of sorption. Finally, the Polanyi potential theory assumes the existence of an adsorption space at the sorbent surface, where the adsorption potential depends on the distance of the sorbate to the surface. The experimental data were fit with one of the mathematical formulations of the Polanyi theory: the Dubinin-Ashtakhov model (DAM; as used in[11]). Model parameters were determined by least square error optimisation (Marquardt-Levenberg algorithm). Given that the concentration range studied spanned six to seven orders of magnitude, the standard deviation of the scatter cannot be considered uniform along the x-axis. Data were therefore weighted by $1/y^2$ (where y is the concentration sorbed to the CNTs; mg/kg) which generally resulted in a significant improvement of fit.

The goodness of fit of the six models tested was evaluated and compared based on the r^2 values, mean weighted square errors (MWSE), distribution of residuals along the x-axis, mechanistic considerations, and statistical testing. Differences in the quality of fit between nested models (LM and DLM) were tested using a F-test on the ratio of mean square of residuals, as described in Pikaar et al.[17]: [(SS1/DF1)/(SS2/DF2)] = F; with SS being the sum of squares and DF the number of degrees of freedom, 2 refers to the best fitting model). This procedure accounts for different numbers of fitting parameters among models, so that models with more fitting parameters are not automatically favored. Model fits were also compared based on Akaike's Information Criterion (AIC). This method is based on information theory and determines which model is more likely to be correct. Probabilities were calculated considering differences in residual errors and the number of parameters between each model. An advantage of AIC over the F-test is that it can be used to compare non-nested models (see[20]). Akaike's Information Criterion (AIC) was calculated for each model following:

$$AIC = N * \ln\left(\frac{WSS_{res}}{N}\right) + 2 * p + \frac{2 * p * (p+1)}{N - p - 1}$$

Where N is the number of data points, p is the number of fitting parameters and WSS_{res} is the weighted sum of squares residual:

$$WSS_{res} = \sum \frac{(y_{data} - y_{fit})^2}{{y_{data}}^2}$$

The model with the smallest AIC value is most likely the best. The probability to choose the best model can be computed based on the difference of AIC values between two models compared:

$$probability = \frac{e^{-0.5*\Delta AIC}}{1 + e^{-0.5*\Delta AIC}}$$

The evidence ratio is defined as the ratio of the probability associated with the two models:

$$evidence\ ratio = \frac{1}{e^{-0.5*\Delta AIC}}$$

For more information, see Burnham and Anderson. [20] All statistical tests and parameter optimizations were performed with SigmaPlot 11.0 for Windows.

3.4 Results and Discussion

3.4.1 Batch/Centrifugation vs POM-SPE

In Figure 3.2, the sorption isotherms for Phen and Pyr on CNTs measured by the batch/centrifugation and the POM-SPE method are compared. The six sorption models described above were fit to the isotherms measured by both methods in the high concentration range. Note that 'high concentration range' here refers to the range that can be investigated by both the batch/centrifugation and POM-SPE method. In contrast, 'low concentration range' will be used below to indicate the range that can only be investigated using POM-SPE and for which data have not been reported so far. The aim of the fitting at this stage was to identify the model that describes the data adequately, allowing a statistical comparison of the two experimental methods based on differences in model parameters. Based on the r^2 and MWSE, the DLM was selected for this purpose (fitting parameters presented in Table 3.2). Analysis of variance on the four fitting parameters confirmed that there was no significant difference between the results obtained by batch/centrifugation and POM-SPE for both PAHs (p<0.001). This implies that the centrifugation yielded a complete separation of CNTs and water, which is in accordance with the observation that under the present experimental conditions (i.e. pre-treatment and the addition of $CaCl_2$ 0.01M to the solution) CNTs form fairly large aggregates (see electron microscopy images in Figures 3.3, 3.4 and 3.5). As such, a relatively low-speed centrifugation is sufficient to efficiently separate the CNTs from the liquid phase. Even though the POM-SPE method yielded similar results as the faster batch/centrifugation method, the former has a clear advantage. The passive sampling approach concentrates the freely

dissolved PAHs and therefore allows studying strongly sorbing compounds at environmentally-relevant low concentrations. Understanding sorption behavior in the low concentration range is of primary importance when assessing sorption likely to occur in the natural environment. It is also required to understand the possible succession of sorption mechanisms occurring at the surface of complex sorbents.

***Figure 3.2**. Sorption isotherms of Phen and Pyr to CNTs as measured by batch/centrifugation (●) and POM-SPE (o). The straight lines represent the fit by the Freundlich model in the low concentration range. Triangles represent sorption coefficients measured in the presence of 12 other PAHs.*

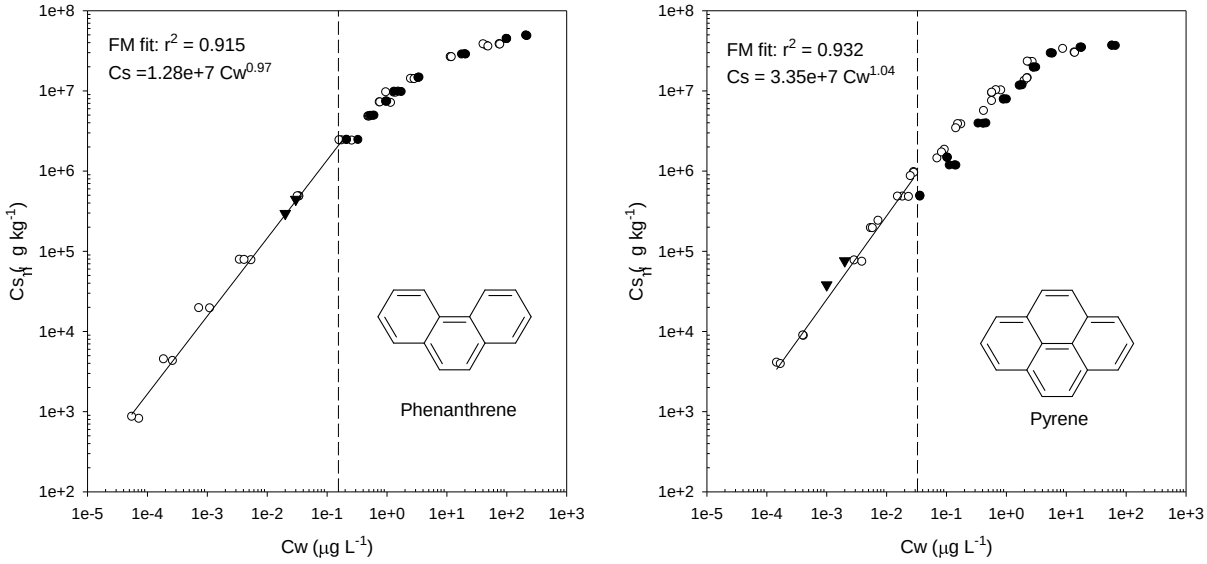

3.4.2 Sorption in the Low Concentration Range

Sorption isotherms of Phen and Pyr appeared linear in the low concentration range and the FM fit the isotherms very well (Figure 3.2). Freundlich exponents were close to unity (n = 0.97 and 1.04 for Phen and Pyr, respectively), indicating also linear isotherms on a non-logarithmic scale. Sorption of these PAHs can be thus be described by a single sorption coefficient over several orders of magnitude in the low concentration range (log K_f = 7.11 and 7.53 L/kg for Phen and Pyr, respectively).

***Figure 3.3**. Scanning electron microscope images of dried CNT powder before (BP) and after pre-treatment (AP). The purification procedure seems to significantly affect the physical aspects of CNT aggregates (much larger aggregates, more condensed structure).*

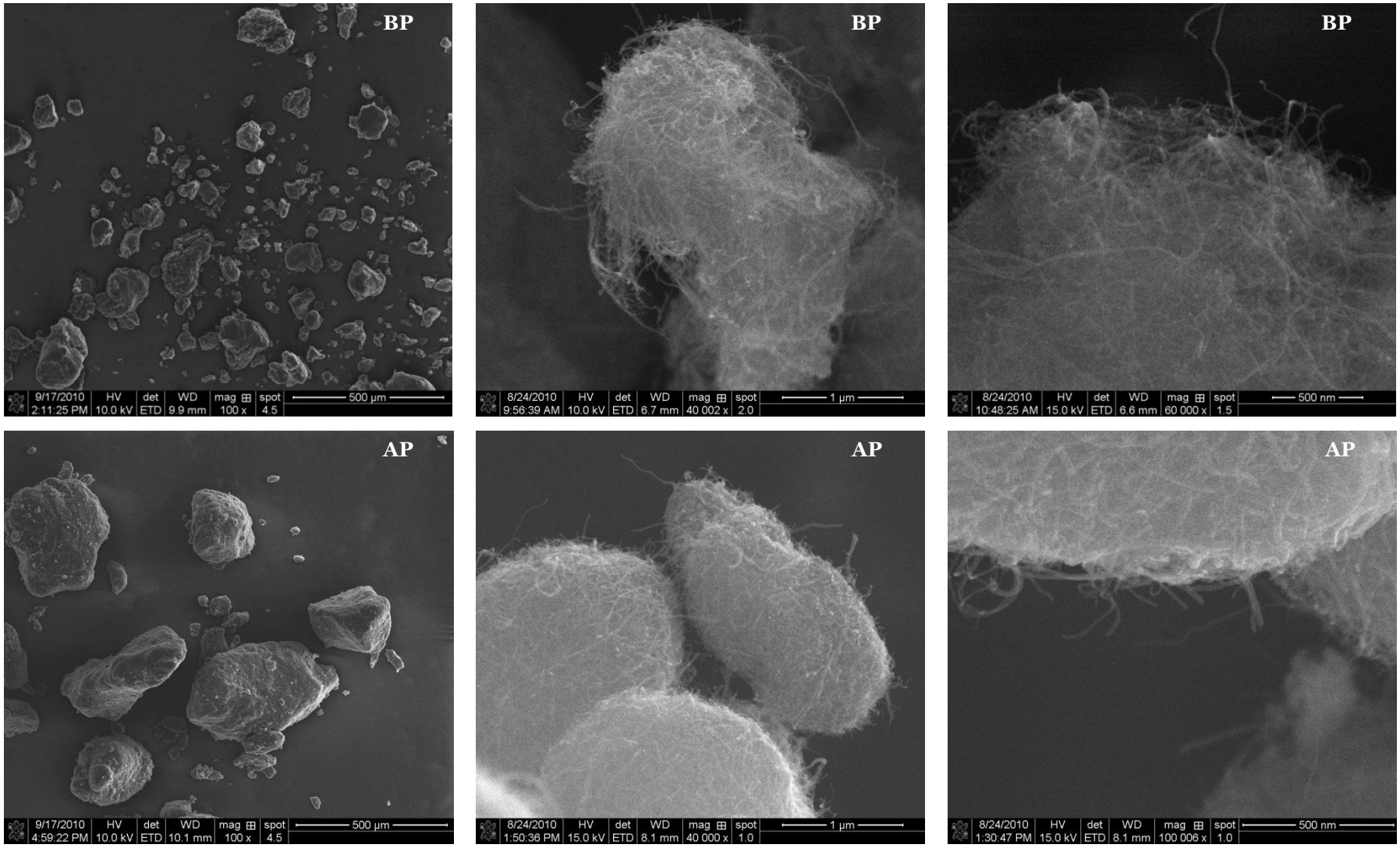

***Figure 3.4**. Scanning electron microscope images of a cross section of an aggregate of CNTs after pre-treatment. The interstitial spaces between the tubes appear very heterogeneous within an aggregate (coexistance of regions of very low and high density).*

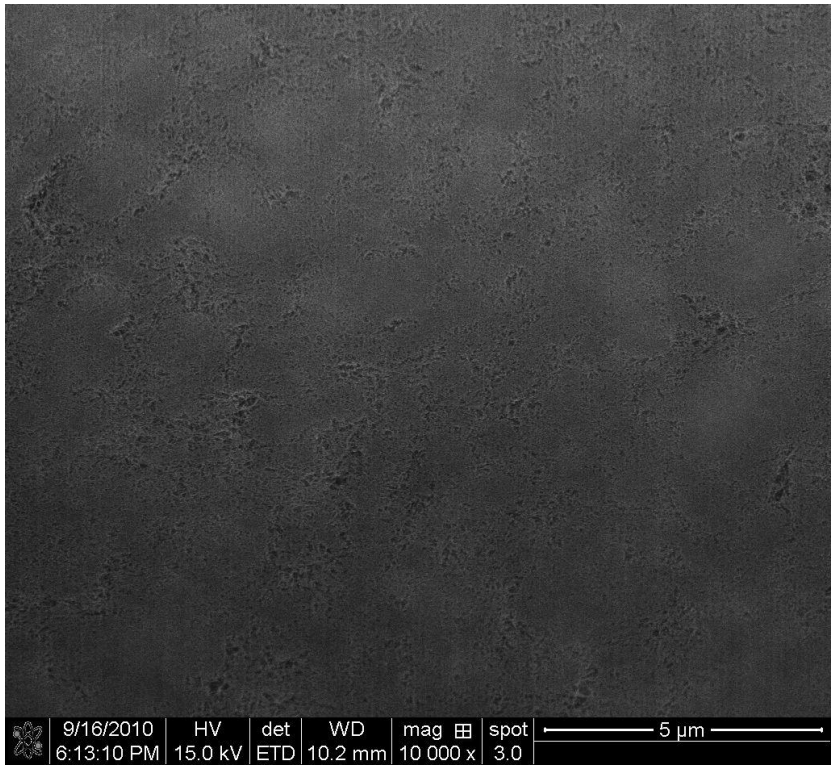

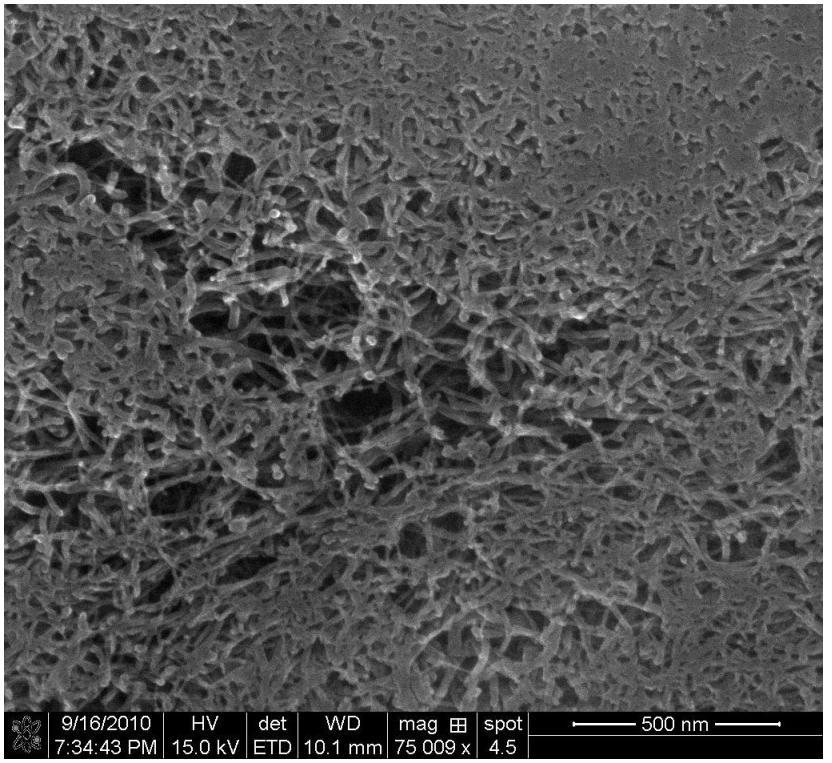

***Figure 3.5**. Electron microscope images of pre-treated CNTs shaken for 28 days with a POM strip in background solution (i.e., under the same conditions as applied during sorption tests). The TEM grid was dipped into the suspension to collect CNTs and dried at room temperature for 2 days before imaging.*

SEM

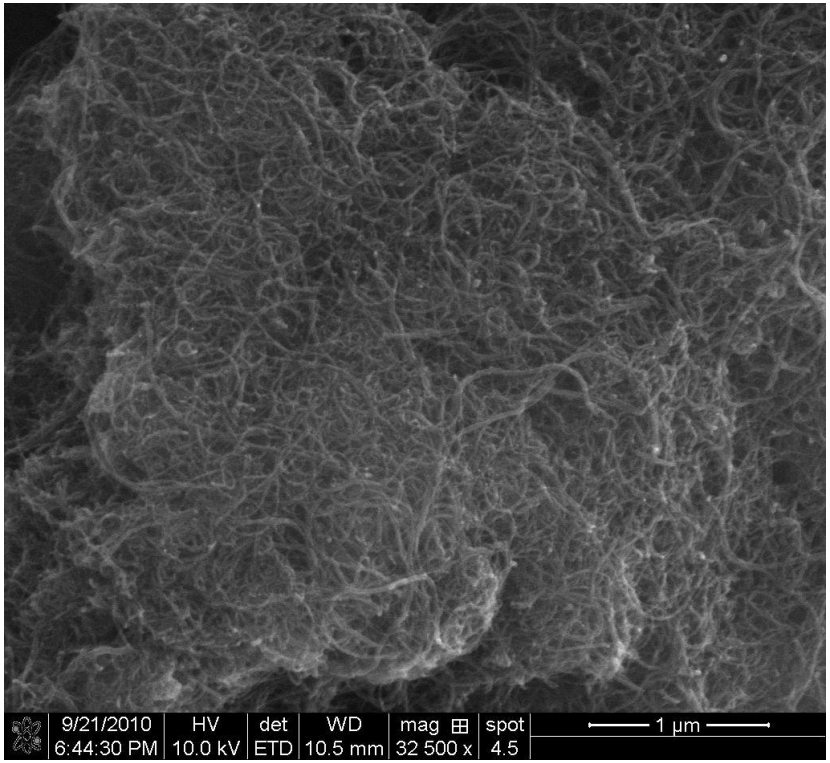

STEM

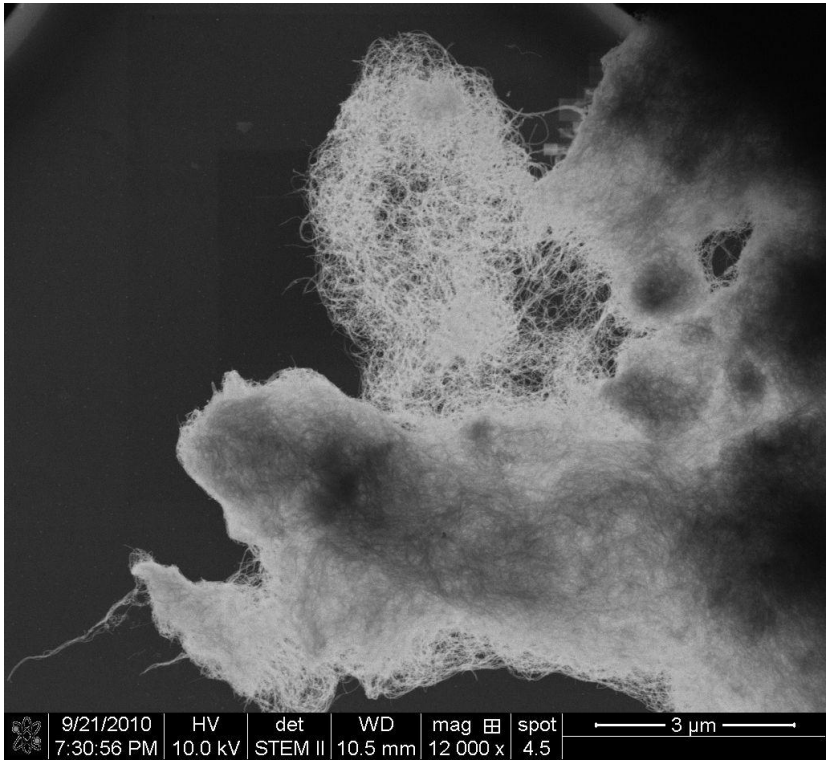

***Table 3.2**. Fitting parameters ± standard error, mean weighted square error (MWSE), and r^2 for six sorption models fitting the isotherm of phenanthrene (Phen) and pyrene (Pyr) on CNTs in the high concentration range: comparison of the batch/centrifugation (PhenC and PyrC) and POM-SPE (PhenP and PyrP) method.*

Freundlich Model (FM)					
	K_f	n	**MWSE**	r^2	**N**[a]
PhenC	6.12E+06±3.72E+05	0.43±0.02	0.00257	0.9079	24
PhenP	6.65E+06±3.57E+05	0.45±0.02	0.00219	0.9224	24
PyrC	4.84E+06±3.92E+05	0.59±0.03	0.00554	0.5743	30
PyrP	8.96E+06±4.92E+05	0.59±0.02	0.00261	0.7974	24
Langmuir Model (LM)					
	Q^0	$K_{d`}$	**MWSE**	r^2	**N**
PhenC	4.17E+07±2.50E+06	4.66±0.44	0.00101	0.9450	24
PhenP	3.68E+07±2.11E+06	3.42±0.32	0.00088	0.9780	24
PyrC	4.16E+07±2.58E+06	3.69±0.32	0.00077	0.9834	30
PyrP	2.68E+07±2.80E+06	1.10±0.17	0.00184	0.8900	24
Brunauer-Emmett-Teller Model (BETM)					
	Q^0	B	**MWSE**	r^2	**N**
PhenC	3.81E+07±1.86E+06	309.86±24.42	0.00071	0.9732	24
PhenP	3.53E+07±1.91E+06	359.91±34.95	0.00081	0.9830	24
PyrC	2.59E+07±2.03E+06	60.97±6.97	0.00164	0.8367	30
PyrP	2.52E+07±2.41E+06	127.54±18.67	0.00170	0.9060	24
Dual-Mode Model (DMM)					
	K_P	Q^0	K_d	**MWSE**	r^2	**N**
PhenC	1.07E+05±1.89E+04	3.01E+07±2.25E+06	3.05±0.32	0.00047	0.9833	24
PhenP	1.87E+05±5.67E+04	2.72E+07±2.94E+06	2.32±0.35	0.00066	0.9842	24
PyrC	-1.05E+05±1.10E+05	4.63E+07±5.79E+06	4.14±0.59	0.00077	0.9905	30
PyrP	1.13E+06±4.06E+05	1.82E+07±3.05E+06	0.71±0.15	0.00149	0.9187	24
Dual-Langmuir Model (DLM)						
	Q_1^0	K_{d1}	Q_2^0	K_{d2}	**MWSE**	r^2	**N**
PhenC	1.78E+07±3.68E+06	1.75e±0.38	3.77E+07±3.54E+06	38.42±17.10	0.00028	0.9994	24
PhenP	5.93E+06±4.29E+06	0.54e±0.39	3.62E+07±3.45E+06	7.95±3.16	0.00046	0.9962	24
PyrC	1.27E+05±1.84E+5	1.97e-10±0.05	4.31E+07±2.66E+06	4.21±0.51	0.00065	0.9780	30
PyrP	4.47E+05±4.16E+05	2.32-11±0.02	3.21E+07±3.60E+06	1.79±0.44	0.00121	0.9377	24
Dubinin-Ashtakhov Model(DAM)						
	log Q^0	E	b	**MWSE**	r^2	**N**
PhenC	7.72±0.02	1.86E+04±1.88E+02	2.38±0.12	0.00029	0.9983	24
PhenP	7.68±0.03	1.93E+04±2.78E+02	2.52±0.18	0.00047	0.9935	24
PyrC	7.65±0.04	1.39E+04±3.50E+02	1.99±0.12	0.00120	0.9435	30
PyrP	7.67±0.08	1.52E+04±7.71E+02	1.85±0.20	0.00126	0.9311	24

[a]N is the number of experimental point

To date, CNTs have generally been described as heterogeneous sorbents. The explanations provided were (i) the presence of high energy adsorption sites (e.g., defects, functional

groups, and interstitial/groove regions between CNT bundles); and/or (ii) the occurrence of condensation (e.g., surface and capillary condensation of gas or liquid adsorbates).[1] The presence of high energy sites would impact the low concentration range, whereas condensation would occur at relatively high concentration (when a multilayer of sorbates may form at the surface of the sorbent). The linearity of the isotherm in the low concentration range observed in our study does however not support the presence of a limited number of highly energetic sites; rather it indicates a large number of sites exhibiting similar sorption energy.

3.4.3 Sorption over the Full Concentration Range

Six sorption models were fit to the isotherms of Phen and Pyr over the whole concentration range investigated (Table 3.3, Figures 3.6 and 3.7). All the nonlinear models appeared to fit the isotherms very well ($r^2 \geq 0.950$). The exception was the FM with r^2=0.618 and 0.458 for Phen and Pyr, respectively. Although several authors used the FM to fit sorption isotherms of organic chemicals to CNTs[7] and reasonable fits were sometimes observed (e.g., over narrow concentration ranges), most graphs clearly show that the curvatures observed on a logarithmic scale cannot be represented by a straight line. The FM has undisputed advantages when comparing several sorbents/sorbates, due to its simplicity. However, it apparently is not suitable for describing the sorption behavior of PAHs on CNTs over a wide concentration range.

For both Phen and Pyr, the highest r^2 and lowest MWSE were calculated for the DLM, which however also has the highest number of parameters. Still, the F-test indicated that the better fit of DLM compared to LM was not due to over-parametrisation (p<0.001). According to Akaike's Information Criterion (AIC), the goodness of fit followed the order DLM>DMM=DAM>BETM>LM for Phen, and DMM>DLM>BETM>LM>DAM for Pyr. AIC helps quantifying discrepancies between models. For Phen, the evidence ratio indicated a large improvement of fit by the DLM, compared to the other models, whereas differences between models were smaller for Pyr (Table 3.4). Overall, the various evaluation methods fairly consistently indicated that the DLM and/or DMM were most likely the best models to describe sorption of the two PAHs to CNTs over a wide concentration range.

Yang and Xing[7] recently reviewed the literature on the adsorption of organic compounds to CNTs. The authors concluded that Polanyi theory-based equations seemed to be superior when describing sorption of PAHs to CNTs. This conclusion was mainly based on the bad fits obtained for other models, including DLM, DMM, BETM and LM. Parameter optimization is

an essential step when comparing the goodness of fit among different models. Transformation of the model equations (e.g., linearization), data weighting, and the number of iterations and steps can significantly influence the optimization and thus the quality of the fit, as well as fitting narrow concentration ranges. It is possible that the low fitting quality for several models reported previously in the literature was due to the optimisation procedure. However, the sometimes limited concentration ranges studied may also contribute to the low fitting qualities.

Table 3.3*. Fitting parameters ± standard error, mean weighted square error (MWSE), and r^2 for six sorption models fitting the isotherms of phenanthrene (Phen) and pyrene (Pyr) on CNTs considering the whole concentration range investigated with the POM-SPE method.*

Freundlich Model (FM)						
	K_f	n		**MWSE**	r^2	**N**[a]
Phen	2.30E+06±3.05E+05	0.76±0.02		0.01070	0.6181	36
Pyr	6.95E+06±7.42E+05	0.81±0.02		0.00671	0.4581	36
Langmuir Model (LM)						
	Q^0	K_d		**MWSE**	r^2	**N**
Phen	3.22E+07±2.77E+06	2.39±0.28		0.00142	0.9500	36
Pyr	2.64E+07±2.48E+06	1.06±0.13		0.00118	0.9185	36
Brunauer-Emmett-Teller Model (BETM)						
	Q^0	B		**MWSE**	r^2	**N**
Phen	3.11E+07±2.58E+06	557.63±63.83		0.00135	0.9568	36
Pyr	2.50E+07±2.20E+06	129.88±14.64		0.00112	0.9318	36
Dual-Mode Model (DMM)						
	K_P	Q^0	K_d	**MWSE**	r^2	**N**
Phen	3.01E+05±6.41E+04	2.00E+07±2.45E+06	1.36±0.21	0.00100	0.9697	36
Pyr	1.05E+06±4.11E+05	1.92E+07±3.04E+06	0.77±0.13	0.00104	0.9459	36
Dual-Langmuir Model (DLM)						
	Q_1^0	K_{d1}	Q_2^0	K_{d2}	**MWSE**	r^2	**N**
Phen	4.45E+06±3.01E+06	0.40±0.21	3.72E+07±3.25E+06	7.00±2.72	0.00071	0.9973	36
Pyr	1.08E+07±1.02E+07	0.51±0.34	3.10E+07±9.70E+06	6.04±8.42	0.00103	0.9578	36
Dubinin-Ashtakhov Model(DAM)						
	log Q^0	E		b	**MWSE**	r^2	**N**
Phen	7.83±0.04	1.75E+04±4.17E+02		1.88±0.05	0.00100	0.9685	36
Pyr	7.75±0.06	1.43E+04±5.03E+02		1.73±0.07	0.00116	0.9405	36

[a]N is the number of experimental point

Good fits by the Dubinin-Ashtakhov model (DAM) were also observed in the present study. However, there are some arguments that would not support the selection of the DAM as the most appropriate model. First, better fits were observed for DLM and DMM for both PAHs.

Second, the Dubinin-Ashtakhov theory describes sorption phenomena, which are not supported by the linear isotherms observed in the low concentration range. Third, as discussed in Yang and Xing[7], two assumptions behind the use of the DAM may not to be fulfilled as (i) no scaling factor could be derived to obtain a single correlation curve for molecules expected to sorb according to similar mechanisms[10], and (ii) it is possible that the adsorbed phase may be different from the corresponding bulk phase. In addition, Polanyi theory-based models did not adequately describe competitive sorption of PAHs to CNTs.[11] Fourth, in the perspective of developing predictive approaches, models that do not include solubility (i.e., all models tested except DAM and BETM) may be preferred as solubility data are not always available and are often associated with large uncertainties.

The DMM describes sorption to matrices that are structurally heterogeneous and in which partitioning dominates in a flexible domain (e.g., an aliphatic moiety), whereas adsorption dominates in a more rigid domain (e.g., an aromatic moiety). Competition experiments with PAHs in the high concentration range showed an enhanced isotherm linearity of the primary solute, which was explained by a DMM.[11] However, the authors calculated a decrease in the adsorption contribution at high concentration, which does not support a DMM (adsorption should reach a maximum value and remain constant with increasing concentration). On the other hand, partitioning should continue once the adsorption domain has reached saturation, which was not observed here or in previous studies focussing on the high concentration range. Finally, crystalline and graphitic carbon dominates in CNTs and the existence of a flexible domain in the pretreated CNTs is unlikely. Hence, the DMM does not seem appropriate on a mechanistic basis.

Similarly, in spite of the fairly good isotherm fits (r^2=0.932 and 0.957 for Phen and Pyr, respectively), the BETM is most likely inadequate. The model describes a multilayer deposition process, where the lower part of the isotherm corresponds to the formation of a monolayer, followed by condensation to a multilayer at higher concentration. Although the formation of multilayers on CNTs has been suggested to occur at high concentration, the observations leading to this suggestion only applied to systems containing several solutes.[11] Condensation at concentrations close to the solubility limit should also result in an increase in sorption in the high concentration range, which was not observed here or in previous studies.

***Figure 3.6**. Isotherms of sorption of phenanthrene to CNTs fit by six commonly-used sorption models with corresponding coefficients of determination (r^2) and mean weighted square errors (MWSE).*

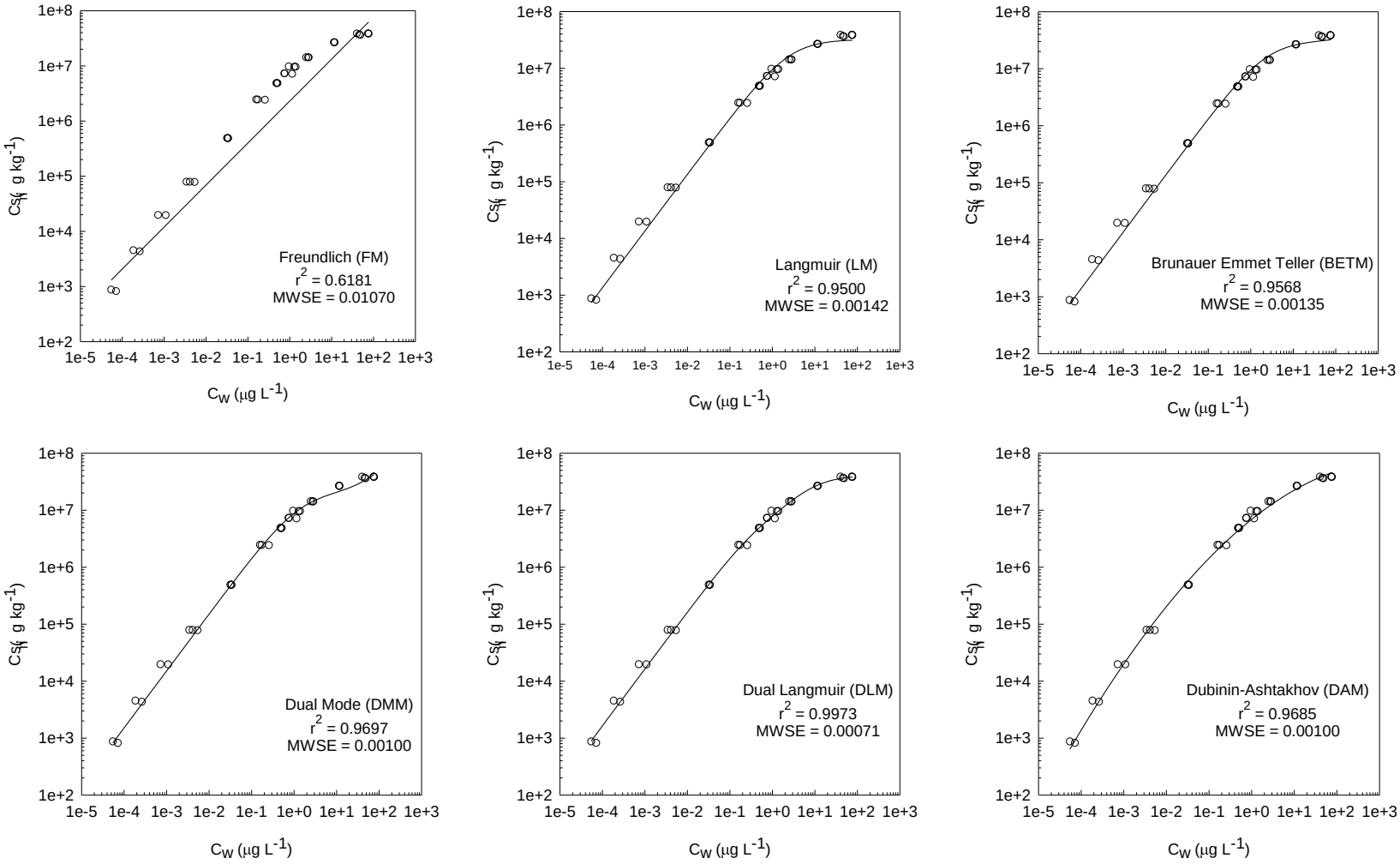

***Figure 3.7**. Isotherms of sorption of pyrene to CNTs fit by six commonly-used sorption models with corresponding coefficients of determination (r^2) and mean weighted square errors (MWSE).*

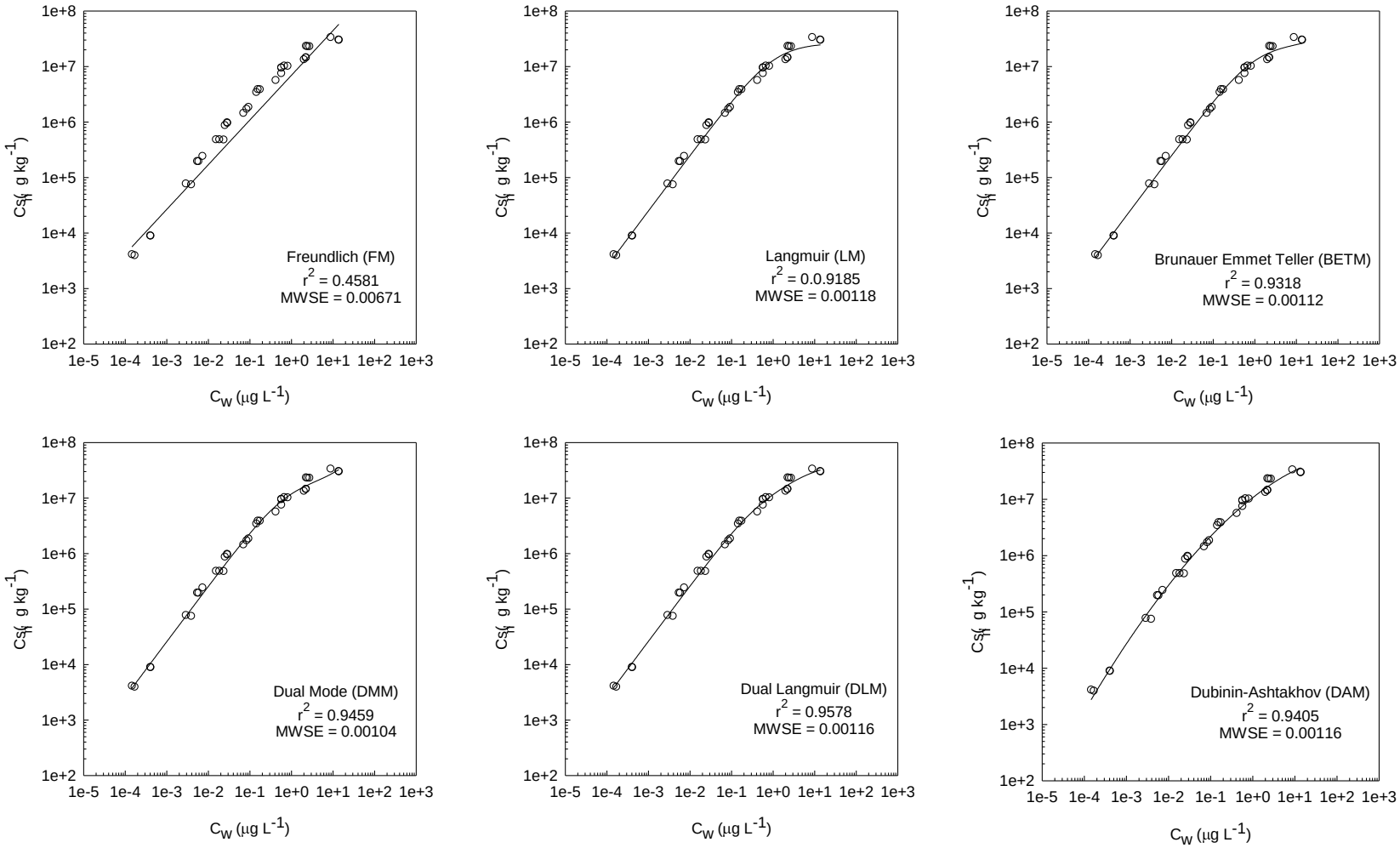

***Table 3.4**. Probability and evidence ratio for each pair of models compared, based on Akaike's Information Criterion.*

Probability for phenanthrene

	FM	LM	BETM	DM	DLM	DAM
FM	0.50	1.00	1.00	1.00	1.00	1.00
LM		0.50	0.70	1.00	1.00	1.00
BETM			0.50	0.99	1.00	0.99
DM				0.50	1.00	0.50
DLM					0.50	0.00
DAM						0.50

Evidence ratio for phenanthrene

	FM	LM	BETM	DM	DLM	DAM
FM	1	7.E+15	2.E+16	2.E+18	4.E+20	2.E+18
LM		1	2	282	65978	278
BETM			1	122	28520	120
DM				1	234	1
DLM					1	0
DAM						1

Probability for pyrene

	FM	LM	BETM	DM	DLM	DAM
FM	0.50	1.00	1.00	1.00	1.00	1.00
LM		0.50	0.72	0.84	0.73	0.38
BETM			0.50	0.66	0.51	0.19
DM				0.50	0.35	0.11
DLM					0.50	0.18
DAM						0.50

Evidence ratio for pyrene

	FM	LM	BETM	DM	DLM	DAM
FM	1	4.E+13	1.E+14	2.E+14	1.E+14	2.E+13
LM		1	3	5	3	1
BETM			1	2	1	0
DM				1	1	0
DLM					1	0
DAM						1

Isotherm curvature is generally attributed to (i) the solubility limit being reached (which is unlikely in the present study) or (ii) saturation of the surface or adsorption sites. The theoretical maximum sorption capacity (i.e., the number of sorption sites) can be estimated based on the PAHs' molecular area (199.4 and 213.5 $Å^2$ for Phen and Pyr, respectively[21]), the surface area of the CNTs (200–500 m^2/g, as provided by the supplier), and assuming flat surface sorption. Interestingly, the theoretical values (i.e., 2.97–7.42 and 3.15–7.86E+07

µg/kg for Phen and Pyr, respectively) are in the same order of magnitude as the sorption capacities calculated by the five models tested (Table 3.3). This also applied when examining sorption isotherms to other CNTs reported in the literature for Phen and Pyr.[10, 22] These observations, together with the best isotherm fit by the DLM, support the formation of a monolayer of PAHs at the surface of the CNTs until saturation occurs, similarly to what was suggested for activated carbon.[17] Good fit by the DLM does not prove the existence of two singular types of sorption sites. Equilibrium constants may also be interpreted as a bimodal distribution of sorption energies, which could represent different accessibilities of sorption sites located in loose and more condensed structures of the CNTs aggregates (as shown on electron microscope images in Figures 3.3, 3.4 and 3.5).The present results demonstrate the importance of investigating wide concentration ranges when interpreting isotherm fits. Maximum sorption capacities of CNTs can be derived from the high range and are of particular interest in situations where the sorption capacity may be reached (i.e., for sorbent applications). On the other hand, results in the low concentration range are representative of sorption behavior under environmentally-relevant conditions. The latter provides (i) the maximum sorption affinity (studies performed at higher concentration may underestimate sorption affinity occurring at low concentration) and indicate, if it exists, (ii) the concentration range where sorption is linear and can be described using a single sorption coefficient.

3.4.4 Sorption of 13 PAHs to CNTs

Chemicals exist concurrently in the environment and competition phenomena are thus key issues to consider. Significant competition between naphthalene, Phen, and Pyr for sorption sites on CNTs was observed previously in the high concentration range.[11] Yang et al.[11] determined sorption isotherms of a primary solute over two to three orders of magnitude up to the solubility limit and in the presence of extremely high concentrations of competing solutes (equilibrium concentration reaching the solubility limit). The authors proposed that the surface of CNTs was oversaturated and that the formation of multilayers occurred. In the present study, we compared sorption coefficients measured for Phen and Pyr spiked (i) individually and (ii) together with 12 other PAHs at concentrations in the ng/L range. Sorption coefficients measured by the single and multiple solute set ups were statistically identical (see triangles in Figure 3.2), indicating that competition phenomena between PAHs do not occur in the low concentration range. The theoretical surface saturation ranged from 4 to 10 % for the sum of 13 PAHs.

***Table 3.5**. Sorption coefficients of 13 PAHs to CNTs measured in the low concentration range, together with the standard deviation (Stdev), the number of points (N), octanol-water partitioning coefficient (log K_{OW}), polarizability, and solubility of the subcooled liquid (logSi). C_w gives the range of equilibrium aqueous concentrations investigated.*

	C_w (ng/L)	logK_{CNT}	Stdev; N	log*K*ow Literature[b]	log*K*ow EPI[c]	log*K*ow SPARC[d]	Polarizability[e] (cm^3)	logSi[f]
Phen [a]	20-30	7.17	(0.02; 4)	4.57	4.35	4.74	2.46E-23	-1.64
Antr	1-20	7.36	(0.07; 9)	4.68	4.35	4.69	2.46E-23	-1.67
Flu	2.5-16	7.56	(0.06; 6)	5.16	4.93	5.29	2.87E-23	-2.30
Pyr	2-10	7.58	(0.08; 6)	5.22	5.54	5.25	2.87E-23	-2.35
BaA	0.2-6	7.82	(0.12; 9)	5.91	5.52	5.85	3.16E-23	-3.21
Chr	0.2-6.5	7.73	(0.11; 9)	5.81	5.52	5.90	3.16E-23	-3.39
BeP	0.1-0.7	8.00	(0.10; 6)	6.44	6.11	6.59	3.58E-23	-3.67
BbF	0.1-0.6	8.00	(0.10; 6)	6.20	6.11	6.58	3.58E-23	-4.13
BkF	0.1-0.6	8.05	(0.09; 6)	6.20	6.11	6.50	3.58E-23	-3.86
BaP	0.1-0.6	8.10	(0.09; 6)	6.20	6.11	6.54	3.58E-23	-4.21
BghiPe	0.1-0.5	8.10	(0.09; 6)	6.90	6.70	7.04	4.00E-23	-4.22
dBahAntr	0.1-0.5	8.01	(0.09; 6)	7.00	6.70	7.39	3.87E-23	-3.70
InP	0.07-0.4	8.14	(0.08; 6)	7.00	6.70	7.09	4.00E-23	-4.88

[a] Explanation of abbreviations: Phen: Phenanthrene, Antr: Antracene, Flu: Fluoranthene; Pyr: Pyrene; BaA: Benz[*a*]anthracene; Chr: Chrysene; BeP: Benzo[*e*]pyrene; BbF: Benzo[*b*]fluoranthene; BkF: Benzo[*k*]fluoranthene; BaP: Benzo[*a*]pyrene; BghiPe: Benzo[*g,h,i*]perylene; dBahAntr: Dibenz[*a,h*]anthracene; InP: Indeno[1,2,3-*c,d*]pyrene.
[b] Taken from Jonker & Van der Heijden[16]
[c] Derived by EPI Suite[23]
[d] Derived by SPARC[24]
[e] Predicted by ACD Lab prediction software and available in the Chemspider database[25]
[f] Taken from Van Noort[26]. Value for InP was not available and was taken from Ma et al.[27]

For most of the 13 PAHs investigated, sorption coefficients were measured at two or three concentrations within the range investigated and the results turned out to be similar (range available in Table 3.5, p>0.05). The following analysis was therefore based on single, averaged sorption coefficients that can be considered as the maximum sorption affinity of the CNTs studied (K_{CNT} in L/kg; average of the concentrations investigated). These averaged values are presented in Table 3.5 and indicate that sorption of PAHs to CNTs is considerably weaker (1.4–1.8 log units) than to activated carbon (data measured by the same POM-SPE approach[28]). Even though sorption coefficients normalized to the specific surface area are slightly higher for the CNTs, the benefit of using CNTs instead of activated carbon as superior sorbent for organic contaminants such as PAHs is therefore questionable, especially considering the cost of production and the potential toxicity of the material.

***Figure 3.8**. Correlation matrix between sorption coefficients of 13 PAHs on CNTs (log K_{CNT}) and PAH molecular properties. The three values presented for each pair of variables are the correlation coefficient (r), the p value, and the number of points (N), respectively.*

		log K_{CNT}			(a) MW		
		r	*p*	N	*r*	*p*	N
(a)	MW	0.947	9.23e-07	13	-	-	-
	Molec. Vol.	0.922	2.05e-05	12	0.982	1.31e-08	12
	Total surf.area	0.873	2.08e-04	12	0.961	6.49e-07	12
(b)	Log K_{OW} literature	0.941	1.62e-06	13	0.985	1.09e-09	13
(c)	Log K_{OW} EPI	0.945	1.14e-06	13	0.975	1.64e-08	13
(d)	Log K_{OW} SPARC	0.940	1.80e-06	13	0.990	1.36e-10	13
(e)	Log Si	-0.964	1.08e-07	13	-0.946	9.79e-07	13
(f)	Molar refraction	0.912	1.41e-05	13	0.941	1.59e-06	13
	Molar volume	0.940	1.85e-06	13	0.988	2.29e-10	13
	Edonor	0.865	1.34e-04	13	0.887	5.29e-05	13
	Polarizability	0.943	1.38e-06	13	0.903	2.31e-05	13
(g)	Log P hexade c./w	0.859	1.71e-04	13	0.960	2.02e-07	13
	Log P alkane/w.	0.861	1.55e-04	13	0.957	2.94e-07	13
	Log P cyclohex./w.	0.880	7.40e-05	13	0.967	7.51e-08	13
(h)	Polarizability	0.960	2.05e-07	13	0.991	6.97e-11	13
(i)	EHOMO	0.420	1.74e-01	12	0.339	2.82e-01	12
	ELUMO	-0.657	2.03e-02	12	-0.515	8.69e-02	12
	TE	-0.956	1.14e-06	12	-1.000	8.48e-20	12
	μ	0.399	1.98e-01	12	0.356	2.56e-01	12
	QH+	0.458	1.34e-01	12	0.515	8.67e-02	12
	QC-	-0.558	5.92e-02	12	-0.470	1.23e-01	12
	LCC	0.397	2.01e-01	12	0.447	1.46e-01	12
	Re	0.849	4.76e-04	12	0.926	1.59e-05	12
		(a) Molec. Vol.			(a) Total surf.area		
		r	*p*	N	*r*	*p*	N
(a)	Total surf.area	0.956	1.12e-06	12	-	-	-
(b)	Log K_{OW} literature	0.979	3.11e-08	12	0.913	3.43e-05	12
(c)	Log K_{OW} EPI	0.946	3.23e-06	12	0.898	7.40e-0.5	12
(d)	Log K_{OW} SPARC	0.988	1.56e-09	12	0.932	1.01e-05	12
(e)	Log Si	-0.924	1.73e-05	12	-0.880	1.57e-04	12
(f)	Molar refraction	0.924	1.72e-05	12	0.846	5.23e-04	12
	Molar volume	0.996	7.42e-12	12	0.945	3.69e-06	12
	Edonor	0.896	7.95e-05	12	0.822	1.04e-03	12
	Polarizability	0.916	2.85e-05	12	0.832	7.96e-04	12
(g)	Log P hexade c./w	0.947	3.15e-06	12	0.915	3.01e-05	12
	Log P alkane/w.	0.942	4.80e-06	12	0.913	3.38e-05	12
	Log P cyclohex./w.	0.953	1.72e-06	11	0.917	2.69e-05	11
(h)	Polarizability	0.967	3.05e-07	11	0.915	2.97e-05	11
(i)	EHOMO	0.261	4.38e-01	11	0.266	4.29e-01	11
	ELUMO	-0.341	3.05e-01	11	-0.392	2.33e-01	11
	TE	-0.982	7.30e-08	11	-0.982	8.05e-08	11
	μ	0.140	6.82e-01	11	0.185	5.87e-01	11
	QH+	0.667	2.49e-02	11	0.656	2.84e-02	11
	QC-	-0.454	1.61e-01	11	-0.486	1.29e-01	11

	LCC	0.379	2.50e-01	11	0.412	2.08e-01	11
	Re	0.969	8.83e-07	11	0.969	9.69e-07	11
		(b) Log K_{OW} literature			(c) Log K_{OW} EPI		
		r	*p*	N	*r*	*p*	N
(c)	Log K_{OW} EPI	0.975	1.54e-08	13	-	-	-
(d)	Log K_{OW} SPARC	0.989	1.65e-10	13	0.972	2.71e-08	13
(e)	Log Si	-0.930	4.03e-06	13	-0.925	5.88e-06	13
(f)	Molar refraction	0.959	2.24e-07	13	0.957	2.88e-07	13
	Molar volume	0.989	2.16e-10	13	0.963	1.23e-07	13
	Edonor	0.881	6.98e-05	13	0.871	1.08e-04	13
	Polarizability	0.915	1.19e-05	13	0.944	1.24e-06	13
(g)	Log P hexade c./w	0.967	7.52e-08	13	0.920	8.68e-06	13
	Log P alkane/w.	0.965	1.01e-07	13	0.917	9.99e-06	13
	Log P cyclohex./w.	0.975	1.61e-08	13	0.933	3.26e-06	13
(h)	Polarizability	0.988	2.71e-10	12	0.982	2.60e-09	13
(i)	EHOMO	0.365	2.44e-01	12	0.378	2.25e-01	12
	ELUMO	-0.513	8.83e-02	12	-0.515	8.65e-02	12
	TE	-0.994	8.45e-11	12	-0.980	2.66e-08	12
	μ	0.343	2.75e-01	12	0.328	2.98e-01	12
	QH+	0.485	1.10e-01	12	0.395	2.04e-01	12
	QC-	-0.468	1.25e-01	12	-0.421	1.72e-01	12
	LCC	0.437	1.55e-01	12	0.353	2.61e-01	12
	Re	0.927	1.47e-05	12	0.879	1.68e-04	12
		(d) Log K_{OW} SPARC			(e) Log Si		
		r	*p*	N	*r*	*p*	N
(e)	Log Si	-0.928	4.74e-06	13	-	-	-
(f)	Molar refraction	0.953	4.73e-07	13	-0.869	1.13e-04	13
	Molar volume	0.995	2.35e-12	13	-0.928	4.87e-06	13
	Edonor	0.902	2.44e-05	13	-0.874	9.31e-05	13
	Polarizability	0.925	6.00e-06	13	-0.875	8.92e-05	13
(g)	Log P hexade c./w	0.957	2.85e-07	13	-0.854	2.02e-04	13
	Log P alkane/w.	0.953	5.03e-07	13	-0.852	2.20e-04	13
	Log P cyclohex./w.	0.965	1.05e-07	13	-0.867	1.26e-04	13
(h)	Polarizability	0.988	2.48e-10	13	-0.954	4.32e-07	13
(i)	EHOMO	0.312	3.24e-01	12	-0.325	3.02e-01	12
	ELUMO	-0.488	1.07e-01	12	0.592	4.24e-02	12
	TE	-0.996	1.31e-11	12	0.949	2.45e-06	12
	μ	0.341	2.79e-01	12	-0.483	1.11e-01	12
	QH+	0.533	7.46e-02	12	-0.484	1.10e-01	12
	QC-	-0.484	1.11e-01	12	0.497	1.01e-01	12
	LCC	0.437	1.55e-01	12	-0.434	1.59e-01	12
	Re	0.945	3.68e-06	12	-0.821	1.05e-03	12
		(e) Molar refraction			(f) Molar volume		
		r	*p*	N	*r*	*p*	N
(f)	Molar volume	0.952	5.46e-07	13	-	-	-
	Edonor	0.888	5.16e-05	13	0.909	1.67e-05	13
	Polarizability	0.932	3.67e-06	13	0.923	7.09e-06	13
(g)	Log P hexade c./w	0.924	6.24e-06	13	0.961	1.83e-07	13
	Log P alkane/w.	0.922	7.21e-06	13	0.957	3.14e-07	13
	Log P cyclohex./w.	0.941	1.64e-06	13	0.968	5.92e-08	13
(h)	Polarizability	0.949	7.42e-07	13	0.979	5.82e-09	13
(i)	EHOMO	0.582	8.15e-02	12	0.333	2.89e-01	12

	ELUMO	-0.436	1.57e-01	12	-0.454	1.38e-01	12
	TE	-0.957	1.12e-06	12	-0.991	3.54e-10	12
	μ	0.115	7.21e-01	12	0.295	3.51e-01	12
	QH+	0.412	1.83e-01	12	0.561	5.77e-02	12
	QC-	-0.438	1.54e-01	12	-0.496	1.01e-01	12
	LCC	0.212	1.08e-01	12	0.421	1.73e-01	12
	Re	0.875	1.97e-04	12	0.959	9.03e-07	12
		(f) Edonor			(f) Polarizability		
		r	*p*	N	*r*	*p*	N
(f)	Polarizability	0.840	3.22e-04	13	-	-	-
(g)	Log P hexade c./w	0.796	1.14e-03	13	0.832	4.25 e-04	13
	Log P alkane/w.	0.782	1.58e-03	13	0.831	4.34e-04	13
	Log P cyclohex./w.	0.810	7.94e-04	13	0.854	2.00e-04	13
(h)	Polarizability	0.886	5.44e-05	13	0.917	1.03e-05	13
(i)	EHOMO	0.426	1.67e-01	12	0.416	1.79e-01	12
	ELUMO	-0.324	3.04e-01	12	-0.493	1.03e-01	12
	TE	-0.898	7.15e-05	12	-0.931	1.11e-05	12
	μ	0.187	5.61e-01	12	0.218	4.96e-01	12
	QH+	0.427	1.67e-01	12	0.455	1.38e-01	12
	QC-	-0.539	7.05e-02	12	-0.479	1.15e-01	12
	LCC	0.255	4.24e-01	12	0.223	4.86e-01	12
	Re	0.864	2.95e-04	12	0.875	1.94e-04	12
		(g) Log P hexade c./w			(g) Log P alkane/w.		
		r	*p*	N	*r*	*p*	N
(g)	Log P alkane/w.	0.999	1.68e-16	13	-	-	-
	Log P cyclohex./w.	0.998	8.87e-15	13	0.999	2.87e-15	13
(h)	Polarizability	0.944	1.24e-06	13	0.941	1.64e-06	13
(i)	EHOMO	0.301	3.44e-01	12	0.310	3.27e-01	12
	ELUMO	-0.426	1.67e-01	12	-0.450	1.42e-01	12
	TE	-0.959	8.95e-07	12	-0.956	1.24e-06	12
	μ	0.264	4.07e-01	12	0.267	4.02e-01	12
	QH+	0.556	5.52e-02	12	0.553	6.24e-02	12
	QC-	-0.394	2.05e-01	12	-0.399	1.99e-01	12
	LCC	0.466	1.33e-01	12	0.459	1.34e-01	12
	Re	0.916	2.84e-05	12	0.912	3.59e-05	12
		(g) Log P cyclohex./w.			(h) Polarizability		
		r	*p*	N	*r*	*p*	N
(h)	Polarizability	0.953	4.68e-07	13	-	-	-
(i)	EHOMO	0.336	2.86e-01	12	0.339	2.81e-01	12
	ELUMO	-0.452	1.40e-01	12	-0.557	6.01e-02	12
	TE	-0.966	3.52e-07	12	-0.997	1.54e-12	12
	μ	0.255	4.24e-01	12	0.400	1.97e-01	12
	QH+	0.543	6.80e-02	12	0.474	1.19e-01	12
	QC-	-0.413	1.82e-01	12	-0.445	1.47e-01	12
	LCC	0.435	1.58e-01	12	0.462	1.30e-01	12
	Re	0.918	2.48e-05	12	0.892	9.82e-05	12
		(i) EHOMO			(i) ELUMO		
		r	*p*	N	*r*	*p*	N
(i)	ELUMO	-0.331	2.94e-01	12	-	-	-
	TE	-0.339	2.81e-01	12	0.521	8.21e-01	12
	μ	-0.320	3.11e-01	12	-0.674	1.63e-02	12
	QH+	-0.267	4.02e-01	12	0.636	9.12e-01	12
	QC-	-0.466	1.27e-01	12	0.572	5.20e-02	12

	LCC	-0.439	1.53e-01	12	-0.413	1.82e-01	12
	Re	0.282	3.75e-01	12	-0.365	2.43e-01	12
		(i) TE			(i) μ		
		r	*p*	N	*r*	*p*	N
(i)	μ	-0.363	2.46e-01	12	-	-	-
	QH+	-0.509	9.12e-02	12	0.117	7.17e-01	12
	QC-	0.466	1.27e-01	12	-0.240	4.52e-01	12
	LCC	-0.449	1.43e-01	12	0.750	5.01e-03	12
	Re	-0.921	2.16e-05	12	0.234	4.64e-01	12
		(i) QH+			(i) QC-		
		r	*p*	N	*r*	*p*	N
(i)	QC-	-0.196	5.41e-01	12	-	-	-
	LCC	0.482	1.12e-01	12	-0.087	7.87e-01	12
	Re	0.578	4.91e-02	12	-0.573	5.17e-02	12
		(i) LCC					
		r	*p*	N			
(i)	Re	0.395	2.04e-01	12	-	-	-

(a) Molecular weight, volume and surface area taken from Mackay[21]
(b) Log K_{OW} collected from the literature[16]
(c) Log K_{OW} derived by EPI Suite[23]
(d) Log K_{OW} derived by SPARC[24]
(e) Solubility of the subcooled liquid[26]; Value for InP was not available and was taken from Ma et al.[27]
(f) Linear free energy relationship parameters[30] (excess molar refraction, molar volume, electron donor capability, polarizability)
(g) Hexadecane, alkane, and cyclohexane-water partitioning coefficients[31]
(h) Polarizability predicted by ACD Lab prediction software and available in the Chemspider database[25]
(i) Quantum chemical descriptors[32]: eigenvalues of the highest occupied and lowest unoccupied molecular orbital (EHOMO and ELUMO), molecular total energy (TE), dipole moment (μ), the most negative Mulliken atomic charges on a carbon atom (QC−), the most positive Mulliken atomic charges on a hydrogen atom (QH+), the largest bond length between two aromatic carbon atoms (LCC), and the electronic spatial extent (Re).

To date, sorption from the aqueous phase to CNTs was only reported for three low molecular weight PAHs. The present data set provides the opportunity to study in more detail how sorption affinity is influenced by PAHs properties. To this end, a series of molecular descriptors was collected for the 13 PAHs studied. These included several estimates of hydrophobicity, solubilities of the subcooled liquid, solvent-water partitioning coefficients, molecular surfaces, linear free energy relationship parameters, and quantum chemical descriptors. A correlation matrix was built to identify which parameters explained best the variation amongst PAHs (Figure 3.8). All molecular descriptors were significantly correlated with K_{CNT}. Exceptions were the quantum chemistry parameters: only two out of eight significantly correlated with K_{CNT} (molecular total energy and electronic spatial extent). Overall, the highest correlation coefficients were calculated for the solubility of the subcooled liquid[26, 27] and polarizability[25] followed by molecular weight and log K_{OW} as estimated by

Figure 3.9. *Relationships between CNT-water distribution coefficients (log K_{CNT}) in the low concentration range and molecular properties of 13 PAHs, being (a) solubility of the subcooled liquid (Si)*[26, 27]*; (b); polarizability*[25]*, and (c) log K_{OW} values collected from the literature*[16] *and derived by SPARC*[24] *and EPI Suite.*[23]

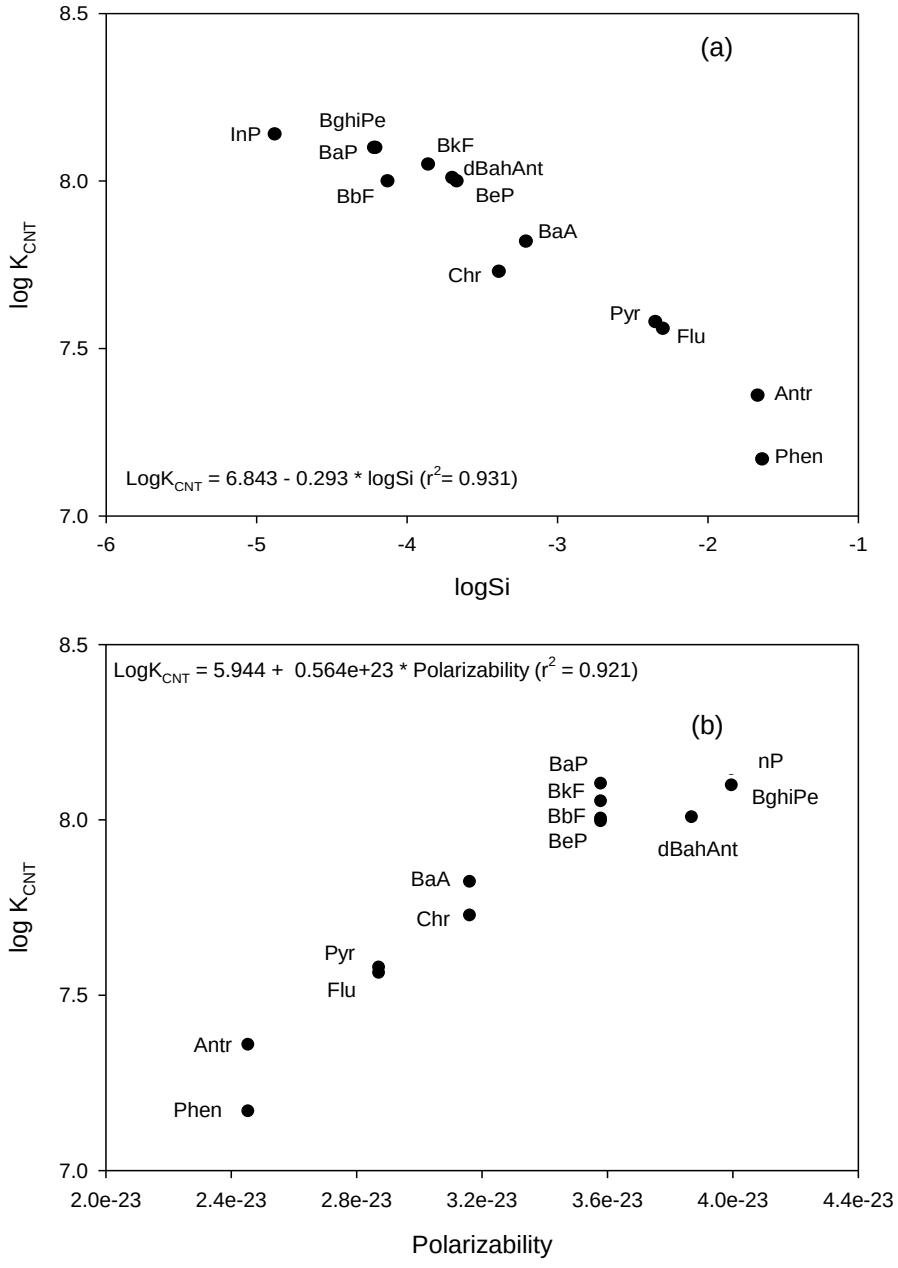

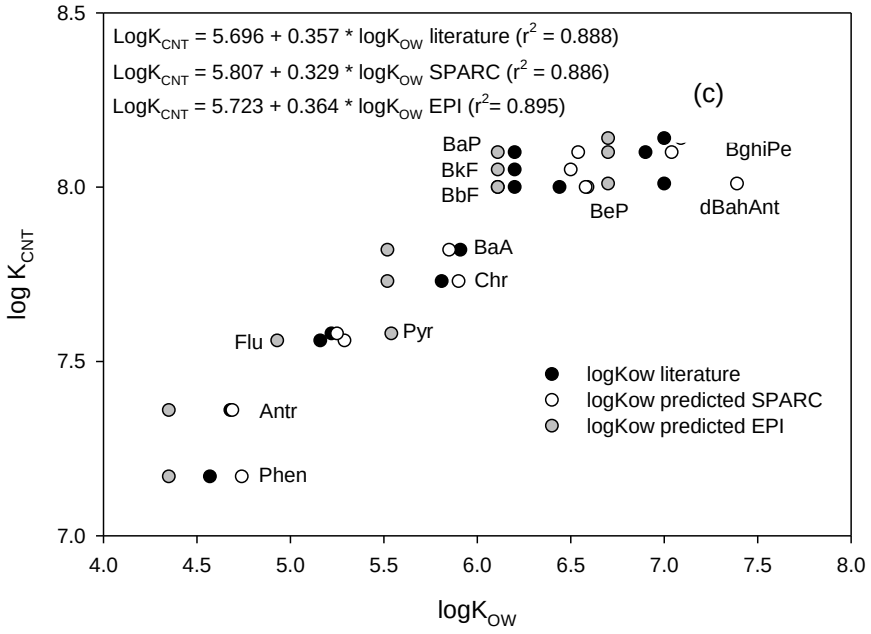

EPISuite[23] (Figure 3.9). Relationships between log K_{OW} and sorption coefficients for sediments and soils generally have slopes close to 1 (e.g.,[29]), whereas the slope observed for sorption to CNT was much lower (i.e., 0.3). Hence, an increase in hydrophobicity of almost three orders of magnitude resulted in merely one order of magnitude increase in sorption to CNTs. A similar effect was observed previously for charcoal.[28]

It has been reported that PAHs sorb to CNTs by a combination of hydrophobic and π–π interactions.[7] The ratio K_{CNT}/K_{OW} may be useful to estimate that part of sorption that is not due to hydrophobic interactions. Phen was previously shown to have greater K_{CNT}/K_{OW} values than naphthalene.[22] This was explained by the higher polarizability of Phen, which would allow stronger π–π interactions with the highly polarizable graphene sheets of CNTs. In the same study, K_{CNT}/K_{OW} was also positively related to molecular size, suggesting that micropore-filling was not a dominant mode of sorption on the CNTs studied. Interestingly, the opposite relationships were observed with the present dataset of 13 PAHs in the low concentration range. K_{CNT}/K_{OW} negatively correlated with steric hindrance parameters (molecular weight and volume, $p<0.001$) and polarizability ($p<0.001$). These relationships could indicate (i) a possible molecular sieving effect, and (ii) that the stronger sorption of PAHs with more benzene rings cannot be explained by stronger π–π interactions. It is important to note however that correlations between K_{CNT}/K_{OW} and molecular descriptors must be interpreted cautiously since most parameters significantly correlated with K_{OW}.

Differences in the subcooled liquid solubility, polarizability or hydrophobicity cannot explain the stronger sorption of anthracene and benz[*a*]anthracene as compared to Phen and chrysene, respectively. Although having the same number of benzene rings, the more linear compounds apparently adsorbed significantly better to CNTs ($p<0.001$). This may be explained by the nanoscale curvature of the tube surface, which may result in a better contact of more linear molecules, as previously suggested in Gotovac et al.[30]

It was not possible to test the predictive power of the regression equations from Figure 3.9 on published data, as (i) K_{CNT} values from the literature were generally measured at much higher concentrations and therefore may not represent the maximum sorption affinity evaluated here, and (ii) additional parameter(s) are required to account for differences among different CNTs. Further experimental data are hence necessary to determine whether properties of the carbon nanomaterial (e.g., surface area, aggregation status) can be integrated in a predictive equation.

3.5 Literature Cited

(1) Pan, B.; Xing, B. S. Adsorption mechanisms of organic chemicals on carbon nanotubes. *Environ. Sci. Technol* **2008**, *42*, (24), 9005-9013.

(2) Mauter, M. S.; Elimelech, M. Environmental applications of carbon-based nanomaterials. *Environ. Sci. Technol.* **2008**, *42*, (16), 5843-5859.

(3) Cai, Y. Q.; Jiang, G. B.; Liu, J. F.; Zhou, Q. X. Multi-walled carbon nanotubes packed cartridge for the solid-phase extraction of several phthalate esters from water samples and their determination by high performance liquid chromatography. *Anal. Chim. Acta* **2003**, *494*, (1-2), 149-156.

(4) Wu, H.; Wang, X. C.; Liu, B.; Lu, J.; Du, B. X.; Zhang, L. X.; Ji, J. J.; Yue, Q. Y.; Han, B. P. Flow injection solid-phase extraction using multi-walled carbon nanotubes packed micro-column for the determination of polycyclic aromatic hydrocarbons in water by gas chromatography-mass spectrometry. *J. Chromatography A* **2010**, *1217*, (17), 2911-2917.

(5) Ma, J. P.; Xiao, R. H.; Li, J. H.; Yu, J. B.; Zhang, Y. Q.; Chen, L. X. Determination of 16 polycyclic aromatic hydrocarbons in environmental water samples by solid-phase extraction using multi-walled carbon nanotubes as adsorbent coupled with gas chromatography-mass spectrometry. *J. Chromatography A* **2010**, *1217*, (34), 5462-5469.

(6) Hofmann, T.; von der Kammer, F. Estimating the relevance of engineered carbonaceous nanoparticle facilitated transport of hydrophobic organic contaminants in porous media. *Environ. Pollut.* **2009**, *157*, (4), 1117-1126.

(7) Yang, K.; Xing, B. S. Adsorption of organic compounds by carbon nanomaterials in aqueous phase: Polanyi theory and its application. *Chem. Rev.* **2010**, *110*, (10), 5989-6008.

(8) Hyung, H.; Kim, J. H. Natural organic matter (NOM) adsorption to multi-walled carbon nanotubes: Effect of NOM characteristics and water quality parameters. *Environ. Sci. Technol.* **2008**, *42*, (12), 4416-4421.

(9) Lin, D. H.; Liu, N.; Yang, K.; Xing, B. S.; Wu, F. C. Different stabilities of multiwalled carbon nanotubes in fresh surface water samples. *Environ. Pollut.* **2010**, *158*, (5), 1270-1274.

(10) Yang, K.; Zhu, L. Z.; Xing, B. S. Adsorption of polycyclic aromatic hydrocarbons by carbon nanomaterials. *Environ. Sci. Technol.* **2006**, *40*, (6), 1855-1861.

(11) Yang, K.; Wang, X. L.; Zhu, L. Z.; Xing, B. S. Competitive sorption of pyrene, phenanthrene, and naphthalene on multiwalled carbon nanotubes. *Environ. Sci. Technol.* **2006**, *40*, (18), 5804-5810.

(12) Jonker, M. T. O.; Koelmans, A. A. Polyoxymethylene solid phase extraction as a partitioning method for hydrophobic organic chemicals in sediment and soot. *Environ. Sci. Technol.* **2001**, *35*, (18), 3742-3748.

(13) Chen, W.; Duan, L.; Zhu, D. Q. Adsorption of polar and nonpolar organic chemicals to carbon nanotubes. *Environ. Sci. Technol.* **2007**, *41*, (24), 8295-8300.

(14) Su, S. H.; Chiang, W. T.; Lin, C. C.; Yokoyama, M. Multi-wall carbon nanotubes: Purification, morphology and field emission performance. *Physica E* **2008**, *40*, (7), 2322-2326.

(15) Lin, D. H.; Xing, B. S. Adsorption of phenolic compounds by carbon nanotubes: Role of aromaticity and substitution of hydroxyl groups. *Environ. Sci. Technol.* **2008**, *42*, (19), 7254-7259.

(16) Jonker, M. T. O.; van der Heijden, S. A. Bioconcentration factor hydrophobicity cutoff: An artificial phenomenon reconstructed. *Environ. Sci. Technol.* **2007**, *41*, 7363-7369.

(17) Pikaar, I.; Koelmans, A. A.; van Noort, P. C. M. Sorption of organic compounds to activated carbons. Evaluation of isotherm models. *Chemosphere* **2006**, *65*, (11), 2343-2351.

(18) Jantunen, A. P. K.; Koelmans, A. A.; Jonker, M. T. O. Modeling polychlorinated biphenyl sorption isotherms for soot and coal. *Environ. Pollut.* **2010**, *158*, (8), 2672-2678.

(19) Allen-King, R. M.; Grathwohl, P.; Ball, W. P. New modeling paradigms for the sorption of hydrophobic organic chemicals to heterogeneous carbonaceous matter in soils, sediments, and rocks. *Advances in Water Resources* **2002**, *25*, (8-12), 985-1016.

(20) Burnham, K. P.; Anderson, D. R., *Model Selection and Multimodel Inference: A Practical Information-Theoretic Approach*. 2nd ed.; Springer-Verlag: 2002.

(21) Mackay, D.; Shiu, W. Y.; Ma, K. C., *Illustrated Handbook Of Physical-Chemical Properties And Environmental Fate For Organic Chemicals. Vol. I and II.* Lewis Publishers, Boca Raton, Ann Arbor, London, Tokyo: 1992.

(22) Wang, X. L.; Tao, S.; Xing, B. S. Sorption and competition of aromatic compounds and humic acid on multiwalled carbon nanotubes. *Environ Sci Technol* **2009**, *43*, (16), 6214-6219.

(23) US-EPA EPI Suite Package. Estimation Program Interface from the U.S. Environmental Protection Agency. Available at http://www.epa.gov/oppt/exposure/pubs/episuitedl.htm. Last accessed Nov. 2010. **2000**.

(24) Yang, W. C.; Mang, J.; Zhang, C. D.; Zhu, L. Y.; Chen, W. Sorption and resistant desorption of atrazine in typical chinese soils. *J. Environ.l Qual.* **2009**, *38*, (1), 171-179.

(25) Yu, S. M.; Chen, C. L.; Chang, P. P.; Wang, T. T.; Lu, S. S.; Wang, X. K. Adsorption of Th(IV) onto Al-pillared rectorite: Effect of pH, ionic strength, temperature, soil humic acid and fulvic acid. *Appl Clay Sci* **2008**, *38*, (3-4), 219-226.

(26) van Noort, P. C. M. Estimation of amorphous organic carbon/water partition coefficients, subcooled aqueous solubilities, and n-octanol/water distribution coefficients of alkylbenzenes and polycyclic aromatic hydrocarbons. *Chemosphere* **2009**, *74*, (8), 1018-1023.

(27) Ma, Y. G.; Lei, Y. D.; Xiao, H.; Wania, F.; Wang, W. H. Critical review and recommended values for the physical-chemical property data of 15 polycyclic aromatic hydrocarbons at 25 degrees C. *J. Chem. Engin. Data* **2010**, *55*, (2), 819-825.

(28) Jonker, M. T. O.; Koelmans, A. A. Sorption of polycyclic aromatic hydrocarbons and polychlorinated biphenyls to soot and soot-like materials in the aqueous environment mechanistic considerations. *Environ. Sci. Technol.* **2002**, *36*, (17), 3725-3734.

(29) Schwarzenbach, R. P.; Gshwend, P. M.; Imboden, D. M., *Environmental organic chemistry. 3rd, ed.* . John Wiley & Sons: Hoboken, U.S.: 2003.

(30) Gotovac, S.; Honda, H.; Hattori, Y.; Takahashi, K.; Kanoh, H.; Kaneko, K. Effect of nanoscale curvature of single-walled carbon nanotubes on adsorption of polycyclic aromatic hydrocarbons. *Nano Lett.* **2007**, *7*, (3), 583-587.

4. Influence of Dispersion State

Dispersion State and Humic Acids Concentration-Dependent Sorption of Pyrene to Carbon Nanotubes

Zhang, X. R.; Kah, M.; Jonker, M. T. O.; Hofmann, T.

Environ. Sci. Technol. **2012**, *46*, (13), 7166–7173.

4.1 Abstract

Sonication and humic acids (HA) are known to disperse CNT suspensions, but potential effects on sorption of chemicals to CNTs remain poorly understood. We applied a passive sampling method to investigate the influence of dispersion/aggregation on sorption of pyrene to CNTs. Sonication broke down CNT aggregates and increased pyrene sorption affinity by up to 1.39 orders of magnitude. Sorption surfaces newly exposed by sonication remained available to pyrene even after re-aggregation occurred, suggesting an irreversible effect of sonication. The presence of HA decreased sorption of pyrene to CNTs, but at the highest HA concentration investigated (200 mg/L), sorption affinity was still 1.80 orders of magnitude larger than sorption of pyrene to HA alone. Specific interactions between pyrene and CNTs were thus still taking place, in spite of the presence of a HA coating on the CNTs' surface. A greater suppression of sorption by CNTs occurred when the HA addition was combined with a sonication pre-treatment. Sorption isotherm fitting indicated that the maximum sorption capacity, sorption affinity, and heterogeneity of the CNT surface were all affected by sonication and the presence of HA at a concentration as low as 1 mg/L. The present results contribute to an improved understanding of the sorption behavior of CNTs in both natural and waste water systems.

4.2 Introduction

Over the past decade, CNTs have gained increasing attention due to their unique properties. CNTs have a strong affinity towards organic compounds and have therefore been proposed as superior sorbents for water treatment or solid-phase extraction cartridges.[1] In addition, the production of CNTs increases rapidly and release of the particles into the environment is inevitable. There is concern that CNTs might facilitate the relocation of hydrophobic organic contaminants in the environment.[2] Both during CNT usage as sorbents and relocation of

contaminants in the environment, sorption to CNTs might be influenced by their aggregation state. Depending on the production and release routes, CNTs may be discharged as large aggregates and/or in dispersed forms.[3] After their release, interactions with substances present in the environment will further affect the dispersion status of CNTs. For instance, NOM has been shown to significantly increase the stability of CNT suspensions.[4, 5]

Potential effects of dispersion/aggregation events on sorption behavior towards organic contaminants remain poorly understood. Several researchers have reported a decrease in the sorption potential of pristine CNTs in the presence of NOM.[6-7] However, in these studies, dispersed CNTs were preliminarily excluded from the analysis by centrifugation[6, 7] or settling.[8] Existing results therefore only refer to large CNT aggregates and there is currently very limited data on the sorption potential of partially/fully dispersed CNT systems. Yet, understanding the influence of dispersion/aggregation phenomena on sorption is essential for evaluating the potential environmental impact of CNTs and their application as sorbent.

The lack of data relating to dispersed CNTs can be mainly explained by limitations associated with the generally-applied batch sorption test set ups that do not allow investigations on dispersed systems, consisting of inseparable nanoparticles. We previously validated a passive sampling method (POM-SPE) which allows studying sorption of PAHs onto both aggregated and dispersed CNTs.[9] Even though long equilibrium times are needed for POM-SPE, in the present study we applied this method to investigate the influence of dispersion on sorption behavior of CNTs. The objectives were to investigate the effects of (i) CNT pre-treatments (sonication, shaking) and (ii) natural dispersants (humic acids; HA) on the sorption characteristics of the CNT system. Sonication is an efficient method to disperse CNTs and is often applied in the presence of dispersants, such as polymers, surfactants, and HA.[10] To our knowledge, the effect of an efficient dispersion (e.g., by sonication in the presence of dispersants) on the sorption potential of CNTs has however not been investigated yet. Single point sorption coefficients and sorption isotherms for pyrene were measured over a wide range of concentrations and in the presence of HA (1–200 mg/L). CNT suspensions were extensively characterized by microscopic, spectroscopic, and size distribution measurements in order to support mechanistic interpretations of the results.

4.3 Materials and Methods

4.3.1 Sorbents and Chemicals

A POM sheet (thickness 0.5 mm; density 1.41 g/cm^3) was purchased from Vink Kunststoffen BV, Didam, The Netherlands. The POM sheet was cut into strips (1 cm × 1 cm; 1 cm × 10 cm) and cold-extracted with hexane (30 min) and methanol (3 times for 30 min) as described in Jonker and Koelmans.[11] Multiwalled CNTs were provided by Baytubes. The CNTs were purified and their properties were listed in Table 3.1 of Chapter 3.

Suwannee river HA were selected as model HA. HA standard II "2S101H" was purchased from the International Humic Substance Society. HA solutions of 1–200 mg/L were prepared in 25 mg/L NaN_3 background (as biocide). First, 300 mg HA were dissolved in 5 mL 0.1 M NaOH. The solution was then diluted with background solution to obtain a 1 g/L HA stock solution. The pH was adjusted from acidic to neutral (pH 7.06) using 0.1 M NaOH. The HA stock solution was then gradually diluted to concentrations of 1–200 mg/L (1, 5, 10, 20, 40, 100, 200 mg/L).

Table 4.1. *Properties of HA used (as provided by the suppliers).*

The elemental composition and carbon type distribution as provided by the supplier (detailed characteristic data is provided by the supplier http://www.humicsubstances.org/) are as follows:

Elemental composition (% w/w) and stable isotopic ratio

H_2O	Ash	C	H	O	N	S	P
20.4	1.04	52.63	4.28	42.04	1.17	0.54	0.013

13C NMR estimates of carbon distribution (%)

Carbonyl 220-190	ppm Carboxyl 190-165 ppm	Aromatic 165-110 ppm	Acetal 110-90 ppm	Heteroaliphatic 90-60 ppm	Aliphatic 60-0 ppm
6	15	31	7	13	29

Pyrene (99.0%) and pyrene-d10 (99.5%) were purchased from Dr. Ehrenstorfer (Germany). All stock solutions were prepared in methanol. Hexane and methanol were of residue analysis grade (Lab Scan, Dublin, Ireland and Acros Organics, Geel, Belgium).

4.3.2 Sorption Experiments

4.3.2.1 Batch setup for pyrene sorption to CNTs

All experiments were carried out at 20 ± 1 °C and using background solution prepared with 25 mg/L NaN_3 as biocide (pH 7.06). One milligram of CNTs (weighed on a Mettler Toledo MX5 micro balance) and 50.00 mL of HA solution (0–200 mg/L) were added to glass vials (diameter 2.3 cm, depth 13.8 cm). Samples (CNT concentration 20 mg/L) were then pre-treated according to one of the following three protocols: (i) shaking by hand for 1 min (Bulk/CNTs), (ii) sonication for 2 h (So/CNTs) or (iii) sonication for 2 h followed by horizontal shaking (180 rpm) for 6 d (So-Sh/CNTs). When sonicating, 20 sample vials were immersed into the sonication bath (Bandelin sonorex super rk106 bath, 35 kHz, diameter 24.5 cm). The water level in the bath was the same as in the samples (depth 10.2 cm). A POM strip (approximately 0.1–1 g, depending on the intended concentration) was subsequently added to each sample and pyrene was spiked. The volume of methanol (spiking solvent) was kept at 0.16% for all samples to minimize solvent effects. For each of the three pre-treatments, sorption coefficients (K_{CNT}) were measured for a single initial concentration of pyrene (150 µg/L). In addition, full sorption isotherms were measured for So-Sh/CNTs (pyrene equilibrium concentration ranged over five orders of magnitude from 0.0001 to 20 µg/L). All vials were horizontally shaken (180 rpm) for 28 d to ensure equilibration. POM strips were then taken out of the vials, rinsed with deionized water and wiped with a wet tissue. They were then extracted with methanol by accelerated solvent extraction (ASE 200, Dionex, USA; 1500 psi, 100 °C), with pyrene-d10 as internal standard. Extracts were concentrated under N_2 prior to GC-MS analysis, as described in our previous study.[9] Blanks without pyrene were prepared for each pre-treatment as method blanks and used as characterization samples in the following section. Control samples with pyrene indicated that losses were < 6% after 28 d of shaking.

4.3.2.2 Calculation of sorption data

The calculation of sorption data is shown in Table 4.2 similarly to Koelmans et al.[12] We here assume that adsorbed HA behave the same as dissolved HA. Even though HA may be partially fractionated during the adsorption process, this assumption is necessary and commonly applied when measuring sorption of HA to CNTs.[13, 14]

***Table 4.2**. Equations used to derive sorption coefficients of pyrene to (a) humic acid (HA) and (b) carbon nanotubes (CNTs) using the polyoxymethylene-solid phase extraction (POM-SPE) method.*

(a) HA-POM-water system

Mass balance for partitioning of total amount of pyrene between 3 phases: water (w), POM, and HA	$m_0=C_wV_w+C_{POM}M_{POM}+C_{HA}M_{HA}$
Pyrene concentration in POM	$C_{POM}=K_{POM}C_w$
Pyrene concentration in HA	$C_{HA}=K_{HA}C_w$
Sorption coefficient for HA calculated from system characteristics, K_{POM}, and C_{POM}	$K_{HA}=1/M_{HA}+(m_0K_{POM}/C_{POM}-V_W-K_{POM}M_{POM})$

(b) CNTs-HA-POM-water system

Mass balance for partitioning of total amount of pyrene concentration between 4 phases: CNTs, water (w), POM, and HA	$m_0= C_{CNT}M_{CNT}+C_wV_w+C_{POM}M_{POM}+C_{HA}M_{HA}$
Adsorbed pyrene concentration on CNTs calculated from K_{CNT} and C_W	$C_{CNT}=K_{CNT}C_w$
Pyrene concentration on CNTs calculated from system characteristics, K_{POM}, K_{HA}, and C_{POM}	$C_{CNT}=1/M_{CNT}(m_0-C_{POM}V_W/K_{POM}-C_{POM}M_{POM}-K_{HA}M_{HA}C_{POM}/K_{POM})$

$m_{0:}$ total mass of pyrene in the system (μg).
C_{CNT}, C_{POM} and C_{HA}: pyrene concentration in CNTs, POM, and HA, respectively (μg/kg).
M_{CNT}, M_{POM}, and M_{HA}: mass of CNTs, POM, and HA (kg), respectively.
C_w: freely dissolved pyrene concentration in water (μg/L).
V_w: volume of solution (L).
K_{CNT}, K_{POM}, and K_{HA}: sorption coefficient of pyrene by CNTs, POM, and HA, respectively (L/kg).
K_{POM} value measured by Jonker and Koelmans (2001)[11] was applied in this study (log K_{POM} = 3.76 ± 0.05).

4.3.2.3 Batch setup for pyrene sorption to HA

The sorption coefficient of pyrene by HA (K_{HA}) was measured at 100 and 200 mg/L HA (pyrene initial concentration of 50 μg/L) and included in the mass balance calculations to derive CNT sorption coefficients (Table 4.2). Sonication of HA did not influence the partition coefficients of pyrene to HA (t test, p=0.680). The literature most often supports that K_{HA} is independent of the concentration and can be measured by single-concentration experiments.[15-18] Pan et al.[19] reported nonlinear sorption of PAHs to HA and reported that the nonlinearity was mainly affected by HA mass. In their study, K_{DOC} at 2 mg DOC/L was about 0.3 orders of magnitude smaller than at 40 mg OC/L. In order to evaluate the effect of nonlinear K_{HA} on the final log K_{CNT} values, we here assume that log K_{HA} decreased by 1.5 orders of magnitude (from 6.33 down to 4.73 over the range 1–200 mg/L HA). Log K_{CNT} in Pyr-CNTs-HA systems were subsequently calculated based on the corresponding log K_{HA} values. The

calculated log K_{CNT} increased by only 0.06 orders of magnitude (maximum) compared with the values in the present study." Reason is that pyrene has a much stronger affinity for CNTs than for HA and variation in K_{HA} has thus a minimal impact on the mass balance calculations when considering a pyrene-CNTs-HA system. The absorbed pyrene mass by HA increases with increasing of HA concentration. At low levels, the absorbed mass is too low to allow an accurate calculation of K_{HA}.

***Table 4.3**. HA-water partition coefficients of pyrene determined at a HA concentration, [HA], of 100 and 200 mg/L, as measured by POM-SPE.*

[HA]	**log K_{HA}**	**log K_{DOC}**[a]
100 mg/L	4.87 ± 0.06	4.59 ± 0.06
200 mg/L	4.73 ± 0.05	4.45 ± 0.05
Average	4.80 ± 0.09	4.52 ± 0.09

[a] Normalization to dissolved organic carbon (log K_{DOC}, L/kg) is based on a C content of 52.63% (International Humic Substance Society).

4.3.2.4 Influence of POM on HA Concentration

Sorption of HA to POM was tested at three HA concentrations (5, 100 and 200 mg/L) and was shown to be negligible (Figure 4.1). The absence of any effect supports a lack of interaction between HA and POM. HA concentrations were determined by UV-spectrometry at 400 nm.

***Figure 4.1**. Influence of POM on the concentration of HA (34 d of exposure).*

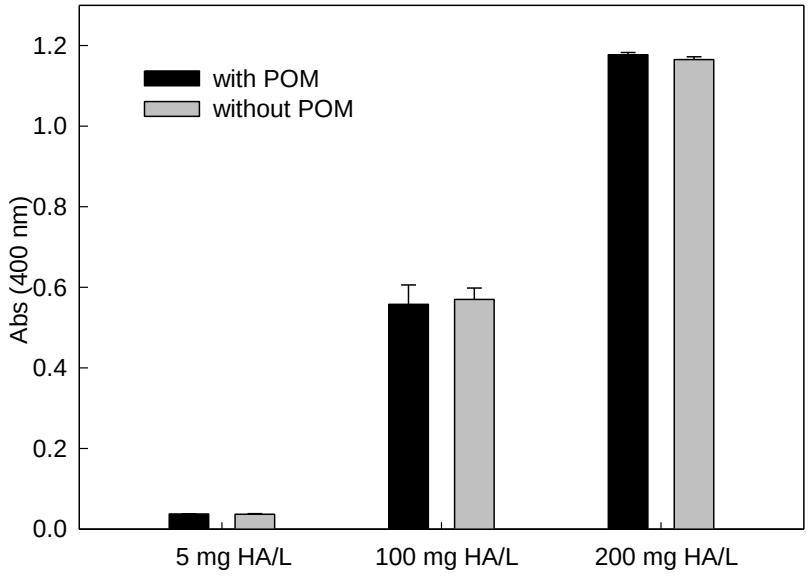

4.3.3 Characterization of CNTs

Extensive characterization of CNTs was carried out as follows.

Images:

For each pre-treatment, CNTs were imaged by scanning electron microscopy (SEM). Particular attention was paid to maintaining the structure of the CNT aggregates as they occurred in the sorption test. Bulk/CNTs: aliquots of CNT suspensions were dropped onto SEM stubs, using a glass pipette. Excess water was withdrawn carefully using a paper tissue and samples were left to dry overnight. So-Sh/CNTs: copper grids were dipped into the CNT suspensions using a pair of tweezers and dried overnight.

Settling behavior:

CNT settling behavior was characterized by UV-Vis spectrometry at 800 nm absorbance (Varian Cary 50 UV-Vis spectrophotometer).[4]

Three mL of suspension were withdrawn from each sample and settling behavior was monitored by UV-Vis spectrometry at 800 nm. The optical density (*OD* = absorbance (*t*)/absorbance (*t* = 0)) was recorded within a 20 h time period. Settling curves were fit by a least squares method using an exponential model:

$$y = OD_{plateau} + OD_1 \exp(-R_0 t)$$

t: settling time (h).
OD_1: optical density of the first point > *t* =0.
R_0: settling rate (*OD*/h).
$OD_{plateau}$: value where the settling curve plateaus.

Size distribution:

Size distribution was determined using a particle size analyzer based on a time of transition principle (TOT, GALAI Production Ltd., Israel). Three mL of suspension were withdrawn from each sample and added to a cuvette for size distribution measurement by a laser time-of-transition (TOT) technique (GALAI Production Ltd., Israel). TOT is a laser-based analyser, using laser obscuration time on the detector and pulse-length analysis to measure particle diameter and size distribution. [20, 21] Particles were counted until a 95% number based confidence level of the distribution was achieved. Size distribution was determined in the range of 0.6–60 µm.

Size of small particles:

The hydrodynamic diameter of CNT aggregates remaining in suspension after 2 d of settling was measured by dynamic light scattering (DLS, Malvern ZetaSizer Nano). Particle size was measured by dynamic light scattering using a Zetasizer Nano-ZS equipped with a 4 mW He-Ne laser (633 nm) after settling the suspension for 2 d. Light scattering was quantified at a fixed backscattering angle of 173˚ and each sample was measured 10 times for 30 seconds. The hydrodynamic diameter of the aggregates was calculated from the particle diffusion coefficient (D) with the Stokes-Einstein equation, using the cumulant method for fitting the stacked autocorrelation functions of the 10 individual measurements.

Functional groups:

The surface functional groups of CNTs were detected with Fourier transform infrared spectroscopy (FTIR). CNT samples were freeze dried and ground with KBr to uniformity and pressured into pellets. Then, IR absorption was measured in the range of 4000–350 cm^{-1}, based on 600 scans.

Surface area:

CNT suspensions were freeze-dried and outgassed before measuring adsorption-desorption isotherms of nitrogen at 77 K (Quantachrome, NOVA 2000e) and deriving the surface area and pore volume of CNT aggregates. CNT-HA suspensions were freeze-dried (Alpha 1-4 LSC). Samples were then outgassed (105°C, >16h) before measuring full adsorption-desorption isotherms of nitrogen at 77 K (Quantachrome NOVA 2000e).

4.3.4 Sorption Models and Statistics

Six sorption models previously applied to describe sorption by carbonaceous materials[22-25] were fit to the isotherms: Freundlich (FM), Langmuir (LM), dual Langmuir (DLM), Toth (TM), dual-mode (DMM) and Dubinin–Ashtakhov model (DAM). Description of the models and their parameters are available in Table 2.3 of Chapter 2. The goodness of fit was evaluated and compared based on the r^2 values, mean weighted square errors (MWSE), and Akaike's Information Criterion (AIC), as described in Chapter 3[9]. All statistical tests and parameter optimizations were performed with *SigmaPlot 11.0* for Windows.

4.4 Results and Discussion

4.4.1 Characterization Results

4.4.1.1 Images

From Figure 4.2–4.4, shaking did not affect the size distribution of Bulk/CNTs as compared to Figure 3.3 in Chapter 3. So-Sh/CNTs exhibit much smaller aggregates and looser structures relative to Bulk/CNTs. Increasing numbers of single CNTs were observed with increasing HA concentration.

Figure 4.2. *Scanning electron microscopy images and digital photos of Bulk/CNTs and CNTs pre-treated by sonication followed by 6 d shaking (So-Sh/CNTs), in the presence of 0 (a–b) and 200 mg HA/L (c–d).*

(a) Bulk/CNTs at 0 mg HA/L (b) So-Sh/CNTs at 0 mg HA/L

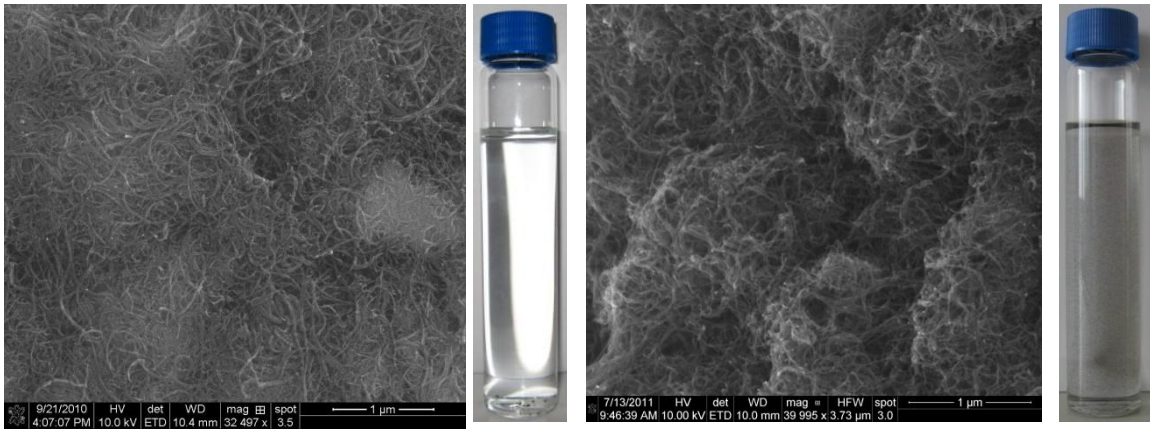

(c) Bulk/CNTs at 200 mg HA/L (d) So-Sh/CNTs at 200 mg HA/L

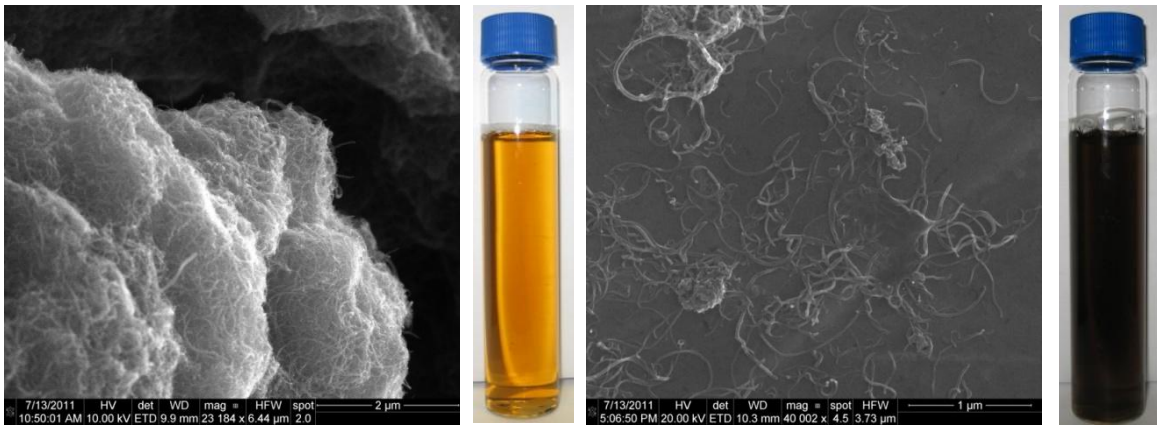

Figure 4.3. *Pictures of the suspensions studied at the end of the sorption experiment: (a) HA alone, (b) Bulk/CNTs (pre-treated by shaking), and (c) So-Sh/CNTs (pre-treated by 2 h sonication + 6 d shaking). The picture of So/CNTs (pre-treated by 2 h sonication) was similar to (c).*

(a) HA

(b) Bulk/CNTs

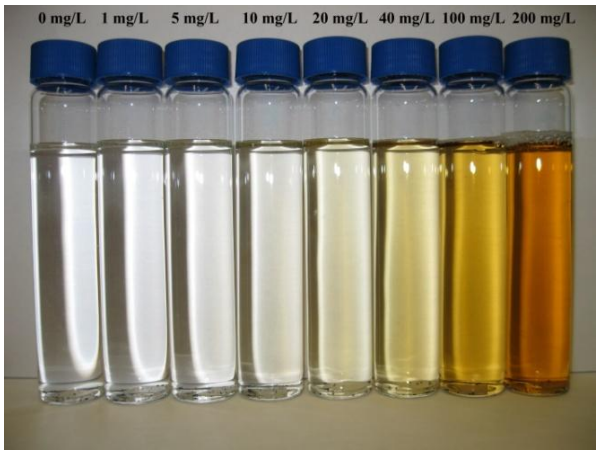

(c) So-Sh/CNTs (similar to So/CNTs)

(d) So/CNTs (after sonication)

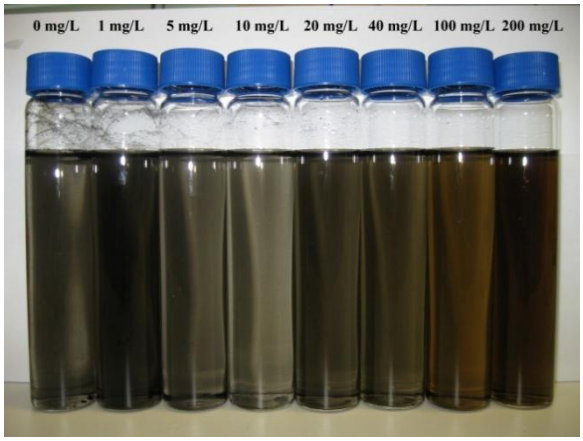

Table 4.4. *Absorbance of So-Sh/CNTs at different conditions*

	So-Sh/CNTs	So-Sh/CNTs	So-Sh/CNTs	So-Sh/CNTs
Methanol (%)	0.16%	0 %	0.16%	0.16 %
Shaking (d)	6 d	6 d	2 d	28 d
[HA]	***Absorbance***	***Absorbance***	***Absorbance***	***Absorbance***
0 mg/L	0.04	0.03	0.04	0.03
1 mg/L	0.04	0.04	0.05	0.05
5 mg/L	0.12	0.11	0.12	0.13
10 mg/L	0.14	0.15	0.15	0.14
20 mg/L	0.16	0.15	0.14	0.15
40 mg/L	0.21	0.20	0.22	0.23
100 mg/L	0.35	0.36	0.37	0.35
200 mg/L	0.37	0.38	0.39	0.39

***Figure 4.4**. Scanning electron microscope (SEM) images of Bulk/CNTs and So-Sh/CNTs in the presence of 0–200 mg HA/L after the sorption experiments.*

Bulk/CNTs at 200 mg HA/L

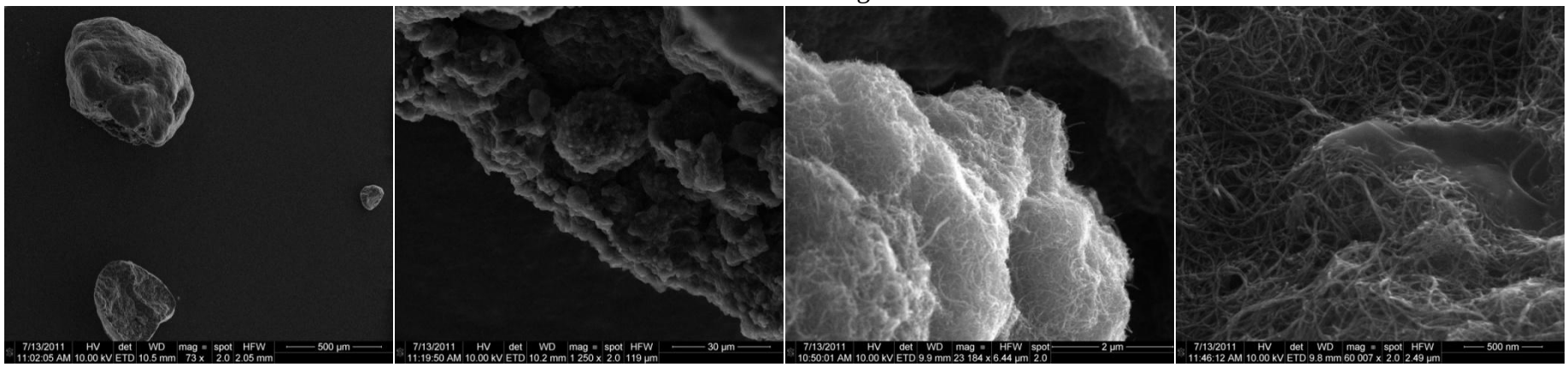

So-Sh/CNTs at 0 mg HA/L

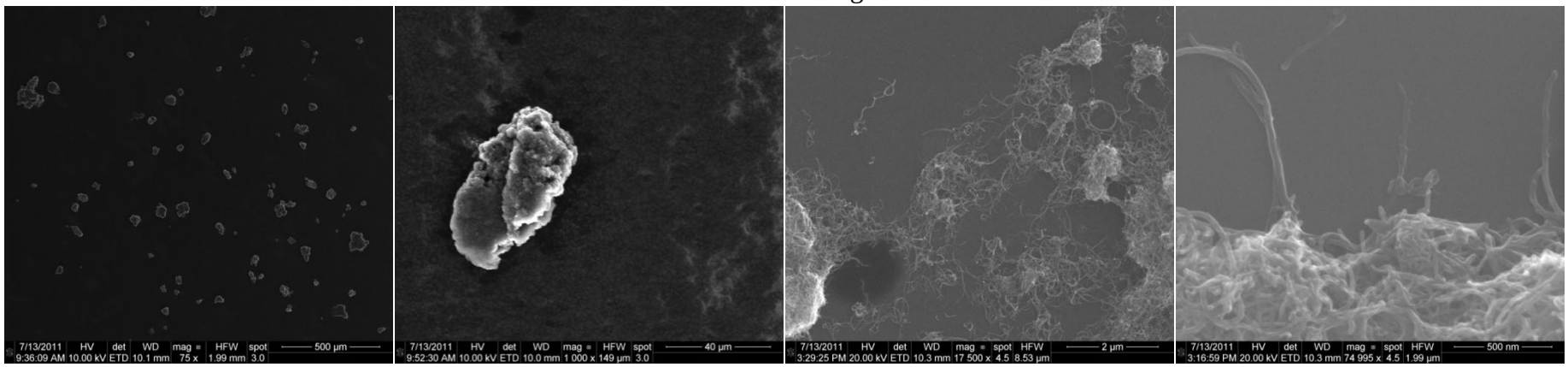

So-Sh/CNTs at 5 mg HA/L

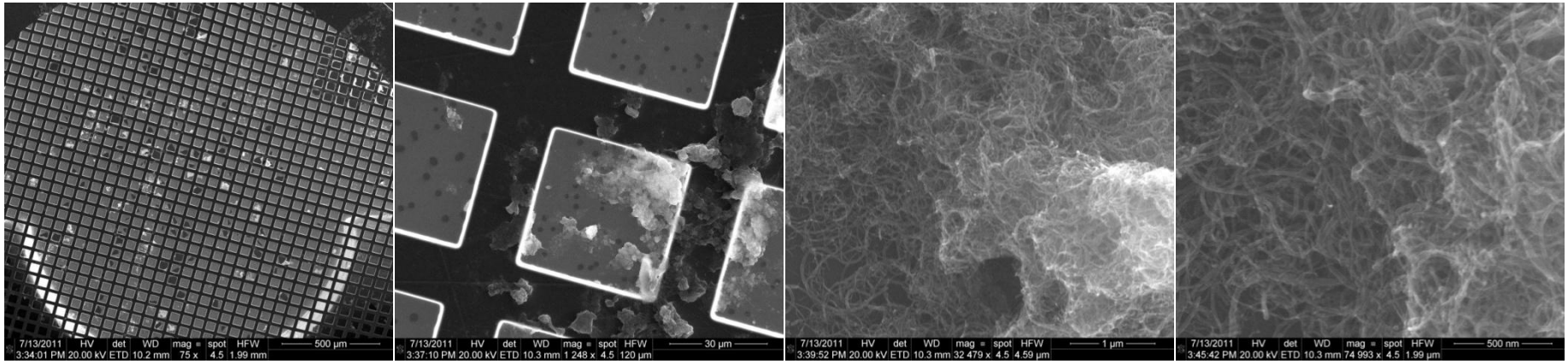

So-Sh/CNTs at 40 mg HA/L

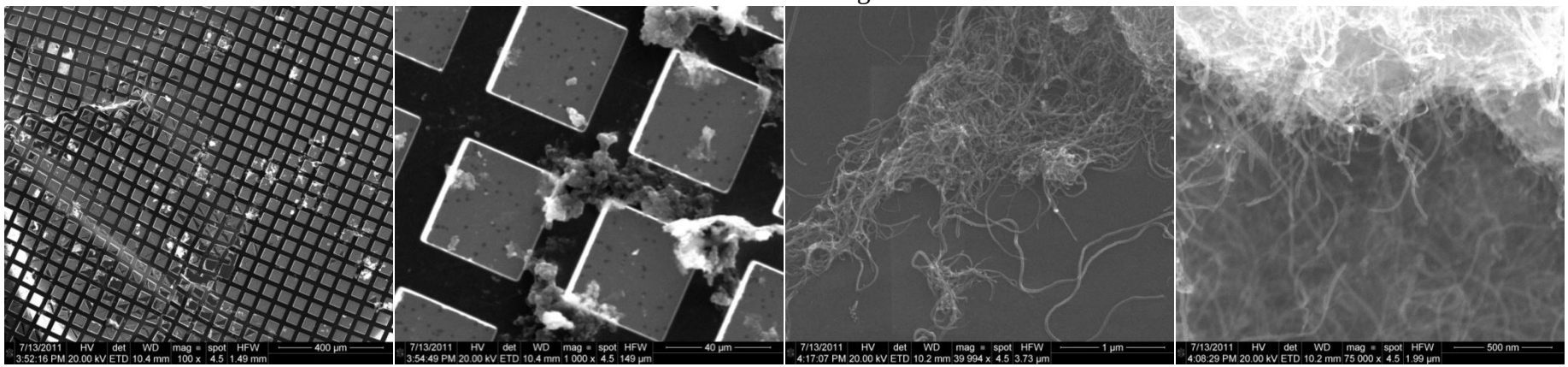

So-Sh/CNTs at 200 mg HA/L

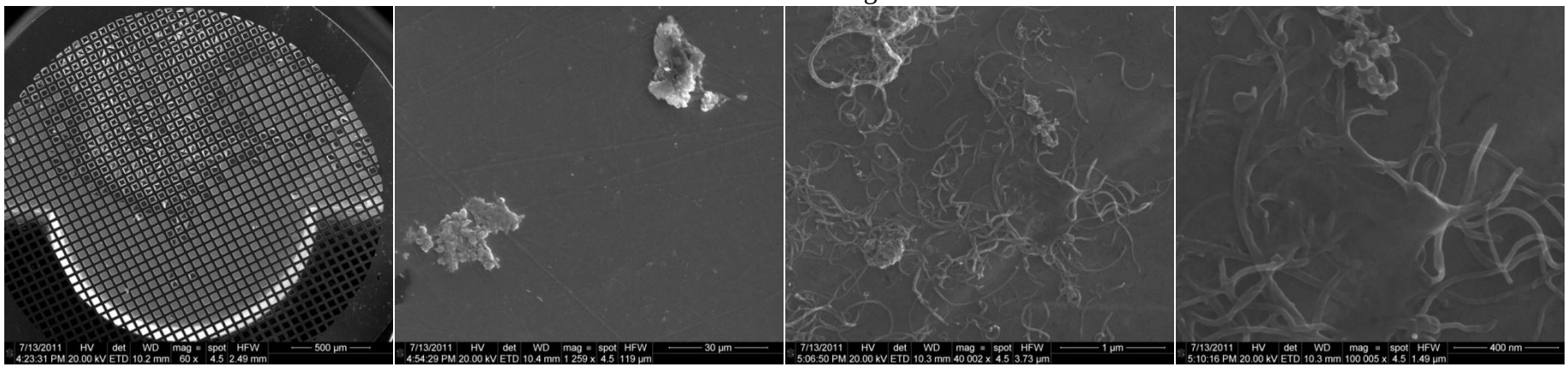

4.4.1.2 Settling behavior

So-Sh/CNTs settled down faster than So/CNTs. Additional shaking probably increased the number of collisions between previously de-bundled CNTs, resulting in re-aggregation (Figure 4.5).

***Figure 4.5**. Settling curves and parameters of (a) So/CNT and (b) So-Sh/CNT suspensions in the presence of 0–200 mg HA/L.*

Settling curves

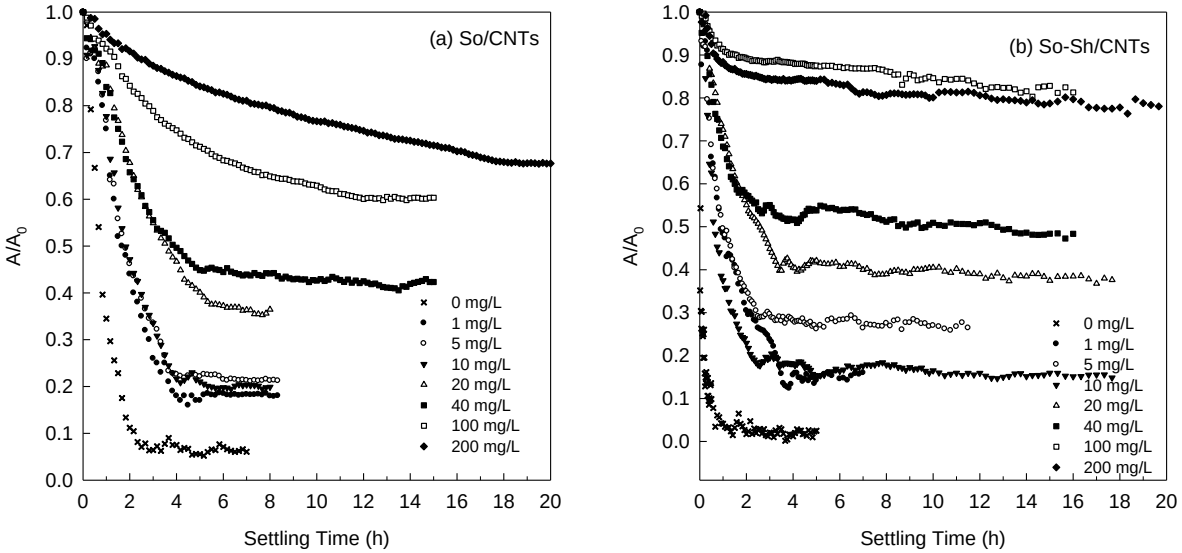

Settling parameters

(a) So/CNTs

[HA]	***Absorbance***	$OD_{plateau}$	OD_1	R_0 (*OD* h^{-1})	r^2
0 mg/L	0.15	0.05±0.01	1.04±0.02	1.23±0.04	0.99
1 mg/L	0.11	0.15±0.01	0.94±0.02	0.60±0.03	0.98
5 mg/L	0.26	0.18±0.01	0.89±0.02	0.57±0.03	0.98
10 mg/L	0.28	0.16±0.01	0.92±0.02	0.53±0.03	0.98
20 mg/L	0.28	0.28±0.01	0.77±0.01	0.34±0.02	0.99
40 mg/L	0.21	0.42±0.00	0.63±0.01	0.48±0.01	0.99
100 mg/L	0.36	0.59±0.00	0.42±0.00	0.24±0.00	1.00
200 mg/L	0.35	0.62±0.01	0.36±0.00	0.09±0.00	0.99

(b) So-Sh/CNTs

[HA]	***Absorbance***	$OD_{plateau}$	OD_1	R_0 (*OD* h^{-1})	r^2
0 mg/L	0.04	0.04±0.01	0.61±0.04	7.87±0.81	0.83
1 mg/L	0.04	0.14±0.01	0.87±0.02	0.82±0.03	0.98
5 mg/L	0.12	0.27±0.00	0.76±0.01	1.15±0.02	0.99
10 mg/L	0.14	0.17±0.00	0.93±0.01	1.45±0.03	0.99
20 mg/L	0.16	0.39±0.00	0.67±0.01	0.72±0.01	0.99
40 mg/L	0.21	0.51±0.00	0.52±0.01	1.07±0.03	0.98
100 mg/L	0.35	0.83±0.00	0.13±0.00	0.22±0.02	0.86
200 mg/L	0.37	0.80±0.00	0.16±0.01	0.41±0.03	0.87

The absolute values of absorbance for So/CNTs are larger than So-Sh/CNTs, which indicates that the So/CNTs are more dispersed than So-Sh/CNTs (Table 4.4). 0.16% of methanol did not affect the characteristics of the CNT aggregates. The aggregation state of the CNTs stabilized within 2 d of shaking (i.e., re-aggregation occurred within the two first days of shaking, after which no significant changes occurred anymore).

4.4.1.3 Size distribution

Figure 4.6 shows the size distribution of So/CNTs and So-Sh/CNTs in the presence of 0–200 mg HA/L. For both pre-treatments, the size range became narrower with increasing [HA]. Size distributions of So-Sh/CNTs were generally wider than those of So/CNTs. Additional 6 d shaking applied to So/CNTs increased the chance of collision between de-bundled particles, resulting in re-aggregation. The effect was less visible at 100 and 200 mg HA/L, where coated CNTs may have thicker electro shells and consequently are less likely to re-aggregate.

Figure 4.6*. Size distributions of (a) So/CNTs and (b) So-Sh/CNTs in the presence of 0–200 mg HA/L.*

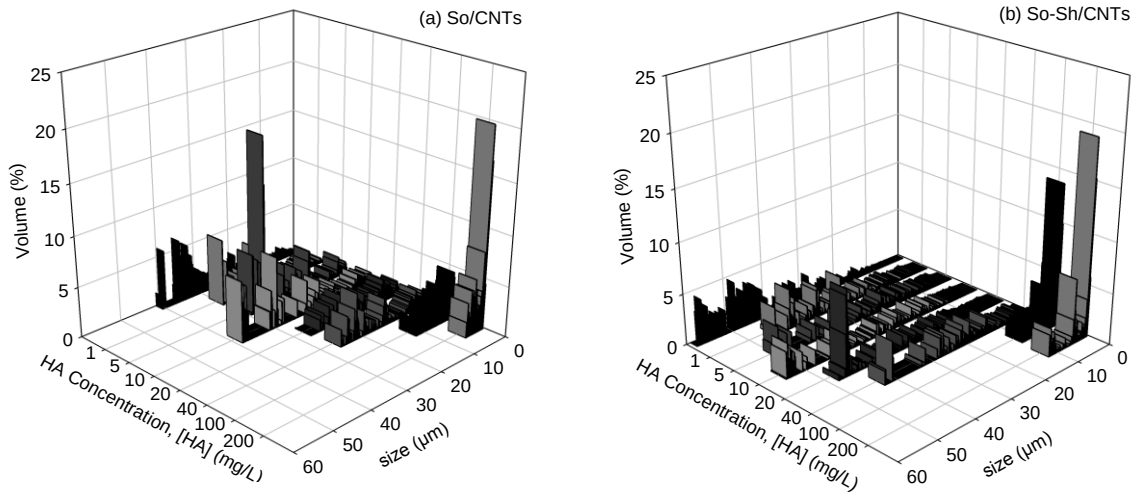

4.4.1.4 Size of small particles

Figure 4.7 shows the size of So/CNTs and So-Sh/CNTs suspended in 0–200 mg HA/L solutions after 2 d of settling. At 0 and 1 mg HA/L, the size of So-Sh/CNTs appeared much larger than that of So/CNTs due to re-aggregation occurring during the additional shaking period. The polydispersity index ranged between 0.6 and 1 for samples > 1000 nm.

Correlograms and derived hydrodynamic diameter > 1000 nm are not reliable; here, TOT data (GALAI Production Ltd., Israel) were used. For sonicated CNTs and in the range of 5–200 mg HA/L, large CNT aggregates rapidly settled down and left behind a fairly monodispersed suspension (polydispersity index between 0.2–0.4) of HA-stabilized CNT aggregates (200–300 nm). There were no particles left in the supernatant for Bulk/CNTs, due to the fast settling of large CNT aggregates.

Figure 4.7*. Size (hydrodynamic particle diameter) of So/CNTs (●) and So-Sh/CNTs (○) suspended in 0–200 mg HA/L solutions after 2 d of settling.*

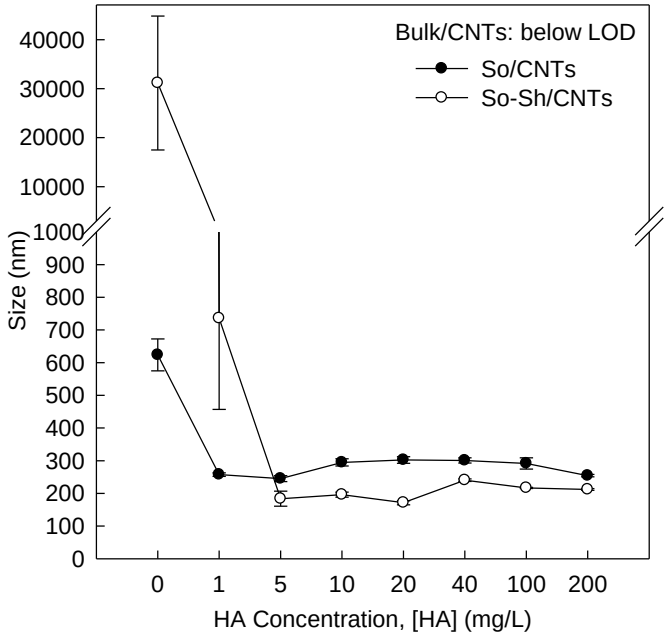

4.4.1.5 Functional groups

Figure 4.8 shows the FTIR results of CNTs without sonication and after sonication with either a bath or a horn. The absorption at 3440 cm^{-1} is due to the H–O stretching vibration of the adsorbed water on the KBr and CNTs. The peak at 1400 cm^{-1} may be in associated with H–O bending vibration in water, phenols and carboxyls.[26] There are significant peaks at 1400 cm^{-1} for sonicated CNTs that indicated CNTs were oxidized after sonication. The relative increase in the 1250 – 950 cm^{-1} wave region upon sonication also points to an increase in the amount of hydrated surface oxides (H–O deformation and C–O stretching combination in the surface phenols, hydroquinones, and aromatic carboxylic acids.[26] Since functional groups are very complex and their vibration rages are adjacent to one another, it is difficult to make quantitative assignments.

***Figure 4.8**. Results of Fourier transform infrared spectroscopy (FTIR) of CNTs without sonication and after 2 h of sonication with either a bath or a horn.*

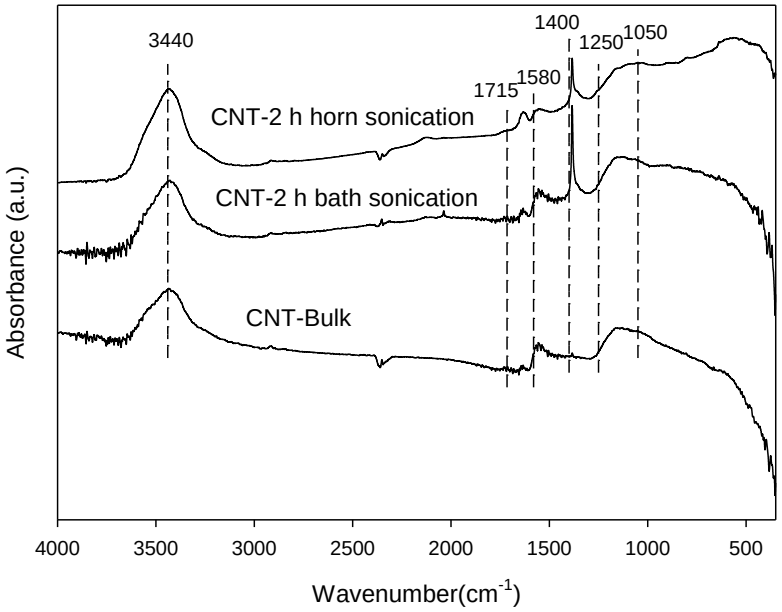

4.4.1.6 Surface area

The BET measurement was performed at the end of the sorption experiment (after 28d of shaking). So/CNTs and So-Sh/CNTs had the same characteristics at this point (size distribution, settling behavior, and sorption data). Comparing Bulk/CNTs to either So/CNTs or So-Sh/CNTs thus leads to the same conclusions.

***Figure 4.9**. Plots of (a) surface area and (b) pore volume against HA concentration for Bulk/CNTs and So-Sh/CNTs, followed by the values.*

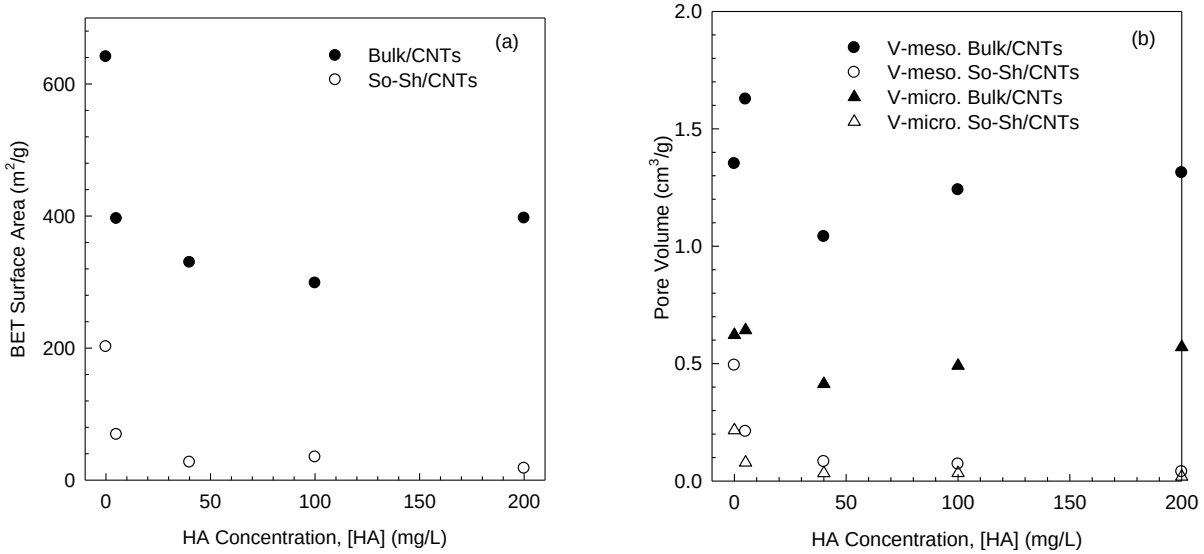

Bulk/CNTs

[HA]	S_{BET} (m^2/g)	S_{BJH} (m^2/g)	V_{meso} (cm^3/g)	V_{micro} (cm^3/g)
0 mg/L	641	660	1.352	0.622
5 mg/L	396	641	1.627	0.643
40 mg/L	330	449	1.041	0.414
100 mg/L	298	511	1.241	0.491
200 mg/L	397	580	1.313	0.570

So-Sh/CNTs

[HA]	S_{BET} (m^2/g)	S_{BJH} (m^2/g)	V_{meso} (cm^3/g)	V_{micro} (cm^3/g)
0 mg/L	202	209	0.493	0.216
5 mg/L	69	89	0.211	0.079
40 mg/L	27	33	0.083	0.034
100 mg/L	35	35	0.072	0.034
200 mg/L	18	18	0.040	0.019

S_{BET}: surface area calculated by the multi-point Brunauer–Emmett–Teller (BET) method.
S_{BJH}: surface area calculated by the Barret–Joyner–Halenda (BJH) method.
V_{meso}: Mesopore volume calculated by the BJH method.
V_{micro}: Micropore volume calculated by the Dubinin–Radushkevic (DR) method.

4.4.2 Effect of Sonication in the Absence of HA

Sorption of pyrene was significantly enhanced by sonication. Log K_{CNT} values were 8.61, 8.64 and 7.24, for So/CNTs, So-Sh/CNTs, and Bulk/CNTs, respectively (Table 4.6). For the first sonication treatment (So/CNTs, for which suspensions were spiked with pyrene directly after sonication), sonication broke down CNT aggregates and reduced their size from 40–500 µm down to 0.6–60 µm (based on SEM, TOT, and DLS; see Figures 4.4, 4.6 and 4.7). The increase in sorption affinity may thus be explained by an increase in the outer surface available for sorption, which would imply that inner surfaces of Bulk/CNTs aggregates were, at least partially, not available for pyrene sorption. This hypothesis was tested by measuring the surface area of particles in both the original and the sonicated suspensions. Unexpectedly, the BET measurements indicated a decrease in surface area of CNTs upon sonication (Figure 4.9). As suggested by Arai et al.,[27] sonication may however result in the formation of amorphous carbon that can block some of the pores during the drying procedure preceding the BET measurement, leading to erroneous measurements.

For the second sonication treatment (So-Sh/CNTs), sonication was followed by an additional 6 d shaking period, during which re-aggregation occurred, as evidenced by a wider particle size distribution and faster settling of So-Sh/CNTs as compared to So/CNTs (Figure 4.4–4.5). At the time of pyrene spiking, the outer surface area of So-Sh/CNTs was thus less than that of So/CNTs. However, the sorption affinity of So-Sh/CNTs was similar to that of So/CNTs (p =

0.959, Table 4.6). This indicates that the extra surface exposed by sonication remained available to pyrene after re-aggregation occurred and suggests that sonication irreversibly increased the sorption potential of CNTs in aqueous suspension. Further characterization by SEM showed that sonicated CNT aggregates exhibited much looser structures than Bulk/CNTs (Figure 4.2a-b). This may be explained by a partial oxidation of the CNT surface during sonication (as suggested by FTIR measurements; see Figure 4.8), which will reduce the van der Waals attractive forces responsible for the tightly bound structure of Bulk/CNT aggregates.[28] Looser structures imply that more pores located within So-Sh/CNT aggregates will be available to pyrene, relative to Bulk/CNTs. Note that "pores" here refer to the space between the aggregates or between individual CNTs (hereafter referred to as inter-aggregate and inter-CNT pores, respectively). Even though oxidation is known to decrease PAHs sorption to CNTs,[29] the present observations confirm that the effect of structure is overwhelming the effect of surface chemistry.

Table 4.5*. Fitting parameters ± standard error, mean weighted square error (MWSE), r^2, and r^2_{adj} for TM and DAM fitting the isotherm of pyrene by Bulk/CNTs in the absence of HA.*

Toth Model (TM)							
[HA]	**log Q^0**	**K_t**	**t**	**MWSE**	**r^2**	**r^2_{adj} [a]**	**N**
0 mg/L	7.27e+0±1.16e-1	1.40e+0±4.67e-1	1.03e+0±2.55e-1	0.00111	0.9892	0.9880	30
Dubinin–Ashtakhov Model (DAM)							
[HA]	**log Q^0**	**E**	**b**	**MWSE**	**r^2**	**r^2_{adj}**	**N**
0 mg/L	7.78e+0±1.01e-1	1.40e+1±7.90e-1	1.69e+0±9.30e-2	0.00135	0.9557	0.9506	30

Because fitting isotherms with model equations can aid in obtaining information on sorption mechanisms, the isotherm of pyrene sorption to So-Sh/CNTs was compared with that of Bulk/CNTs[9] (Figure 4.10). Of the six sorption models tested, the Dubinin–Ashtakhov (DAM) and Toth model (TM) gave the best isotherm fit, based on our multi-criteria evaluation (r^2 > 0.95). Both DAM and TM were originally used to describe gas sorption, but were later also applied to adsorption from aqueous phases. The DAM is based on the Polanyi theory, which assumes that for a molecule located within the attractive force field of a sorbent, an adsorption potential exists between the molecule and the sorbent surface. Polanyi theory based models have often been used to describe sorption of organic compounds by CNTs.[30] The TM is derived from the potential theory, which is an empirical equation developed to improve Langmuir isotherm fittings. TM has proven to be useful for describing sorption of organic

compounds onto carbonaceous materials,[31-33] but the model so far has only been used in one study to describe sorption of acetone, n-hexane, and trichloroethylene to CNTs.[34] Sorption parameters derived from DAM and TM were compared for So-Sh/CNTs and Bulk/CNTs. Sonication increased the maximum sorption capacity of CNTs by 0.17 and 1.28 orders of magnitude as derived from the DAM and TM fit, respectively. Probably, this will be related to the greater surface available for sorption, as discussed above. Similar effects have also been reported for natural talc and activated sludge, for which pre-treatments by sonication increased the maximum sorption capacity of naphthalene[35] and heavy metals,[36] respectively.

***Figure 4.10**. Sorption isotherms of pyrene to Bulk/CNTs (○) and CNTs pre-treated by sonication followed by 6 d shaking (So-Sh/CNTs; ×), in the absence of humic acids. The lines represent the fits by the Dubinin–Ashtakhov (DAM; ——) and Toth (TM; ·····) model.*

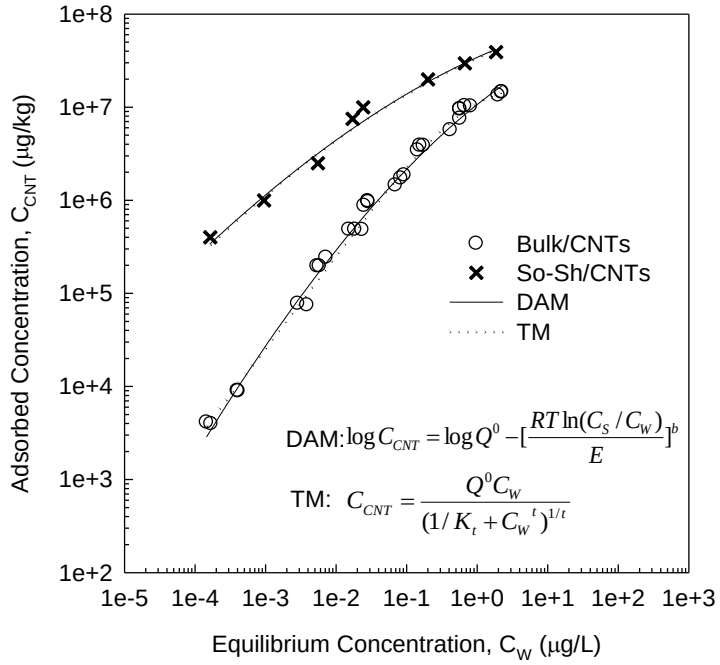

The Toth exponent, *t*, is an indicator of surface heterogeneity. When $t = 1$, TM reduces to LM and represents an homogeneous population of sorption sites.[37] The further *t* deviates from unity, the more heterogeneous the sorbent surface is. For Bulk/CNTs, *t* was close to unity (t = 1.03, Table 4.5), indicating that sorption is likely to be equivalent to a monolayer sorption, as argued previously.[9] For So-Sh/CNTs, t = 0.18 (Table 4.7), indicating that sonication significantly increased the heterogeneity of the CNT surface. By breaking down CNT aggregates, sonication probably produced defects such as bending, buckling, and breaking.[38] Sites of varying energy may be created at the disrupted surfaces, resulting in higher

heterogeneity. The oxidation induced by sonication (based on FTIR, Figure 4.8) may also contribute to the increase in heterogeneity.

To date, only one study considered the potential effect of sonication on the adsorption behavior of CNTs. Cho et al.[29] observed no effect of sonication (and ball-milling) on the sorption isotherms of naphthalene by CNTs. The authors concluded that naphthalene sorption was independent of the CNT aggregate size, due to the full availability of sorption sites in the internal spaces of the aggregates. The discrepancy with the present study in which we found a strong effect of sonication for pyrene may perhaps be explained in terms of steric hindrance: narrow pores inside the Bulk/CNTs aggregates may be accessible to small molecules such as naphthalene, but not to larger molecules such as pyrene. However, it is also possible that the lack of sonication effect observed in ref [29] was (partially) due to insufficient de-bundling of CNTs under their conditions. The solid:liquid ratio of Cho et al.[29] (2 mg : 7 mL) was about 15 times higher than that in the present study (1 mg : 50 mL). Perhaps, a substantial fraction of tightly bundled tubes may remain under high solid:liquid conditions, whereas a low ratio as applied in the present study may allow sufficient de-bundling of the CNTs and consequently lead to a significant increase in sorption.

Overall, the present results highlight the importance of considering both the size and structure of sorbents in addition to performing sorption experiments, in order to gain information on the availability of both outer and inner surfaces. They furthermore indicate an irreversible increase in the sorption of organic contaminants with a molecular size as large as that of pyrene after sonication of CNTs, most probably due to a combined increase in sorption capacity, affinity, and heterogeneity, as suggested by the isotherm fitting. As argued by Laurent et al.[36], the effect of sonication on sorption may however depend on sonication power and duration. Further research is therefore required to fully quantify the impact of these parameters on the sorption behavior of CNTs.

4.4.3 Influence of HA on Single Point Sorption

For all pre-treatments, log K_{CNT} values decreased exponentially with increasing HA concentration (Figure 4.11). The exponential equation was selected to derive numbers that allow an easy comparison of the three treatments, the quantification of discrepancies, and the application of statistical tests. Competition and pore blockage mechanisms have previously been proposed to explain the suppression effect of NOM on the sorption of organic compounds by carbonaceous materials,[6-8] and could also apply in the present case. Note that for all sorption experiments in this study, pyrene was spiked after pre-treating CNTs together

with HA. The effect of HA on pyrene sorption was much more pronounced for sonicated CNTs than for Bulk/CNTs (the exponential decrease rate was three times larger for sonicated CNTs, Figure 4.11). Therefore, HA molecules may have different accessibility to CNTs undergoing different pre-treatments. Similarly to observations made for pyrene, inter-aggregate and –CNT pores of sonicated CNTs were probably accessible to large HA molecules, whereas this was only partly the case for Bulk/CNTs. HA molecules will thus have occupied more sorption sites on sonicated CNTs than on Bulk/CNTs, causing a more pronounced suppression effect for sorption of pyrene. Interestingly, at the highest HA concentration investigated (200 mg HA/L), sorption was similar for all three pre-treatments (Figure 4.11 and Table 4.6). This indicates that sonication has two opposite effects on pyrene sorption in CNT suspensions. On the one hand, it increases the outer surface and widens inter-aggregate and –CNT pores, hence providing more sorption sites for pyrene. On the other hand, the same applies to HA, rendering competition and pore blockage more efficient when combined with sonication. At 200 mg HA/L, both contrasting effects apparently resulted in the same sorption as to Bulk/CNTs.

Figure 4.11. *Log K_{CNT} for pyrene as a function of HA concentration, following three pretreatments: Bulk/CNTs (○); CNTs pre-treated by sonication (So/CNTs; Δ), and CNTs pretreated by sonication and subsequent 6 d shaking (So-Sh/CNTs; ×). Solid lines are exponential fits of the relationships in the range 0–200 mg HA/L, whereas the dashed line is a linear fit for So-Sh/CNTs in the 0–40 mg HA/L range.*

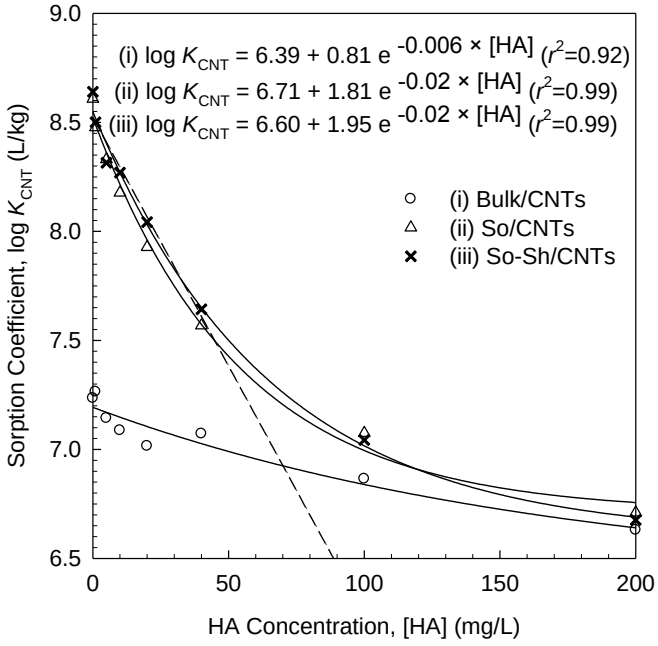

Over the whole HA concentration range, Bulk/CNT aggregates remained large and tightly bound (40–500 µm, Figures 4.2–4.4). They settled down within 5 seconds, whereas the settling of sonicated CNTs took several hours, with the duration increasing with increasing HA concentration (Figure 4.5). In the presence of 5–200 mg HA/L, a significant fraction of sonicated CNTs formed small aggregates that remained in suspension even after 2 d (200–300 nm by DLS, Figure 4.7). At 0 and 1 mg HA/L, the supernatant of CNT suspensions contained larger aggregates relative to higher HA concentrations, with relatively loose structures resulting from the sonication effect (see above).

***Table 4.6**. Logarithmic CNT-water sorption coefficients of pyrene (Log K_{CNT}, L/kg) measured for a single initial concentration of pyrene (C_0=150 µg/L) and three pre-treatments, being (i) shaking by hand (Bulk/CNTs), (ii) 2 h sonication (So/CNTs), and (iii) 2 h sonication + 6 d shaking (So-Sh/CNTs).*

[HA]	Bulk/CNTs	So/CNTs	So-Sh/CNTs
0 mg/L	7.24	8.61	8.64
1 mg/L	7.26	8.48	8.50
5 mg/L	7.14	8.33	8.31
10 mg/L	7.08	8.18	8.27
20 mg/L	7.01	7.93	8.04
40 mg/L	7.07	7.57	7.64
100 mg/L	6.86	7.07	7.04
200 mg/L	6.64	6.72	6.68

Overall, the characterization data indicated that HA could interact to a larger extent with CNTs pre-treated with sonication than with CNTs pre-treated with shaking only. During sonication, HA molecules may adsorb to de-bundled CNTs, with HA preventing re-aggregation of CNTs to more tightly bundled aggregates. HA presumably cannot adsorb into the CNTs aggregates when only shaking was applied (see suspension photographs for the three pre-treatments, Figure 4.3). These observations are consistent with those of Schwyzer et al.[10], who reported that in the presence of dispersants (20 mg/L natural organic matter or 2.5–5000 mg/L anionic, non-ionic, and cationic surfactants), mild shaking for 20 d was not sufficient to separate and suspend CNTs effectively (only 1% suspended), whereas sonication resulted in 65% of suspended CNTs. As such, sonication most probably enhances the suppression effect of HA on sorption of chemicals by allowing more efficient competition and pore blockage to occur. Chen et al.[6] reported that 50 mg HA/L suppressed the sorption of

various non-ionic aromatic compounds by about 0.2 orders of magnitude for pristine CNTs, which agrees with our observation for Bulk/CNTs. For graphite a much larger suppression of sorption was observed by Chen et al.[6] This difference may be explained by the full accessibility of macro pores in graphite for HA molecules of any size, in contrast to the narrow pores in pristine CNT aggregates. The decrease in sorption reported for graphite however matches our results for So/CNTs and So-Sh/CNTs. Hence, sonicated CNTs behave similarly to macro-porous sorbents, in contrast to pristine CNTs.

For all pre-treatments, the suppression effect of HA on pyrene sorption was particularly pronounced in the low HA concentration range (about 0–40 mg/L). This agrees with the more pronounced decrease in CNT surface area and pore volume in this range (Figure 4.9). Wang et al.[7] reported sorption isotherms of HA (extracted from a peat soil) on CNTs to follow a Langmuir-like shape, indicating that sorption of HA by CNTs will increase with increasing HA concentration until saturation occurs (maximum sorption capacity was 53–82 mg/g for the CNTs studied, depending on the CNT outer diameter).[7] Such behavior can well explain the effects observed in this study: the sharp decrease in sorption observed for the HA concentration range 0–100 mg/L could be fit by a linear equation (slope = –0.02; r^2 = 0.96, Figure 4.11), probably reflecting the increase in surface area occupied by HA (initial portion of a Langmuir isotherm). Between 100 and 150 mg HA/L, surface saturation by HA presumably occurred, since further addition of HA only resulted in a slight or no impact on pyrene sorption. If his hypothesis is true, at 200 mg HA/L the sorption capacity of CNTs for HA was most certainly exceeded, with the surface of CNTs then fully being covered with a HA layer. In such a situation, one would expect the HA concentration to be so high that pyrene molecules cannot directly interact with the CNTs surface, and K_{CNT} to be similar to K_{HA}. However, at 200 mg HA/L, log K_{CNT} was still 1.88 orders of magnitude larger than log K_{HA} (6.68 vs. 4.80, respectively). Exponential fits further suggested that log K_{CNT} does not reduce to log K_{HA} with increasing HA concentration (log K_{CNT} is always > 6.30, Figure 4.11). The specific interactions between CNTs and pyrene may be either explained in terms of availability, where some sites are available to pyrene and not to HA and/or in terms of sorption mechanisms (e.g., π–π interactions) still occurring in spite of a HA layer on the CNTs surface.

4.4.4 Influence of HA on Sorption Isotherms

Figure 4.12 shows the sorption isotherms of pyrene measured in partially dispersed suspensions of So-Sh/CNTs in the presence of 1–200 mg HA/L, corresponding to HA/CNT mass ratios ranging from 0.05 up to 10 g of HA/g of CNTs. Two ways of interpreting the sorption of pyrene in the CNT-HA systems are considered below. First, "intrinsic" sorption by CNTs can be calculated by subtracting the amount of pyrene sorbed to HA (based on K_{HA} values presented in Table 4.3) from the total amount sorbed to the combined CNT-HA phase. Although sorption of HA on CNTs may experience fractionation, we assume adsorbed HA to behave the same as dissolved HA, an assumption also previously made when measuring sorption of HA to CNTs.[7] In the second approach, HA and CNTs are considered as a whole sorbent, to which sorption is denoted as "extrinsic". In this case, sorption is calculated from the total amount of pyrene sorbed to the overall CNT-HA matrix, divided by the total mass of HA and CNTs. Expectedly, "extrinsic" isotherms showed much weaker sorption than "intrinsic" isotherms, especially at high HA/CNT mass ratios (i.e., > 1 g of HA/g of CNTs, Figure 4.13). Differences between "intrinsic" and "extrinsic" isotherms are important to

Figure 4.12. *"Intrinsic" sorption isotherms of pyrene by CNTs pre-treated by sonication followed by 6 d shaking (So-Sh/CNTs), in the presence of 0–200 mg HA/L. The isotherms are fit by the Dubinin–Ashtakhov (DAM; ——) and Toth (TM; ·····) model. The horizontal dashed line represents the concentration at which single sorption coefficients were measured.*

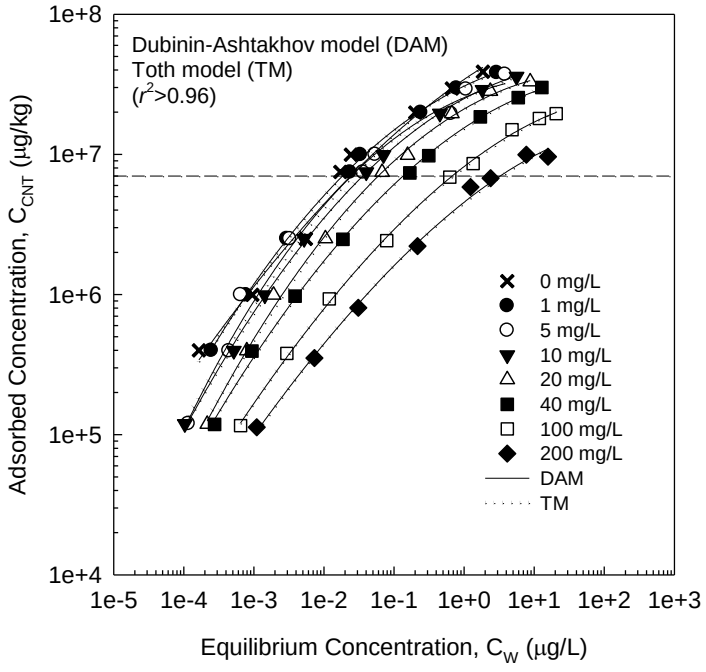

keep in mind when studying large ranges of HA. Neglecting sorption to HA is common practice,[6, 8] but should not be applied in the high HA range, as it may overestimate the effects of HA in decreasing sorption affinity to CNTs and artificially increase isotherm linearity.

The present paper therefore focuses on "intrinsic" sorption. Consistently with the single concentration sorption coefficients discussed above, "intrinsic" sorption isotherms indicated a significant decrease in sorption with increasing HA concentration (Figure 4.12). Based on the multi-criteria evaluation, DAM and TM again gave the best isotherm fit ($r^2 > 0.96$, Table 4.7 and Figure 4.14). Although the Freundlich model (FM) was previously applied to describe sorption isotherms of organic compounds to CNTs in the presence of HA,[8] Figure 4.12 clearly shows that isotherms measured over a wide concentration range are curved on a log-log scale and thus require fitting by more complex models. Below, relationships between DAM and TM parameters and HA concentrations are analyzed to gain further insight into the influence of HA on sorption by So-Sh/CNTs.

Figure 4.13*. Sorption isotherms calculated based on "extrinsic" sorption, considering that sorbents are HA and CNTs as a whole.*

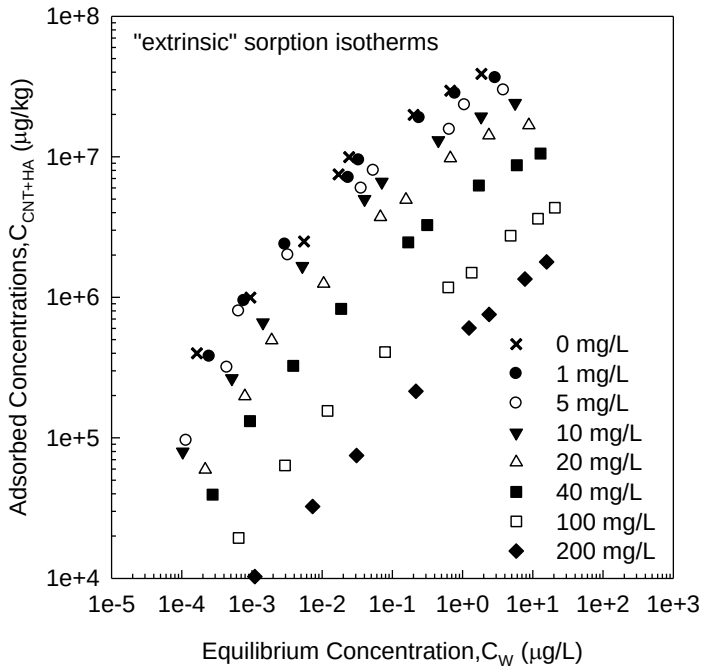

Figure 4.14. *Isotherms of pyrene sorption by CNTs, fit by six commonly-used sorption models. More details on model equations and fitting parameters are available in Table 4.5.*

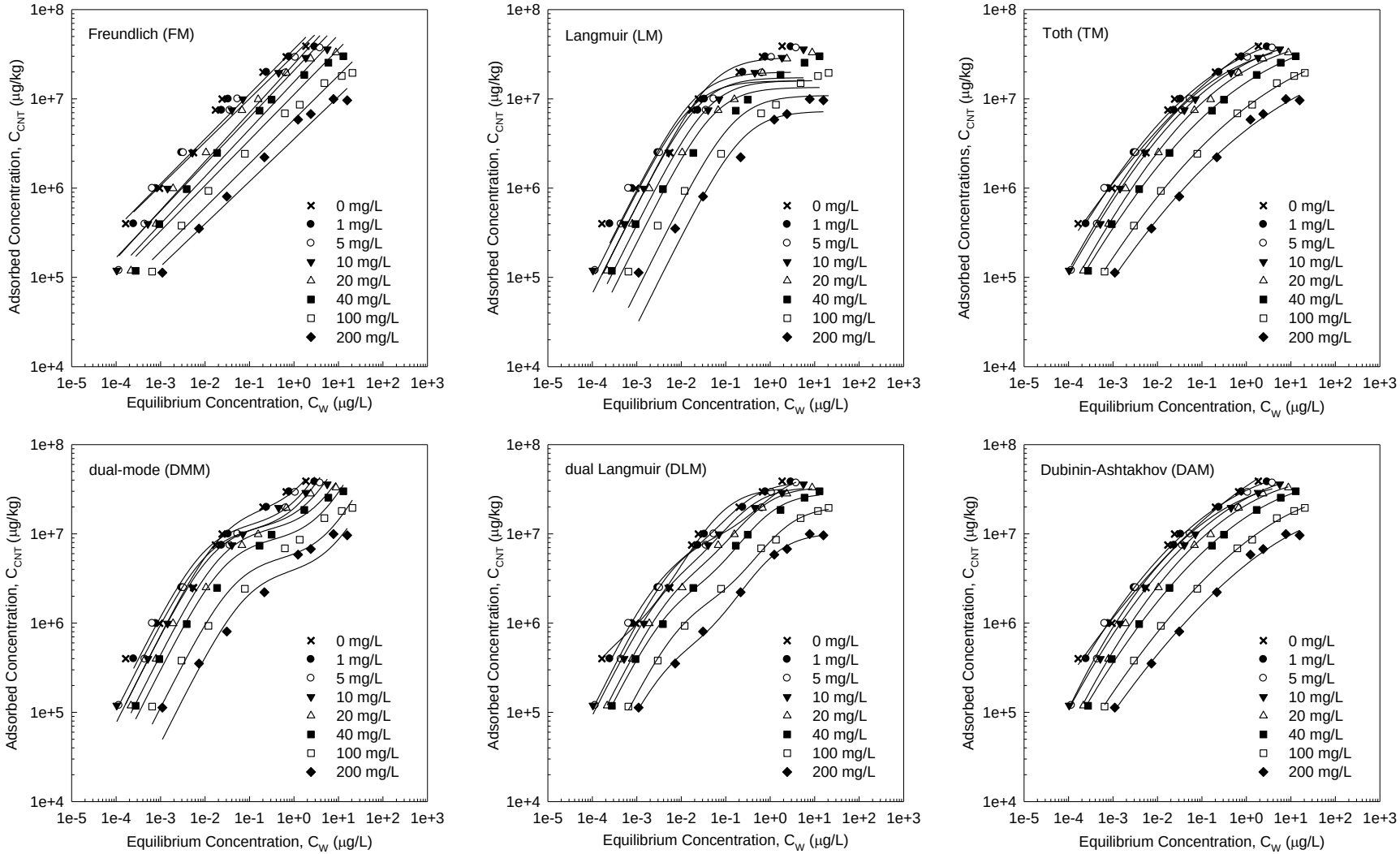

***Table 4.7**. Fitting parameters ± standard error, mean weighted square error (MWSE), r^2, and r^2_{adj} for six models fitting the isotherms of pyrene on So-Sh/CNTs.*

Freundlich Model (FM)						
[HA]	K_f	n	**MWSE**	r^2	r^2_{adj} [a]	**N**[b]
0 mg/L	3.60e+7±5.45e+6	5.03e-1±2.95e-2	0.00985	0.8992	0.8588	8
1 mg/L	3.08e+7±5.25e+6	4.87e-1±3.23e-2	0.01396	0.8335	0.7670	8
5 mg/L	2.46e+7±5.33e+6	5.46e-1±3.76e-2	0.02324	0.8351	0.7802	9
10 mg/L	2.08e+7±4.01e+6	5.24e-1±3.30e-2	0.01959	0.7871	0.7161	9
20 mg/L	1.55e+7±3.10e+6	5.30e-1±3.63e-2	0.02286	0.7247	0.6330	9
40 mg/L	1.12e+7±1.68e+6	5.09e-1±2.94e-2	0.01558	0.8417	0.7890	9
100 mg/L	5.87e+6±6.35e+5	4.93e-1±2.45e-2	0.00975	0.8776	0.8369	9
200 mg/L	3.54e+6±3.63e+5	4.75e-1±2.56e-2	0.00869	0.8435	0.7809	8
Langmuir Model (LM)						
[HA]	Q^0	K_d	**MWSE**	r^2	r^2_{adj}	**N**
0 mg/L	2.91e+7±7.65e+6	4.48e-2±1.87e-2	0.01860	0.9086	0.8721	8
1 mg/L	2.00e+7±5.12e+6	2.01e-2±9.03e-3	0.01740	0.6725	0.5415	8
5 mg/L	1.59e+7±3.73e+6	1.69e-2±6.26e-3	0.01613	0.5530	0.4040	9
10 mg/L	1.73e+7±4.06e+6	2.61e-2±9.89e-3	0.01496	0.6372	0.5162	9
20 mg/L	1.60e+7±3.86e+6	4.06e-2±1.60e-2	0.01621	0.6221	0.4962	9
40 mg/L	1.34e+7±3.49e+6	5.42e-2±2.42e-2	0.02086	0.5548	0.4064	9
100 mg/L	1.09e+7±2.82e+6	1.54e-1±7.45e-2	0.02249	0.6831	0.5774	9
200 mg/L	7.28e+6±1.94e+6	2.47e-1±1.25e-1	0.02313	0.8658	0.8121	8
Toth Model (TM)						
[HA]	$\log Q^0$	K_t	t	**MWSE**	r^2	r^2_{adj}	**N**
0 mg/L	8.55e+0±8.13e-1	1.92e+0±6.69e-1	1.80e-1±9.02e-2	0.00635	0.9856	0.9748	8
1 mg/L	7.88e+0±6.09e-2	3.17e+0±2.54e-1	2.99e-1±2.05e-2	0.00029	0.9988	0.9978	8
5 mg/L	7.69e+0±1.97e-1	3.68e+0±1.43e+0	3.71e-1±9.55e-2	0.00575	0.9682	0.9490	9
10 mg/L	7.80e+0±5.16e-2	2.89e+0±2.06e-1	3.22e-1±1.90e-2	0.00032	0.9999	0.9998	9
20 mg/L	7.76e+0±1.04e-1	2.53e+0±3.43e-1	3.34e-1±4.03e-2	0.00141	0.9949	0.9919	9
40 mg/L	7.85e+0±9.63e-2	2.04e+0±1.51e-1	2.61e-1±2.38e-2	0.00066	0.9996	0.9993	9
100 mg/L	7.85e+0±1.10e-1	1.64e+0±7.86e-2	2.19e-1±1.96e-2	0.00042	0.9950	0.9919	9
200 mg/L	7.73e+0±3.27e-1	1.58e+0±1.67e-1	1.98e-1±4.88e-2	0.00208	0.9652	0.9391	8
Dual-Mode Model (DMM)						
[HA]	K_P	Q^0	K_d	**MWSE**	r^2	r^2_{adj}	**N**
0 mg/L	1.25e+7±1.02e+7	1.84e+7±9.05e+6	2.46e-2±1.70e-2	0.01829	0.9862	0.9758	8
1 mg/L	1.06e+7±3.42e+6	1.26e+7±2.71e+6	9.87e-3±3.27e-3	0.00784	0.9028	0.8300	8
5 mg/L	8.32e+6±2.30e+6	1.12e+7±2.16e+6	1.08e-2±2.85e-3	0.00616	0.9130	0.8608	9
10 mg/L	5.21e+6±1.61e+6	1.20e+7±2.42e+6	1.57e-2±4.54e-3	0.00672	0.9183	0.8693	9
20 mg/L	3.02e+6±1.11e+6	1.13e+7±2.56e+6	2.48e-2±8.21e-3	0.00887	0.8696	0.7913	9
40 mg/L	2.07e+6±6.69e+5	8.59e+6±2.16e+6	2.80e-2±1.06e-2	0.01008	0.9095	0.8552	9
100 mg/L	9.07e+5±2.87e+5	5.30e+6±1.56e+6	4.64e-2±2.11e-2	0.01207	0.8767	0.8027	9
200 mg/L	4.97e+5±2.53e+5	3.75e+6±1.44e+6	8.28e-2±4.98e-2	0.01878	0.8603	0.7556	8
Dual Langmuir Model (DLM)							
[HA]	Q_1^0	K_{d1}	Q_2^0	K_{d2}	**MWSE**	r^2	r^2_{adj}	**N**
0 mg/L	3.21e+7±4.30e+6	7.41e-2±2.14e-2	6.28e+5±3.62e+5	1.47e-4±1.94e-4	0.00420	0.9476	0.8778	8
1 mg/L	3.34e+7±4.01e+6	2.56e-1±1.16e-1	5.35e+6±1.62e+6	3.72e-3±1.29e-3	0.00142	0.9930	0.9836	8
5 mg/L	4.01e+7±1.72e+7	1.40e+0±1.34+0	8.62e+6±2.12e+6	8.18e-3±2.38e-3	0.00398	0.9897	0.9795	9
10 mg/L	3.00e+7±3.63e+6	2.83e-1±1.22e-1	3.63e+6±1.56e+6	4.35e-3±2.05e-3	0.00200	0.9851	0.9703	9
20 mg/L	3.03e+7±2.50e+6	5.34e-1±1.34e-1	3.50e+6±7.92e+5	6.76e-3±1.69e-3	0.00086	0.9982	0.9963	9
40 mg/L	2.64e+7±1.98e+6	7.64e-1±1.54e-1	2.24e+6±4.17e+5	5.36e-3±1.24e-3	0.00090	0.9884	0.9769	9
100 mg/L	1.87e+7±1.53e+6	1.83e+0±4.09e-1	1.61e+6±2.89e+5	9.82e-3±2.35e-3	0.00099	0.9962	0.9924	9
200 mg/L	9.73e+6±6.81e+5	1.01e+0±1.98e-1	5.07e+5±9.54e+4	4.54e-3±1.32e-3	0.00098	0.9912	0.9794	8

Dubinin–Ashtakhov Model (DAM)							
[HA]	**log Q^0**	***E***	***b***	**MWSE**	**r^2**	**r^2_{adj}**	**N**
0 mg/L	7.95e+0±2.11e-1	1.97e+1±2.79e+0	1.71e+0±3.49e-1	0.00622	0.9851	0.9739	8
1 mg/L	7.71e+0±2.67e-2	2.30e+1±3.50e-1	2.24e+0±7.57e-2	0.00025	0.9989	0.9980	8
5 mg/L	7.59e+0±9.74e-2	2.36e+1±1.26e+0	2.49e+0±3.03e-1	0.00484	0.9650	0.9440	9
10 mg/L	7.66e+0±3.06e-2	2.19e+1±4.01e-1	2.16e+0±7.59e-2	0.00047	0.9998	0.9997	9
20 mg/L	7.60e+0±4.43e-2	2.13e+1±5.70e-1	2.18e+0±1.14e-1	0.00107	0.9955	0.9928	9
40 mg/L	7.55e+0±3.26e-2	2.00e+1±4.53e-1	1.93e+0±7.68e-2	0.00060	0.9992	0.9987	9
100 mg/L	7.39e+0±2.69e-2	1.83e+1±3.95e-1	1.71e+0±6.21e-2	0.00041	0.9967	0.9947	9
200 mg/L	7.17e+0±6.23e-2	1.79e+1±8.92e-1	1.64e+0±1.40e-1	0.00167	0.9710	0.9493	8

[a] r^2_{adj} is the adjusted r^2:

$$r^2_{adj} = 1-(N-1)(1-r^2)/(N-p-1)$$

where N and p are the number of experimental data points and fitting parameters, respectively.

Table 4.8*. Probability and evidence ratio for each pair of models compared, based on Akaike's Information Criterion.*[9, 39]

	Probability at different HA concentrations					
1 mg/L	FM	LM	TM	DMM	DLM	DAM
FM	50%	29%	100%	56%	96%	100%
LM	71%	50%	100%	75%	99%	100%
TM	0%	0%	50%	0%	0%	63%
DMM	44%	25%	100%	50%	96%	100%
DLM	4%	1%	100%	4%	50%	100%
DAM	0%	0%	37%	0%	0%	50%
10 mg/L	FM	LM	TM	DMM	DLM	DAM
FM	50%	77%	100%	96%	100%	100%
LM	23%	50%	100%	87%	99%	100%
TM	0%	0%	50%	0%	0%	15%
DMM	4%	13%	100%	50%	94%	100%
DLM	0%	1%	100%	6%	50%	100%
DAM	0%	0%	85%	0%	0%	50%
40 mg/L	FM	LM	TM	DMM	DLM	DAM
FM	50%	21%	100%	56%	100%	100%
LM	79%	50%	100%	83%	100%	100%
TM	0%	0%	50%	0%	1%	61%
DMM	44%	17%	100%	50%	100%	100%
DLM	0%	0%	99%	0%	50%	99%
DAM	0%	0%	39%	0%	1%	50%
100 mg/L	FM	LM	TM	DMM	DLM	DAM
FM	50%	2%	100%	6%	100%	100%
LM	98%	50%	100%	75%	100%	100%
TM	0%	0%	50%	0%	0%	54%
DMM	94%	25%	100%	50%	100%	100%

DLM	0%	0%	100%	0%	50%	100%
DAM	0%	0%	46%	0%	0%	50%

200 mg/L	FM	LM	TM	DMM	DLM	DAM
FM	50%	2%	97%	1%	95%	99%
LM	98%	50%	100%	22%	100%	100%
TM	3%	0%	50%	0%	31%	70%
DMM	99%	78%	100%	50%	100%	100%
DLM	5%	0%	69%	0%	50%	84%
DAM	1%	0%	30%	0%	16%	50%

Evidence ratio at different HA concentrations

1 mg/L	FM	LM	TM	DMM	DLM	DAM
FM	1	0	7.E+05	1	27	1.E+06
LM	2	1	2.E+06	3	66	3.E+06
TM	0	0	1.E+00	0	0	2.E+00
DMM	1	0	6.E+05	1	21	9.E+05
DLM	0	0	3.E+04	0	1	4.E+04
DAM	0	0	1	0	0	1

10 mg/L	FM	LM	TM	DMM	DLM	DAM
FM	1	3	2.E+07	22	322	3.E+06
LM	0	1	6.E+06	7	96	1.E+06
TM	0	0	1.E+00	0	0	2.E-01
DMM	0	0	9.E+05	1	14	2.E+05
DLM	0	0	6.E+04	0	1	1.E+04
DAM	0	0	6	0	0	1

40 mg/L	FM	LM	TM	DMM	DLM	DAM
FM	1	0	3.E+05	1	4.E+03	4.E+05
LM	4	1	1.E+06	5	2.E+04	2.E+06
TM	0	0	1.E+00	0	2.E-02	2.E+00
DMM	1	0	2.E+05	1	3.E+03	3.E+05
DLM	0	0	66	0	1	105
DAM	0	0	1	0	0	1

100 mg/L	FM	LM	TM	DMM	DLM	DAM
FM	1	0	2.E+05	0	3.E+02	3.E+05
LM	43	1	1.E+07	3	1.E+04	1.E+07
TM	0	0	1.E+00	0	1.E-03	1.E+00
DMM	14	0	3.E+06	1	5.E+03	4.E+06
DLM	0	0	730	0	1	846
DAM	0	0	1	0	0	1

200 mg/L	FM	LM	TM	DMM	DLM	DAM
FM	1	0	39	0	18	92
LM	50	1	2.E+03	0	880	5.E+03

TM	0	0	1	0	0	2
DMM	173	3	7.E+03	1	3.E+03	2.E+04
DLM	0	0	2	0	1	5
DAM	0	0	0	0	0	1

In contrast to the sonication effect, the addition of HA significantly decreased the maximum sorption capacity and surface heterogeneity. Figure 4.16a shows that the maximum logarithmic sorption capacity (log Q^0, µg/kg) derived from the DAM fit decreased linearly by 0.54 orders of magnitude going from 1 to 200 mg HA/L. This can be related to the decrease in surface area and/or pore volume (Figure 4.15). The measured surface area corresponds to the combined CNT-HA system because of difficulties in separating HA and CNTs after freeze drying. However, HA have a small surface area relative to CNTs (4.94 m^2/g, soil HA[40]), and the correlation reported was therefore not influenced by the presence of HA. Wang et al.[41] previously reported that the addition of HA had a negligible influence on the sorption capacity of CNTs for phenanthrene, naphthalene, and 1-naphthol (< 0.06 orders of magnitude). However, they (i) considered large CNT aggregates only (dispersed CNTs were discarded by centrifugation prior to the sorption test) and (ii) applied a presumed lower HA concentration (a coating of 85.5 mg of HA/g of CNTs was reported, but this cannot be directly compared to the present experimental conditions, because of possible mass losses during the washing procedure applied in ref [41]. Including both aggregated and dispersed CNTs, the present results support a significant suppression of the sorption capacity by HA, even at very low concentration (e.g., Q^0 decreased by 0.24 orders of magnitude after adding 1 mg HA/L).

Figure 4.15*. Plots of (a) surface area and (b) pore volume against maximum sorption capacity for So-Sh/CNTs.*

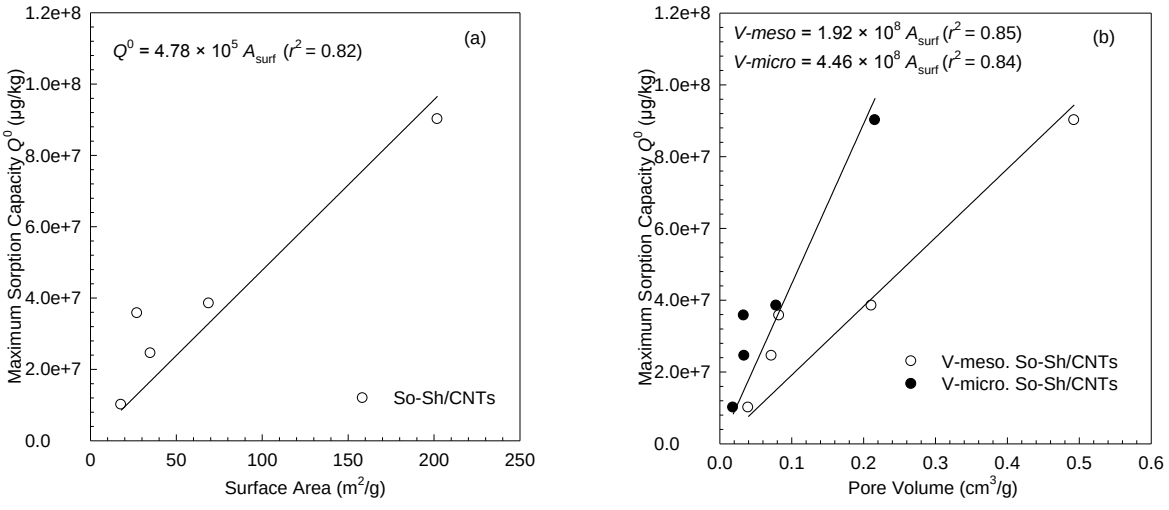

The relationship between HA concentration and Q^0 derived from TM fits was less obvious than for DAM. This may be due to larger standard errors associated with the parameter (Table 4.7). Although the maximum sorption capacity may not easily be reached in the natural environment, a large decrease in the sorption capacity of CNTs can be expected in situations where both the concentrations of DOC and organic contaminants are high (e.g., in waste water).

Figure 4.16*. Decrease in (a) maximum sorption capacity (Q^0, derived from DAM) and (b) Toth exponent (t, derived from TM) with increasing HA concentration. Note that parameters derived from the isotherm measured without HA are not included in the relationships.*

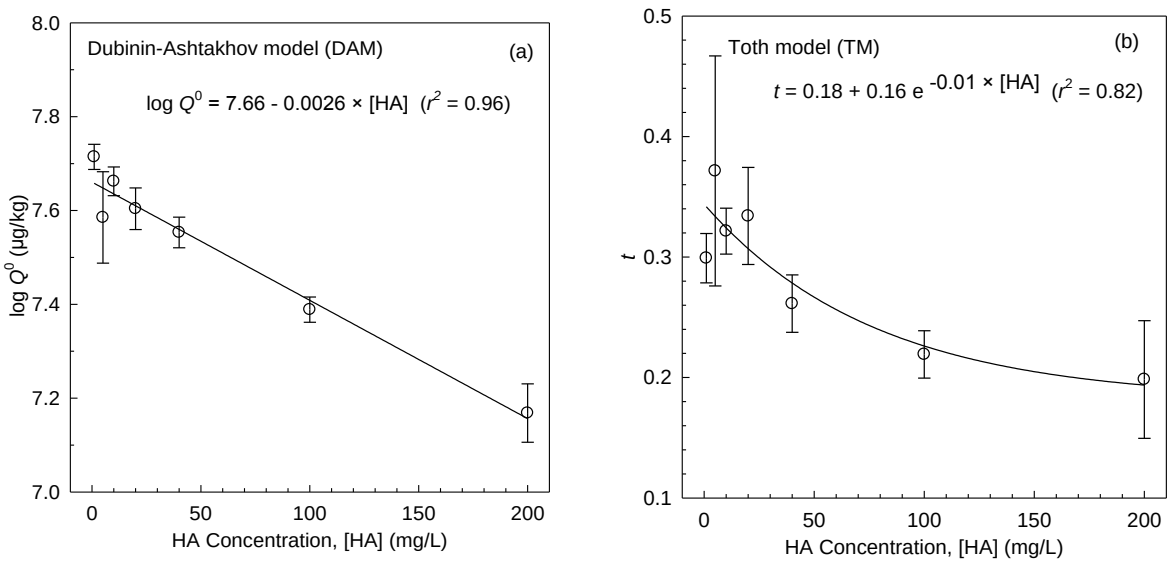

The sorption affinity (E for DAM and K_t for TM) decreased exponentially with increasing HA concentration (Figure 4.17a-b), consistently with the conclusions derived from the single point sorption experiments (Figure 4.11). The extent to which natural dispersants affect the sorption affinity of CNTs towards organic contaminants certainly depends on the concentration and type of contaminants, DOC, and CNTs considered. The present data suggest a difference in sorption affinity of at least one order of magnitude for pyrene when comparing natural water (i.e., low pyrene and HA concentrations) to e.g. waste water systems (i.e., high pyrene and HA [DOC > 40 mg/L] concentrations). Even though sonication will not occur under the natural conditions, it may be part of the production process preceding the environmental release.

***Figure 4.17**. Relationships between HA concentration and model parameters, being (a) E (DAM sorption energy, kg/mol), (b) K_t (TM equilibrium constant, L/µg), and (c) b (DAM fitting parameter). The relationship between E and b is shown in sub graph (d).*

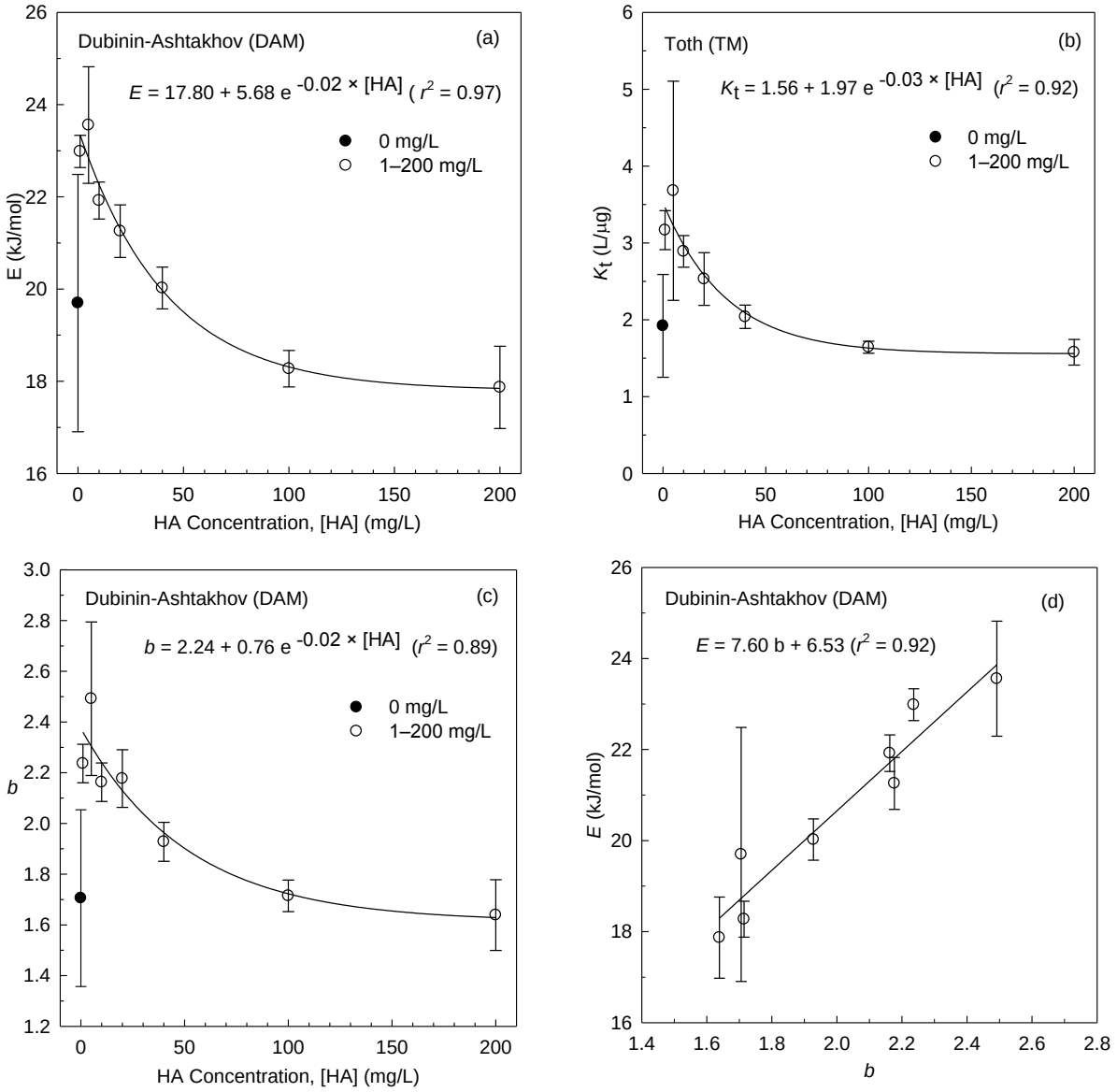

Regarding surface heterogeneity, both the Toth exponent *t* (Figure 4.16b) and the DAM parameter *b* decreased exponentially with increasing HA concentration (Figure 4.17c; the only purpose of the fit was to describe trends numerically and allow easy comparisons). Although *b* is often considered to be only a fitting parameter, it has previously been suggested to be inversely related to sorbent heterogeneity[42, 43], which is also observed in the present results. Both models thus suggest that the CNT surface became more heterogeneous with increasing HA loading, which may be explained by the variety of functional groups

introduced by HA molecules, such as carbonyl, carboxyl, aromatic, acetal, heteroaliphatic, and aliphatic groups (Table 4.1). With increasing HA concentration, the quantity of functional groups will thus have increased, probably leading to the observed increase in CNT surface heterogeneity. Our observations are consistent with those of Koelmans et al.[12], who observed increasing nonlinearity of the "intrinsic" isotherms of polychlorinated biphenyl sorption to charcoal with increasing HA loading. It is important to note that despite the observed increase in heterogeneity with increasing HA, the highest surface heterogeneity was observed for CNTs without HA, as indicated by smaller *t* and *b* values at 0 mg HA/L (0.18 and 1.71, respectively) than at 1–200 mg HA/L (0.30–0.20 and 2.24–1.64, respectively, Table 4.7). Similarly, the results of Zhang et al.[8] suggested that surface heterogeneity of CNTs was reduced after adding 4 mg DOC/L (based on the increase in Freundlich isotherm linearity). The authors hypothesized that (i) DOC preferably adsorbed to high energy adsorption sites on the CNT surface and/or (ii) the aggregation structure of CNTs was changed. The present results support the former hypothesis, with sites of high energy (here mainly generated by sonication) being the main source of surface heterogeneity.

During their life cycle, CNTs can undergo various dispersion/aggregation events that will significantly impact their sorption behavior. The present results demonstrate that both the nature (e.g., sonication or presence of dispersants) and the chronological sequence of the dispersion events are essential in determining the extent and irreversibility of the effects on sorption behavior of organic chemicals.

4.5 Literature Cited

(1) Cai, Y. Q.; Jiang, G. B.; Liu, J. F.; Zhou, Q. X. Multi-walled carbon nanotubes packed cartridge for the solid-phase extraction of several phthalate esters from water samples and their determination by high performance liquid chromatography. *Anal. Chim. Acta* **2003**, *494*, (1-2), 149-156.

(2) Hofmann, T.; von der Kammer, F. Estimating the relevance of engineered carbonaceous nanoparticle facilitated transport of hydrophobic organic contaminants in porous media. *Environmental Pollution* **2009**, *157*, (4), 1117-1126.

(3) Kohler, A. R.; Som, C.; Helland, A.; Gottschalk, F. Studying the potential release of carbon nanotubes throughout the application life cycle. *J Clean Prod* **2008**, *16*, (8-9), 927-937.

(4) Hyung, H.; Fortner, J. D.; Hughes, J. B.; Kim, J. H. Natural organic matter stabilizes carbon nanotubes in the aqueous phase. *Environ. Sci. Technol.* **2007**, *41*, (1), 179-184.

(5) Chappell, M. A.; George, A. J.; Dontsova, K. M.; Porter, B. E.; Price, C. L.; Zhou, P. H.; Morikawa, E.; Kennedy, A. J.; Steevens, J. A. Surfactive stabilization of multi-walled carbon nanotube dispersions with dissolved humic substances. *Environ. Pollut.* **2009**, *157*, (4), 1081-1087.

(6) Chen, J. Y.; Chen, W.; Zhu, D. Adsorption of nonionic aromatic compounds to single-walled carbon nanotubes: effects of aqueous solution chemistry. *Environ. Sci. Technol.* **2008**, *42*, (19), 7225-7230.

(7) Wang, X. L.; Tao, S.; Xing, B. S. Sorption and competition of aromatic compounds and humic acid on multiwalled carbon nanotubes. *Environ. Sci. Technol.* **2009**, *43*, (16), 6214-6219.

(8) Zhang, S. J.; Shao, T.; Bekaroglu, S. S. K.; Karanfil, T. Adsorption of synthetic organic chemicals by carbon nanotubes: Effects of background solution chemistry. *Water Res.* **2010**, *44*, (6), 2067-2074.

(9) Kah, M.; Zhang, X. R.; Jonker, M. T. O.; Hofmann, T. Measuring and modelling adsorption of PAHs to carbon nanotubes over a six order of magnitude wide concentration range. *Environ. Sci. Technol.* **2011**, *45*, (14), 6011-6017.

(10) Schwyzer, I.; Kaegi, R.; Sigg, L.; Magrez, A.; Nowack, B. Influence of the initial state of carbon nanotubes on their colloidal stability under natural conditions. *Environ. Pollut.* **2011**, *159*, (6), 1641-1648.

(11) Jonker, M. T. O.; Koelmans, A. A. Polyoxymethylene solid phase extraction as a partitioning method for hydrophobic organic chemicals in sediment and soot. *Environ. Sci. Technol.* **2001**, *35*, (18), 3742-3748.

(12) Koelmans, A. A.; Meulman, B.; Meijer, T.; Jonker, M. T. O. Attenuation of polychlorinated biphenyl sorption to charcoal by humic acids. *Environmental Science & Technology* **2009**, *43*, (3), 736-742.

(13) Wang, S. G.; Liu, X. W.; Gong, W. X.; Nie, W.; Gao, B. Y.; Yue, Q. Y. Adsorption of fulvic acids from aqueous solutions by carbon nanotubes. *J. Chem. Technol. Biotechnol.* **2007**, *82*, (8), 698-704.

(14) Wang, X. L.; Shu, L.; Wang, Y. Q.; Xu, B. B.; Bai, Y. C.; Tao, S.; Xing, B. S. Sorption of Peat Humic Acids to Multi-Walled Carbon Nanotubes. *Environ. Sci. Technol.* **2011**, *45*, (21), 9276-9283.

(15) Chiou, C. T.; Malcolm, R. L.; Brinton, T. I.; Kile, D. E. Water Solubility Enhancement of Some Organic Pollutants and Pesticides by Dissolved Humic and Fulvic-Acids. *Environ. Sci. Technol.* **1986**, *20*, (5), 502-508.

(16) Doucette, W. J. Quantitative structure-activity relationships for predicting soil-sediment sorption coefficients for organic chemicals. *Environ. Toxicol. Chem.* **2003**, *22*, (8), 1771-1788.

(17) Kopinke, F. D.; Georgi, A.; MacKenzie, K. Sorption of pyrene to dissolved humic substances and related model polymers. 1. Structure-property correlation. *Environ. Sci. Technol.* **2001**, *35*, (12), 2536-2542.

(18) Krop, H. B.; van Noort, P. C. M.; Govers, H. A. J. Determination and theoretical aspects of the equilibrium between dissolved organic matter and hydrophobic organic micropollutants in water (K-doc). *Rev Environ Contam T* **2001**, *169*, 1-122.

(19) Pan, B.; Ghosh, S.; Xing, B. S. Dissolved organic matter conformation and its interaction with pyrene as affected by water chemistry and concentration. *Environ. Sci. Technol.* **2008**, *42*, (5), 1594-1599.

(20) Bohling, B. Variations in grain size analysis with a time-of-transition laser sizer (Galai CIS-50) using a gravitational flow system. *Part Part Syst Char* **2005**, *21*, (6), 455-462.

(21) Tsai, C. H. An assessment of a time-of-transition laser sizer in measuring suspended particles in the ocean. *Mar Geol* **1996**, *134*, (1-2), 95-112.

(22) Yang, K.; Zhu, L. Z.; Xing, B. S. Adsorption of polycyclic aromatic hydrocarbons by carbon nanomaterials. *Environ. Sci. Technol.* **2006**, *40*, (6), 1855-1861.

(23) Pikaar, I.; Koelmans, A. A.; van Noort, P. C. M. Sorption of organic compounds to activated carbons. Evaluation of isotherm models. *Chemosphere* **2006**, *65*, (11), 2343-2351.

(24) Allen-King, R. M.; Grathwohl, P.; Ball, W. P. New modeling paradigms for the sorption of hydrophobic organic chemicals to heterogeneous carbonaceous matter in soils, sediments, and rocks. *Adv Water Resour* **2002**, *25*, (8-12), 985-1016.

(25) Jantunen, A. P. K.; Koelmans, A. A.; Jonker, M. T. O. Modeling polychlorinated biphenyl sorption isotherms for soot and coal. *Environ. Pollut.* **2010**, *158*, (8), 2672-2678.

(26) Chen, J. L.; Chen, Q. H.; Ma, Q. Influence of surface functionalization via chemical oxidation on the properties of carbon nanotubes. *J. Colloid Interface Sci.* **2012**, *370*, 32-38.

(27) Arai, M.; Kanamaru, M.; Matsumura, T.; Hattori, Y.; Utsumi, S.; Ohba, T.; Tanaka, H.; Yang, C. M.; Kanoh, H.; Okino, F.; Touhara, H.; Kaneko, K. Pore characterization of assembly-structure controlled single wall carbon nanotube. *Adsorption* **2007**, *13*, (5-6), 509-514.

(28) Xing, Y. C.; Li, L.; Chusuei, C. C.; Hull, R. V. Sonochemical oxidation of multiwalled carbon nanotubes. *Langmuir* **2005**, *21*, (9), 4185-4190.

(29) Cho, H. H.; Smith, B. A.; Wnuk, J. D.; Fairbrother, D. H.; Ball, W. P. Influence of surface oxides on the adsorption of naphthalene onto multiwalled carbon nanotubes. *Environ. Sci. Technol.* **2008**, *42*, (8), 2899-2905.

(30) Yang, K.; Xing, B. S. Adsorption of organic compounds by carbon nanomaterials in aqueous phase: Polanyi theory and its application. *Chem. Rev.* **2010**, *110*, (10), 5989-6008.

(31) Terzyk, A. P.; Chatlas, J.; Gauden, P. A.; Rychlicki, G.; Kowalczyk, P. Developing the solution analogue of the Toth adsorption isotherm equation. *J. Colloid Interface Sci.* **2003**, *266*, (2), 473-476.

(32) Lee, K.; Wu, Z. J.; Joo, H.; Ahn, L. S.; Haam, S.; Kim, J. H. Organic dye adsorption on mesoporous hybrid gels. *Chem. Eng. J.* **2004**, *102*, (3), 277-282.

(33) Mckay, G.; Ho, Y. S.; Porter, J. F. Equilibrium isotherm studies for the sorption of divalent metal ions onto peat: copper, nickel and lead single component systems. *Water Air Soil Poll* **2002**, *141*, (1-4), 1-33.

(34) Moon, H.; Shim, W. G.; Lee, S. G.; Hwang, M. J.; Park, K. H.; Kim, S. C. Adsorption and thermo desorption characteristics of hydrocarbons on single walled carbon nanotubes. *J Nanosci Nanotechno* **2011**, *11*, (2), 1518-1521.

(35) Sener, S.; Ozyilmaz, A. Adsorption of naphthalene onto sonicated talc from aqueous solutions. *Ultrason. Sonochem.* **2010**, *17*, (5), 932-938.

(36) Laurent, J.; Casellas, M.; Dagot, C. Heavy metals uptake by sonicated activated sludge: relation with floc surface properties. *J. Hazard. Mater.* **2009**, *162*, (2-3), 652-660.

(37) van Noort, P. C. M.; Pikaar, I.; Koelmans, A. A. Sorption of organic compounds to activated carbons. Evaluation of isotherm models. *Chemosphere* **2006**, *65*, (11), 2343-2351.

(38) Vichchulada, P.; Cauble, M. A.; Abdi, E. A.; Obi, E. I.; Zhang, Q. H.; Lay, M. D. Sonication power for length control of single-walled carbon nanotubes in aqueous suspensions used for 2-dimensional network Formation. *J. Phy. Chem. C.* **2010**, *114*, (29), 12490-12495.

(39) Burnham, K. P.; Anderson, D. R., *Model Selection and Multimodel Inference: A Practical Information-Theoretic Approach*. 2nd ed.; Springer-Verlag: 2002.

(40) deJonge, H.; MittelmeijerHazeleger, M. C. Adsorption of CO_2 and N_2 on soil organic matter: Nature of porosity, surface area, and diffusion mechanisms. *Environ. Sci. Technol.* **1996**, *30*, (2), 408-413.

(41) Wang, X. L.; Lu, J. L.; Xing, B. S. Sorption of organic contaminants by carbon nanotubes: influence of adsorbed organic matter. *Environ. Sci. Technol.* **2008**, *42*, (9), 3207-3212.

(42) Carrascomarin, F.; Lopezramon, M. V.; Morenocastilla, C. Applicability of the Dubinin Radushkevich equation to CO_2 adsorption on activated carbons. *Langmuir* **1993**, *9*, (11), 2758-2760.

(43) Dobruskin, V. K. Micropore volume filling. A condensation approximation approach as a foundation to the Dubinin-Astakhov equation. *Langmuir* **1998**, *14*, (14), -3846.

5. Influence of Surface Chemistry

Influence of Surface Chemistry on Sorption of Pyrene to Carbon Nanotubes

Zhang, X. R.; Kah, M.; Hofmann, T.

To be submitted to *Environ. Sci. Technol.*

5.1 Abstract

Surface functionalization has been shown to exert a pronouced effect on the colloidal stability of carbon nanotubes (CNTs) but the effects on sorption of non polar compounds remain poorly understood. We applied a passive sampling method to investigate the influence of dispersion by sonication and presence of natural dispersants on sorption of pyrene to CNTs with different functional groups. Sorption increased following the order: non- < OH- < COOH- < NH_2-functionalized CNTs, which is consistent with their dispersion status. The enhancement of π–π and *n*–π electron donor accepter (EDA) by functional groups may overwhelm the effect of water competition and result in the overall enhancement of sorption affinity with functionalization. Sonication increased both sorption affinity and capacity of all types of CNTs. Interstingly, after sonication the effect of functional groups disappeared and sorption isotherms were similar for all four types of CNTs. This suggests that the effect of sonication on pore structures plays a more important role on sorption than the effect of functional groups on surface chemistry. The presence of HA (0–40 mg/L) decreased sorption for all types of CNTs, especially when combined with a sonication pre-treatment. The decrease in sorption by HA was the greatest for COOH- functionalized CNTs and may be related to a higher affinity of HA to COOH-CNTs. The present results contribute to an improved understanding of the sorption behavior of functionlized CNTs in different dispersion status.

5.2 Introduction

CNTs exhibit unique properties and have potential applications in many areas including material sciences, analytical chemistry and environmental sciences.[1-3] Surface modifications of CNTs can be considered to improve mechanical and chemical properties to suit a particular purpose. For example, functionalized CNTs (e.g., amine founctionalization[4]) have played an important role in the development of nanocomposite materials.[5] Functionalized CNTs by

acid,[6] solvent[7] or gas[8] can be also applied in the trace analysis of organic compounds.[7, 8] Besides intentional modification, CNTs surface can be modified when they are exposed to an oxidative environment.[9] Surface functionalization increases the wettability of CNT surfaces, and consequently makes CNT more hydrophilic,[10] with possible impact on the CNTs sorption behavior. Understanding the influence of surface chemistry on the sorption behavior of CNTs is thus important to evaluate the materials' potential application as well as environmental fate.

A number of studies investigated the influence of CNTs surface chemistry on their sorption behavior. Both increase and decrease in sorption by CNT functional groups were reported for nonpolar compounds. On the one hand, an acid treatment leading to the oxidation of CNTs surfaces was shown to reduce sorption capacity of naphthalene and phenanthrene, due to the competition with water molecules.[11, 12] Higher level of oxidation on CNTs surfaces results in lower sorption capacity.[7] On the other hand, Gotovac et al.[13] and Lu et al.[14] observed that sorption of two PAHs (i.e., phenanthrene and tetracene) and benzene were enhanced by surface oxygen groups on CNTs, respectively. The authors suggested that surface functional groups can enhance the π–π interactions between the aromatic rings of the sorbate and CNTs. Both suppression and enhancement processes probably occur simultaneously and their respective contribution may depend on the nature of sorbate (i.e., the number of aromatic rings).

Substitutions affect organic compounds properties, such as solubility, dissociation constant and chemical reactivity. Similarly, functional groups on CNTs may also affect CNTs properties such as colloidal behaviors and surface charge. Different functional groups may thus exert different influence on sorption. However, the effects of different functionalizations has not been systematically investigated..

To date, examined functional groups are limited to oxygen groups introduced by wet chemical treatment using H_2SO_4, HNO_3, $KMnO_4$ or their mixture. [11-17] Plasma treatment is widely used in industry[18] to functionalize CNTs in dry conditions and using gases such as O_2, N_2 or NH_3 in the plasma reactor.[19, 20] Results on carbon nanofibers suggested that plasma and wet chemical functionalization result in different properties of the materials (e.g., structure, functionalization homogeneity).[21] Therefore, plasma functionalization CNTs may have different effects on the sorption behavior of CNTs relative to wet chemical treatment.

Even though surface functionalization was shown to exert a pronounced effect on colloidal stability, CNTs are only partially dispersed if they only are treated by shaking.[22, 23] Sonication is an effective method to mechanically break down the CNT aggregates. Sonication is also

commonly applied together with polymers[24, 25], surfactants[26, 27] and HA[28] to produce CNT stable suspensions. In a previous study, we showed that sonication increases pyrene sorption to CNTs, but also enhances the suppression effect of HA on sorption.[29] The impact of those two important factors was never examined for functionalized CNTs. HA contain carboxylic and phenolic groups that may react with functional groups on CNTs. The influence of HA on the sorption behavior of functionalized CNTs may thus differ from that on non-functionalized CNTs (non-CNTs).

Passive sampling method allows studying sorption of PAHs onto both aggregated[30] and dispersed CNTs.[29, 31] In the present study, we applied passive sampling method (POM-SPE) to investigate the influence of functional groups as well as the dispersion on sorption behavior on CNTs. The objectives were to investigate the effects of (i) CNT surface functional groups, (ii) CNT pretreatments (sonication and shaking) and (iii) natural dispersants (HA) on the sorption characteristics of the CNT system. CNT suspensions were extensively characterized by microscopic, spectroscopic and size distribution measurements in order to support mechanistic interpretations of the results.

5.3 Materials and Methods

5.3.1 Sorbents and Chemicals

POM sheet, HA, non-CNTs, pyrene and pyrene-d10 were used as described in Chapter 3 and 4. Three types of functionalized multiwalled CNTs including hydroxylated CNTs (OH-CNTs), carboxylated CNTs (COOH-CNTs), and aminoated CNTs (NH_2-CNTs) were purchased from Cheaptubes (Brattleboro, USA). All four types of CNTs types were synthesized by chemical vapor deposition, have purities >99% and exhibit outer mean diameter ranging 13–18 nm. OH-CNTs and COOH-CNTs were functionalized with oxygen based gas plasma, and NH_2-CNTs were treated with nitrogen plasma. Functionalized CNTs contains 7±1.5 wt% functional groups according to XPS and titration results provided by the supplier.

5.3.2 Sorption Experiments

All experiments were carried out at 20±1 °C and using background solution prepared with 25 mg/L NaN_3 as biocide (pH 7.06). One milligram of CNTs and 50 mL of HA solution (0, 5 and 40 mg/L) were added to glass vials. Samples were then pre-treated according to one of the following two protocols: (i) shaking by hand for 1 min (Bulk/CNTs), (ii) sonication for 2 h (So/CNTs). When sonicating, 20 sample vials were immersed into the sonication bath

(Bandelin sonorex super rk106 bath, 35 kHz, diameter 24.5 cm). A POM strip (approximately 100 mg) was subsequently added to each sample and pyrene or multi-PAH standard was spiked. The volume of methanol (spiking solvent) was kept at 0.16% for all samples to minimize solvent effects. For each of the two pre-treatments, sorption coefficients (K_{CNT}) were measured for a single initial concentration of pyrene (50 µg/L). In addition, full sorption isotherms for pyrene were measured at 0 mg/L HA (pyrene equilibrium concentration ranged over five orders of magnitude from 0.0001 to 20 µg/L). All vials were horizontally shaken (180 rpm) for 28 d to ensure equilibration. POM strips were then taken out of the vials, rinsed with deionized water and wiped with a wet tissue. They were then extracted with methanol by accelerated solvent extraction (ASE 200, Dionex, USA; 1500 psi, 100 °C), with pyrene-d10 as internal standard. Extracts were concentrated under N_2 prior to GC-MS analysis, as described in our previous study (Chapter 3 and 4). Blanks without pyrene were prepared for each pre-treatment as method blanks and used as characterization samples in the following section. Control samples with pyrene indicated that losses were < 6% after 28 d of shaking. Sorption was calculated based on mass balance reported in our previous study.[29]

5.3.3 Characterization of CNTs

For each type of CNTs and pre-treatment, CNTs were imaged by scanning electron microscopy (SEM). Particular attention was paid to maintaining the structure of the CNT aggregates as they occurred in the sorption test. The absorbance of CNT suspensions was characterized by UV-Vis spectrometry at 800 nm absorbance (Varian Cary 50 UV-Vis spectrophotometer). Size distribution of So/CNTs was determined using a particle size analyzer (Eyetech) based on a time of transition principle. Size distribution of Bulk/CNTs was measured by laser light scattering with a Malvern Mastersizer (MasterSizer 2000). The hydrodynamic diameter of CNT aggregates remaining in suspension after 2 d of settling was measured by dynamic light scattering (DLS, Malvern ZetaSizer Nano). The surface area of the each type of CNTs (pre-treated by shaking only) was measured by the BET-nitrogen method.

5.3.4 Sorption Models

Among the six models (i.e., FM, LM, DLM, DMM, DAM, TM) tested, the DAM and TM were demonstrated to be the two best models to describe sorption isotherms for both aggregated and dispersed states (Chapter 4). Therefore, DAM and TM were fit to the experimental data. Models equations, parameters and description are available in Table 2.3 of

Chapter 2. All statistical tests and parameter optimizations were performed with *SigmaPlot 11.0* for Windows.

5.4 Results and Discussion

5.4.1 Characterization results

5.4.1.1 Images

Shaking alone did not affect the visual aspect of any of the CNTs suspensions (Figure 5.1) whereas much darker suspensions were obtained after sonication. SEM images of four types of CNTs pretreated with shaking only (Figure 5.2a) show large aggregates with a size distribution ranging 40–500 µm. Images at the largest scale (500 µm scale) indicated that the size of the aggregates decreased in the order: non- > OH- > COOH- > NH_2- functionalized CNTs (sample preparation was identical for all samples; other areas of the stubs that are not shown consistently followed the same trend). SEM images of sonicated COOH-CNTs (Figure 5.2b, images of cross section, Figure 5.2 c) suggest that sonication and the presence of HA had similar effects that those observed for non-CNTs: pore enlargement and debundling, respectively.

The presence of HA also enhanced dispersion, but only when combined with sonication. It was initially hypothesized that functionalized CNTs have much higher solubility than non-CNTs, and that they would be easily dispersed by shaking only (this was also suggested by the supplier). However, the aspect of the suspensions indicated that large aggregates were still present. This may be due to the relatively low functional group content. These results are consistent with previous studies. Schwyzer et al.[22] reported that in the presence of NOM and surfactant, mild shaking for 20 d was not sufficient to separate and suspend CNTs effectively (only 1% suspended), whereas sonication resulted in 65% of suspended CNTs. Zhou et al.[23] reported that in the presence of peat HA, both non- and COOH-functionalized CNTs do not form stable suspension by shaking for 5 d.

Differences in the visual aspect of some suspensions cannot be explained by the types of CNTs, pre-treatment or presence of HA (e.g., non-CNTs in the presence of 40 mg/L HA). The sonication treatment was performed for 20 tubes simultaneously and it is possible that different locations in the sonication bath result in different sonication energy received by the suspensions. The effect of sonication is known to depend on the time, energy and

temperature.[32] The darker vial for non-CNTs at 40 mg/L HA may be due to the location of the tubes in the sonication bath. A systematic study of this effect deserves further work.

Figure 5.1. *Pictures of the suspensions of CNTs without and with three functionalization groups (i.e., non-CNTs, OH-CNTs, COOH-CNTs, NH_2-CNTs) pretreated with shaking and sonication. The pictures were taken directly after pretreatment.*

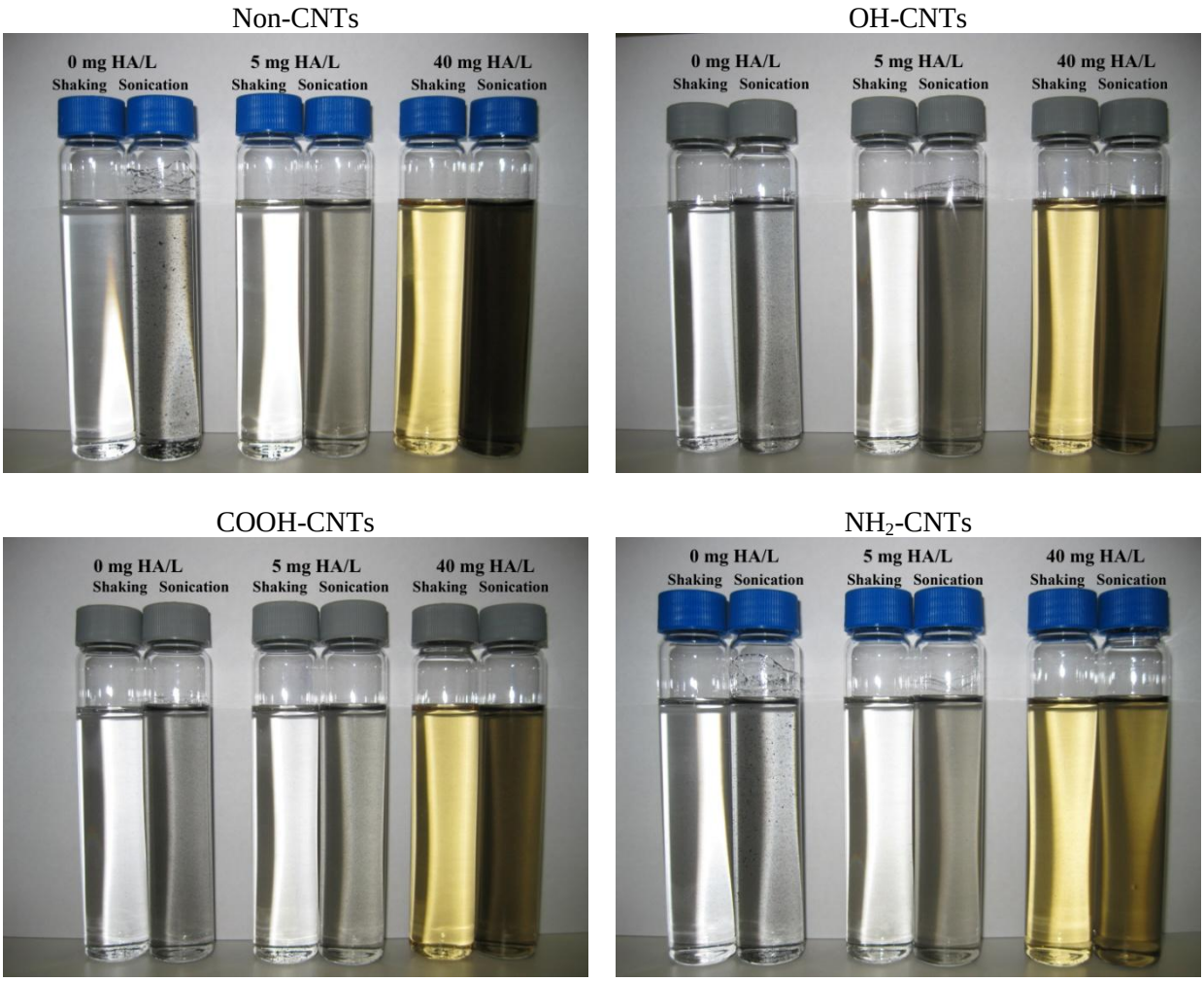

5.4.1.2 Absorbance of CNTs

CNT aggregates are hardly active in the wavelength region between 200 and 1200 nm.[33] Figure 5.3a shows that the absorbance remained very low for Bulk/CNTs and followed the order non- < OH- < COOH- < NH_2- functionalized CNTs, for all HA concentrations investigated. This order is negatively related with the size of the aggregates estimated by SEM.

Figure 5.2. *Scanning electron microscope (SEM) images of four types of CNTs without and with three functionalization groups (i.e., non-CNTs, OH-CNTs, COOH-CNTs, NH_2-CNTs). Images were taken after sorption experiment.*

(a) Four types of CNTs pretreated with shaking (Bulk/CNTs) in the absence of HA

non-CNTs

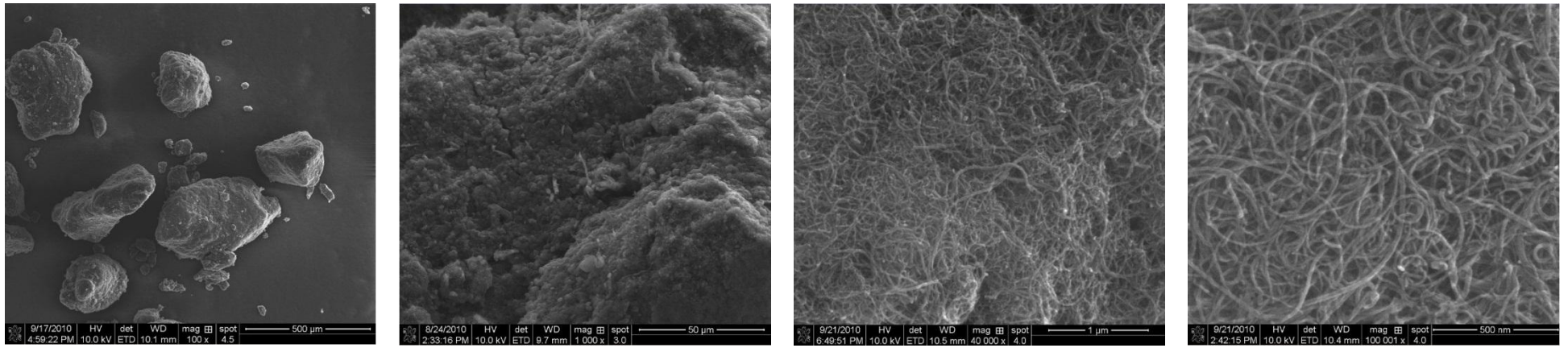

OH-CNTs

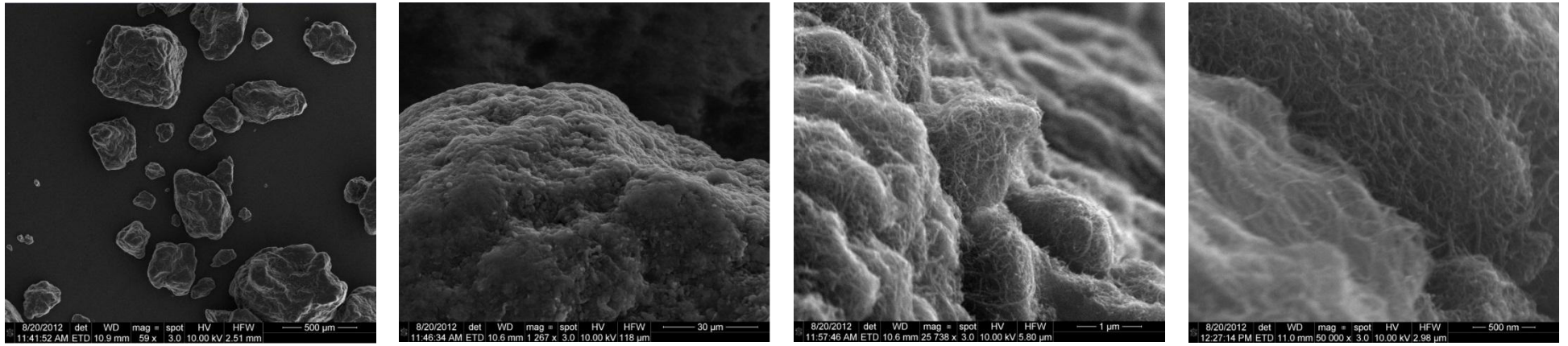

COOH-CNTs

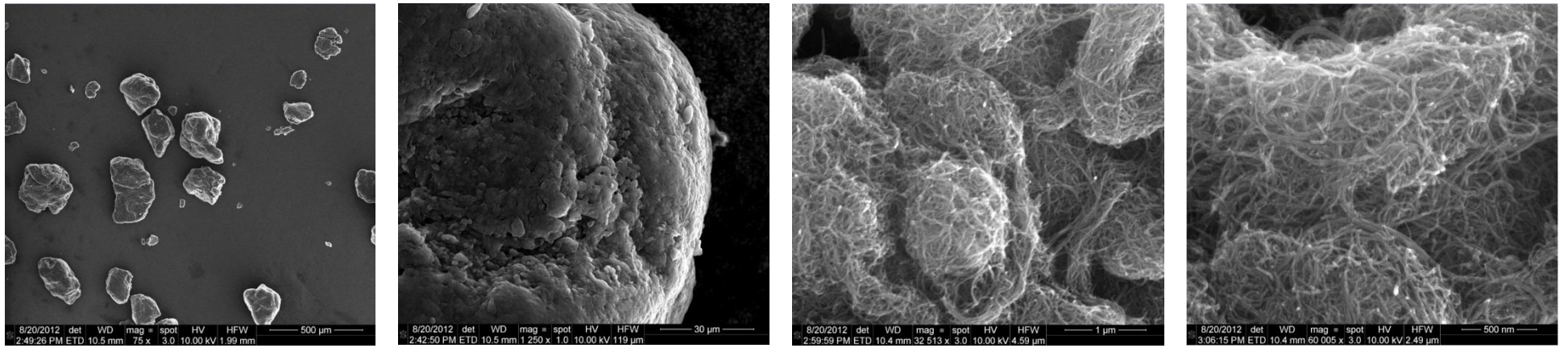

NH_2-CNTs

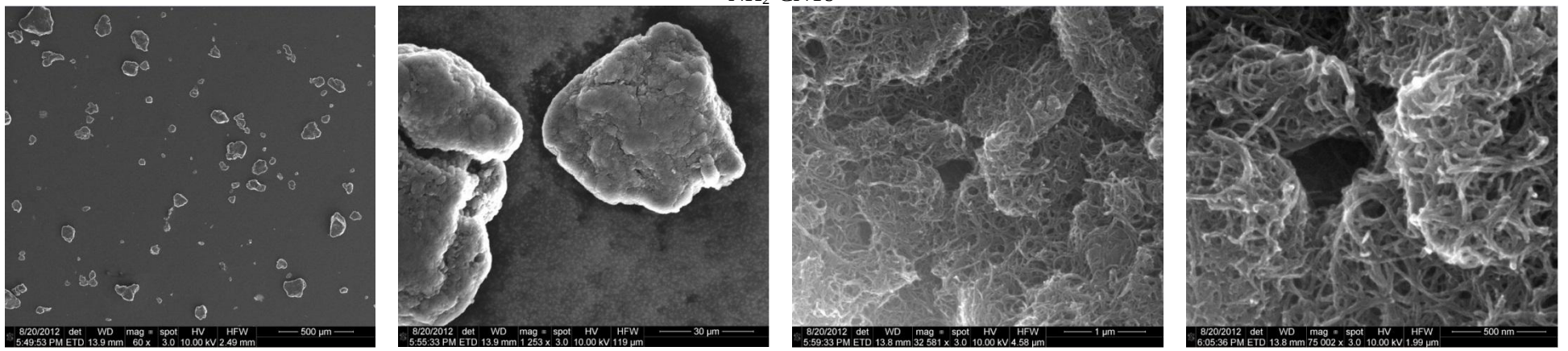

(b) COOH-CNTs pretreated with sonication (So/CNTs) in the presence of 0–40 mg HA/L

0 mg HA/L

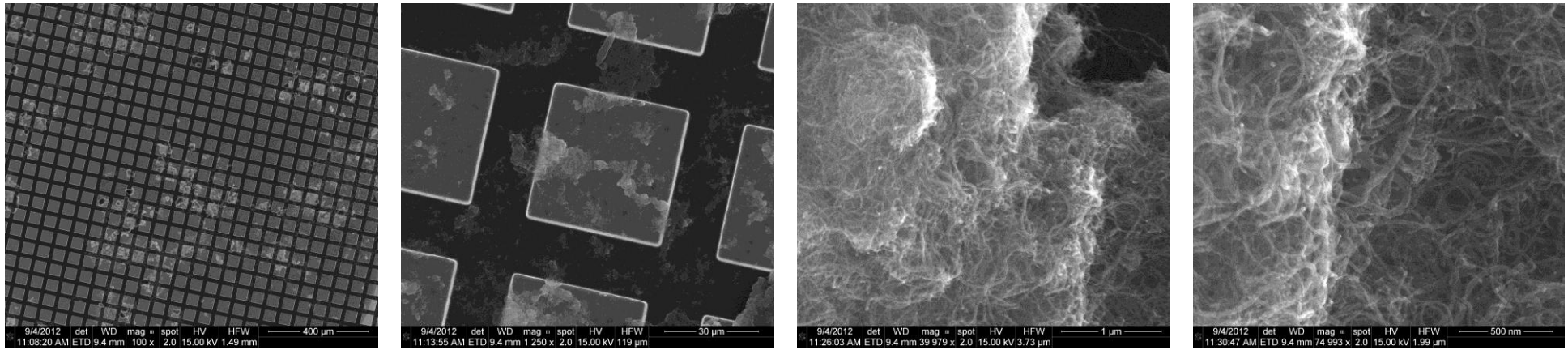

5 mg/L HA/L

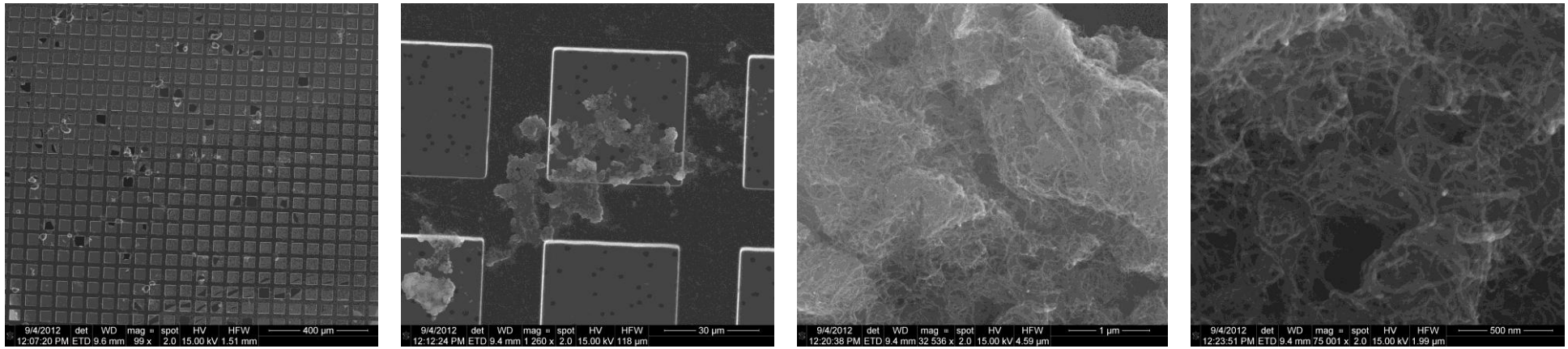

40 mg/L HA/L

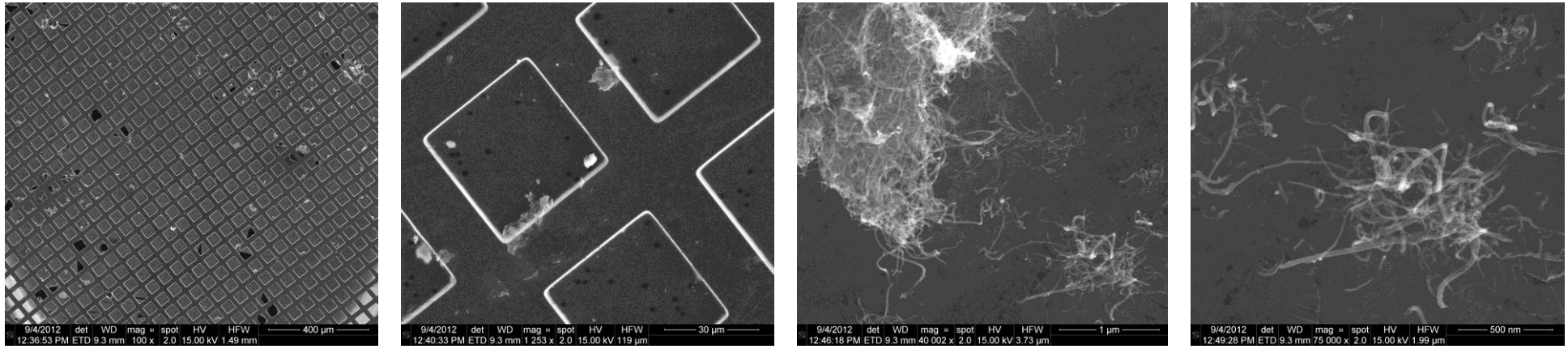

(c) Cross sections of COOH-CNTs pretreated with shaking and sonication in the absence of HA

Shaking

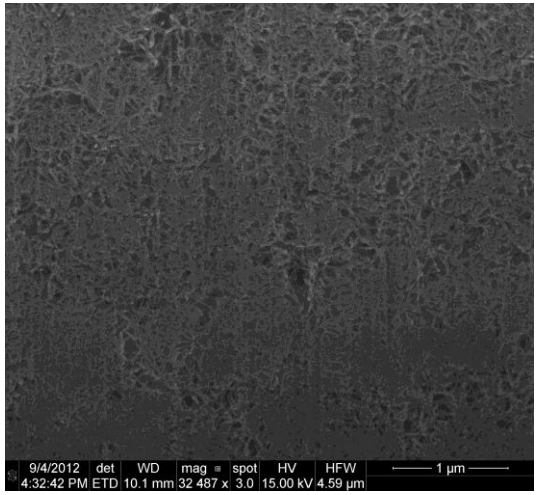

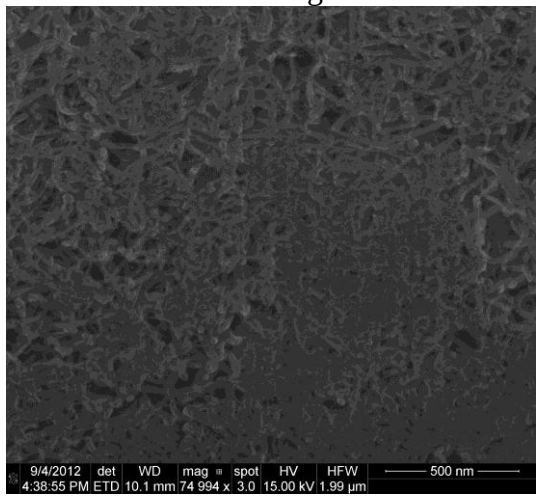

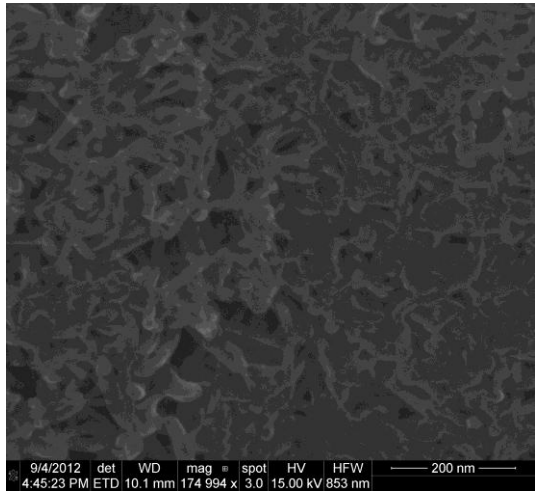

Sonication

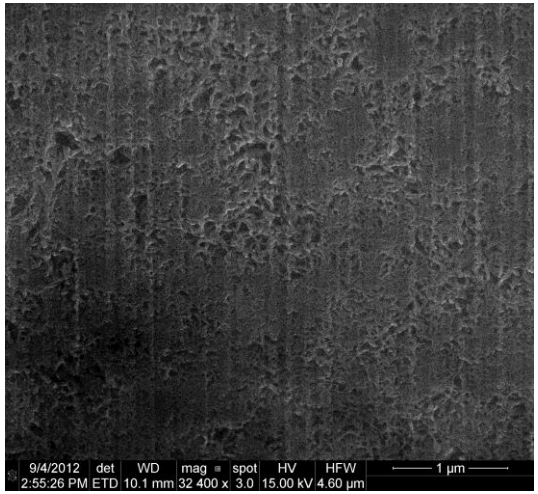

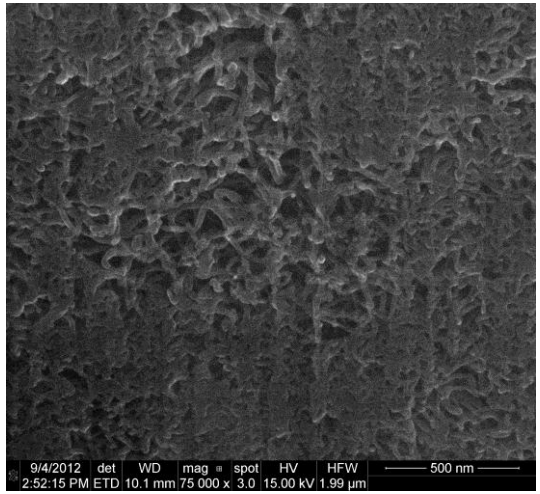

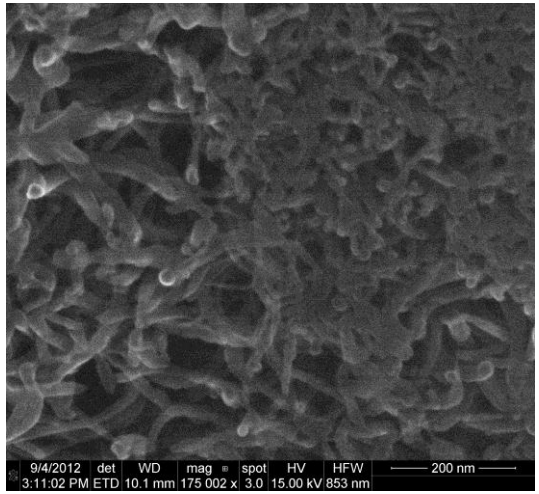

Sonication efficiently dispersed the four types of CNTs, as indicated by higher absorbance value for So/CNTs than for Bulk/CNTs (Figure 5.3 a-b). Absorbance was lower for the So/CNTs at the end of the sorption experiment (i.e., 28 d shaking) than directly after sonication treatment, especially at low HA concentrations (i.e., 0 and 5 mg HA/L, Figure 5.3b). This indicated that re-aggregation occurred after additional shaking for all four types of So/CNTs investigated. Differently from the Bulk/CNTs, the absorbance for So/CNTs followed the order: non- < NH_2- < COOH- < OH- functionalized CNTs, for all HA concentrations investigated.

Figure 5.3*. Absorbance of four types of CNTs pretreated by (a) hand shaking and (b) 2 h sonication in the presence of three HA concentrations: 0, 5 and 40 mg/L. The weight of CNTs was 1 mg and the volume of solution in each vial was 50 mL.*

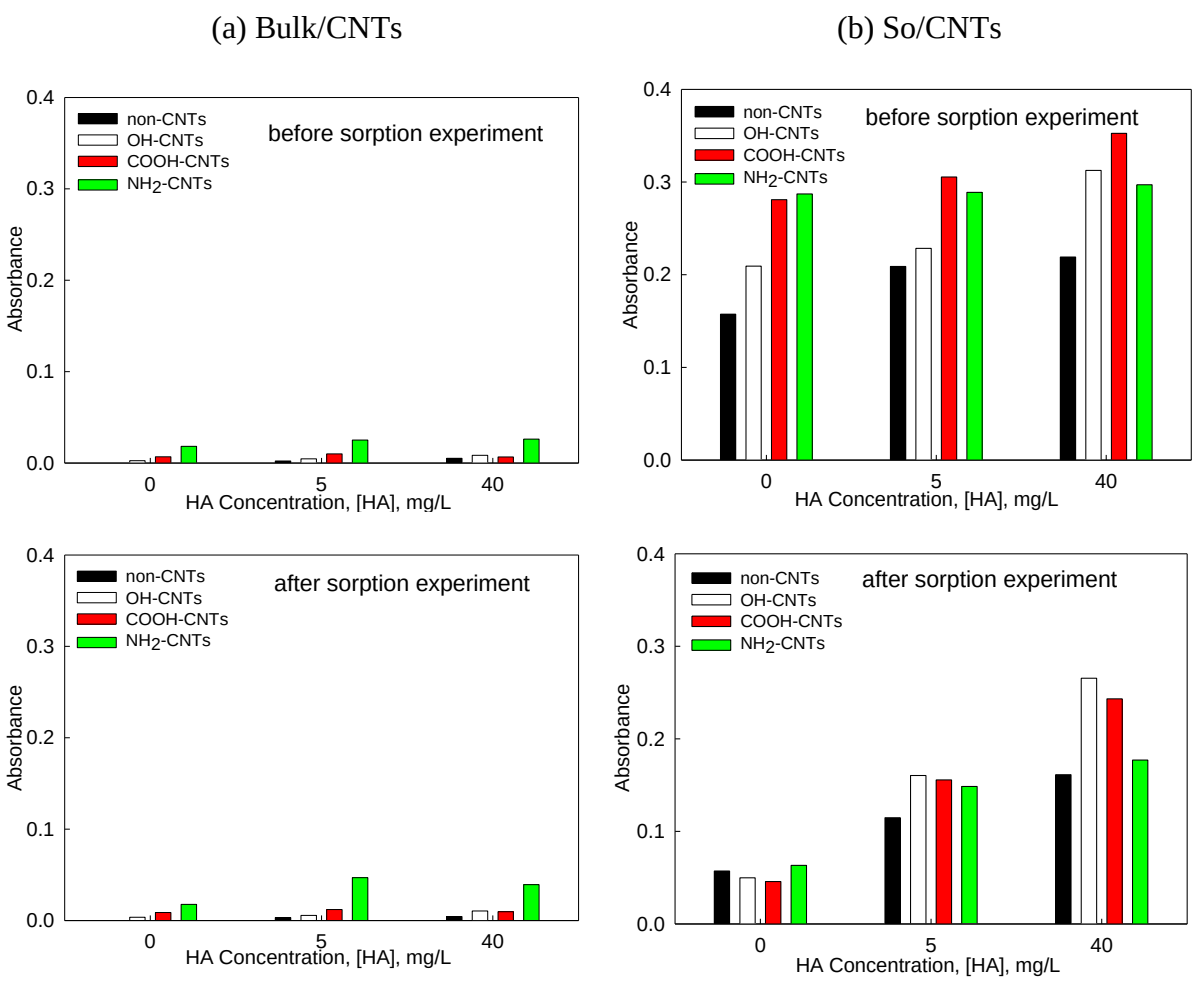

5.4.1.2 Re-aggregation of So/CNTs

With additional shaking, re-aggregation occurred for all So/CNTs (non-CNTs and the three functionalized CNTs, Figure 5.4). Directly after sonication, all types of CNTs exhibited similar size distributions (i.e., 3±2 μm, average size by Eyetech) at the three HA concentration investigated. At the end of the sorption experiment, larger sizes measured indicate that re-aggregation occurred at the two low HA investigated (e.g., at 0 mg HA/L, So/CNT size ranged 15–25 μm). Large standard deviations (i.e., about 10 μm) do not allow differences between CNTs types to be analyzed.

The size of Bulk/CNTs could not be measured by Eyetech because large aggregates quickly settled down to the bottom of the measurement cell. Measurements by Master sizer gave size distributions for the four types of Bulk/CNTs ranging 12–90 μm. There was no significant difference between the four types of CNTs. During the measurement with the Master sizer, the Bulk/CNTs attached to the plastic tubing, which may cause large uncertainties of the measurement.

Figure 5.4*. Size of four types of CNTs pretreated by 2 h sonication in the presence of three HA concentrations: 0, 5 and 40 mg/L (a) before and (b) after sorption experiment.*

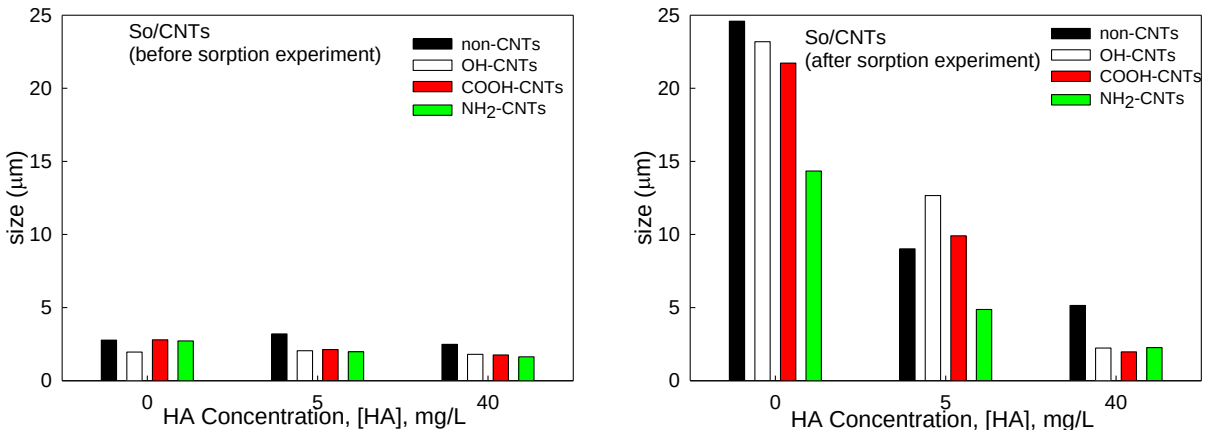

5.4.1.3 Size in the supernatant

DLS gives the size distribution of the particles remaining in suspension after 2 d settling. The presence of HA resulted in much smaller size (average hydrodynamic diameter, 0.2–0.3 μm) compared with CNTs in the absence of HA (4–12 μm, Figure 5.5). The quantity of Bulk/CNTs remaining in suspension was too low to permit measurement by DLS.

***Figure 5.5**. Size (average hydrodynamic diameter, nm) of four types of CNTs pretreated by 2 h sonication (So/CNTs) in the presence of three HA concentrations: 0, 5 and 40 mg/L, the measurement was conducted after settling the suspension for 2 days.*

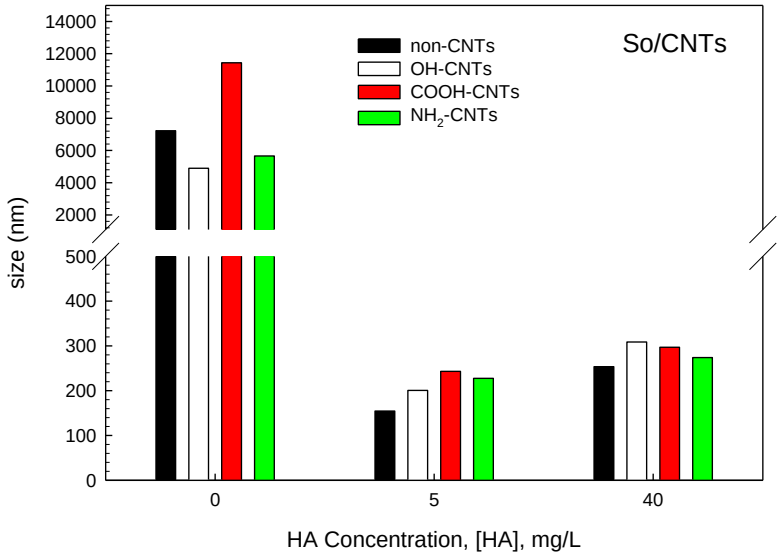

5.4.1.4 Zeta potential

The zeta potential can represent the surface charge of CNTs. At the experimental pH (neutral), all types of CNTs had negative zeta potential. For Bulk/CNTs (pretreated by shaking only), the zeta potentials were small (absolute value) and followed the order: non- < OH- < COOH- < NH_2- functionalized CNTs (Table 5.1). The surface charge of Bulk/CNTs is challenging to measure due to the small amount of the particles remaining in suspension (> 1 μm). Zeta potentials reported in the literature are always measured after sonicating the CNTs, in order to allow measurement.[34, 35] However, the zeta potential measured for So/CNTs may not reflect the surface charge of large Bulk/CNTs aggregates due to the possible modification of CNT surfaces (e.g., damage and/or oxidation) by sonication (as discussed in section 5.4.1).

***Table 5.1**. Zeta potential of four types of CNTs pretreated by (a) hand shaking (Bulk/CNTs) and (b) 2 h sonication (So/CNTs) in the presence of three HA concentrations: 0, 5 and 40 mg/L.*

	(a) Bulk/CNTs			(b) So/CNTs		
[HA]	0 mg/L	5 mg/L	40 mg/L	0 mg/L	5 mg/L	40 mg/L
Non-CNTs	-0.01	-15.7	-21.33	-20.01	-49.67	-59.00
OH-CNTs	-2.45	-24.97	-23.40	-23.22	-51.87	-59.90
COOH-CNTs	-3.02	-26.15	-33.63	-25.31	-52.87	-56.87
NH_2-CNTs	-5.21	-40.40	-41.00	-30.06	-51.03	-57.87

5.4.2 Effects of Functional Groups

5.4.2.1 Sorption capacity of Bulk/CNTs

Both the DAM and TM fitted the isotherms well for all types of CNTs and pre-treatments (Figure 5.6–5.7 and Table 5.2–5.3). The parameters derived for the two models are used below to discuss the discrepancies observed among Bulk/CNTs.

The maximum sorption capacities derived from DAM and TM were similar for the four types of Bulk/CNTs (p>0.05, Table 5.2). The amount of functionnal groups may explain this observation. The non-CNTs were acid-purified (i.e., sorbent used in Chapter 3 and 4), resulting in an O% content between 1.072% and 5.64 wt% (according to elemental analyzer and EDX measurement, respectively). It is thus possible that the O% content of non-CNTs was not significantly smaller than that of the three functionalized CNTs (i.e., 7 ± 1.5 wt% measured by XPS).

Some authors have proposed to normalize the maximum sorption capacity by the surface area, in order to further explore the influence of functional groups on sorption. For instance, Wu et al.[36] observed that oxidation increased the surface area as well as the sorption capacity of CNTs for ten polar and nonpolar compounds (including one PAH, naphthalene). Oxidation thus resulted in a decrease in the surface-normalized sorption capacity. The authors interpreted the results by the competition by water molecules. However, both increase [17, 36, 37] and decrease[12, 14, 17, 38] in BET-nitrogen surface area[12, 14, 17, 38] were reported for oxidized CNTs relative to non-CNTs. For Bulk/CNTs, the BET-nitrogen surface area measured in the present study were 641, 251, 186, 153 m^2/g for non-, OH-, COOH-, NH_2- functionalized CNTs. Hence, the surface-normalized sorption capacity followed the order non- < OH- < COOH- < NH_2- functionalized CNTs for both DAM and TM. The discrepancies between our result and the results from Wu et al.[36] may be due to the uncertainty associated with the BET-nitrogen adsorption method (as discussed in Chapter 4) and variation in surface-normalized sorption capacity should therefore be interpreted with care.

The competition by water molecules was also used to interpret the decrease in sorption capacity with CNTs oxidation for phenanthrene[39] and resorcinol.[40] The authors proposed that the oxidation groups formed H-bond with water, thus the organic compounds cannot be adsorbed due to the formation of water clusters. The possible occurrence of water competition is further discussed in the next section.

Figure 5.6*. Sorption isotherms of pyrene to four types of CNTs pre-treated by shaking in the absence of humic acids. The lines represent the fits by the Dubinin–Ashtakhov (DAM; ——) and Toth (TM; ·····) model.*

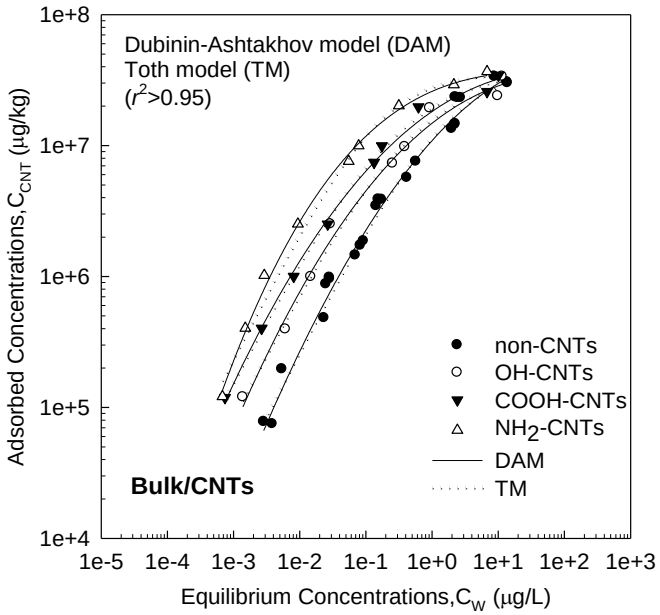

Table 5.2*. Fitting parameters ± standard error and r^2 for Ashtakhov and Toth models fitting the isotherms of pyrene on four types of CNTs pretreated by shaking.*

Shaking	DAM:				TM			
	log Q^0	E(kJ/mol)	b	r^2	log Q^0	Kt (L/μg)	t	r^2
Non-CNTs	7.65±0.07	15.3±0.64	1.93±0.13	0.96	7.65±0.14	0.74±0.09	0.62±0.13	0.95
OH-CNTs	7.55±0.08	18.4±0.93	2.24±0.25	0.96	7.55±0.12	1.67±0.35	0.58±0.13	0.97
COOH-CNTs	7.58±0.06	19.5±0.63	2.27±0.16	0.98	7.59±0.07	2.21±0.30	0.54±0.07	0.99
NH_2-CNTs	7.57±0.05	22.0±0.47	3.01±0.18	0.99	7.56±0.10	4.40±0.22	0.78±0.21	0.96

5.4.2.2 Sorption affinity of Bulk/CNTs

The presence of functional groups on CNTs greatly increased the sorption affinity in the order COOH- < OH- < NH_2- functionalized CNTs (p < 0.001, Table 5.2). Surface functionalization of CNTs can influence sorption via three mechanisms.

Firstly, surface functionalization can enhance the sorption of pyrene via π–π electron donor acceptor (EDA) interactions. Sorption of aromatic compounds to CNTs is mainly driven by π–π interactions. The OH, COOH and NH_2 functional groups can act as electron-donors while pyrene molecules can act as electron-acceptors. Electron donating groups can enhance the π-

polarity of surface aromatic rings of CNTs to form stronger π–π EDA interactions with aromatic molecules.[41] The surface charge reflected by zeta potential (absolute values) the sorption followed the same order (non- < OH- < COOH- < NH_2- functionalized CNTs,Table 5.1). The NH_2-functionalized CNTs are the most negatively charged, thus they can act as strongest electron donors among all the functionalizations and exert strongest enhancement on pyrene sorption. Secondly, functional groups can directly form *n*–π EDA interactions with pyrene molecules and this ability must depend on the nature of the functional group. Theoritical calculations of the energy contribution of each functional groups would be extremely useful to support this mechanism.[42] Thirdly, surface functional groups of CNTs can form H-bonds with water molecules. Conversely to the two effects discussed above, competition with water is expected to suppress the sorption of pyrene to CNTs.[10] Overall, the increase in pyrene sorption affinity observed in the present study (Figure 5.6, Table 5.2) indicated that the enhancement of π–π and *n*–π EDA by functional groups may overwhelm the effect of water competition.

The present result does not agree with previous observations for nonpolar compounds sorption to functionalized CNTs. For example, Wu et al.[43] and Cho et al.[11] observed that the surface oxidation of CNTs did not alter the sorption affinity of naphthalene. In their study, the enhancement and suppression effects by oxidation groups may counterbalance each other and results in the same sorption affinities. The disagreement between the present results and the results observed in ref [11, 43] may be due to differences in sorbates, sorbents, background solution and methods. First, pyrene is more hydrophobic (log K_{OW} is 5.18 and 3.36, respectively), has a higher polarity (π* values are 1.71 and 0.7, respectively) and hydrogen-bonding accepting ability (β_m is 0.29 and 0.15, respectively) than naphthalene.[44] Therefore, the enhancement of π–π and *n*–π EDA interaction may be greater for compounds with higher hydrophobicity and polarity such as pyrene. Second, Wu et al.[43] and Cho et al.[11], as well as the majority of studies[12, 39, 45] examined CNTs oxidized by wet chemical treatment. During the oxidation procedure (e.g., reaction, washing and drying), the structure of CNTs aggregates was altered (e.g., surface area[43]), with possible consequences on sorption. The functional groups may be located mainly at the surface of the CNTs aggregates and likely to form H-bonds with water molecules. As suggested by the supplier of the CNTs investigated here, the functional groups may be more evenly distributed by plasma treatment than by wet chemical treatment. The water competition may thus be weaker for plasma functionalized CNTs than wet chemical functionalized CNTs. Third, Wu et al.[43] and Cho et al.[11] performed their experiments in a $CaCl_2$ background solution (10 mmol/L and 5 mmol/L, respectively) leading

to CNTs aggregation (CCC values of CNTs is 2.6 mM for $CaCl_2$[34]). Metal ions are also likely to form complex with the functional groups on CNTs.[46] Both effects can contribute to the suppression of sorption. In the present study, no $CaCl_2$ was added to coagulate CNTs as solid and liquid phase separation could be achieved by the POM-SPE method. In summary, the effect of sorbate hydrophobicity and polarity, CNTs oxidation methods and ionic strength should be accounted for when examining CNTs functional groups effects on sorption.

5.4.2.3 Sorption heterogeneity of Bulk/CNTs

It was initially hypothesized that the presence of functional groups would make the CNTs surface more heterogeneous. However, no difference in heterogeneity was observed (t, p=0.263). The quantity of functional groups was perhaps not sufficient to significantly affect the heterogeneity of CNT surfaces.

5.4.3 Effect of Sonication

5.4.3.1 Sonication (So/CNTs) vs. shaking (Bulk/CNTs)

Sonication increased sorption capacity, sorption affinity and heterogeneity for the four types of CNTs (Table 5.2–5.3). Our initial hypothesis was that sonication would not influence sorption to functionalized CNTs because of their initially loose structures allowing the access of pyrene to all pores (conversely to non-CNTs, see Chapter 4). However, sonication increased both sorption affinity and capacity for functionalized CNTs, indicating that some surfaces were not available for sorption before sonication. We saw in section 5.4.1 that shaking alone was not efficient to disperse and stabilize the functionalized CNTs suspensions. Sonication efficiently dispersed all four types of CNTs (Figure 5.1–5.3) but re-aggregation occurred rapidly with additional shaking (Figure 5.4) indicating the relatively poor stability of the dispersion. The possible effects of sonication on the properties of CNTs remain unclear. The present results suggest similar effects for functionalized and non-functionalized CNTs: sonication enlarged the pores for functionalized CNTs (Figure 5.2c) and increased the surface heterogeneity (decrease in t value, Table 5.2–5.3). Explanations are much likely similar to those discussed in Chapter 4 and involve oxidization and generation of defects.

The effect of sonication on the sorption to functionalized CNTs has never been studied before. Cho et al.[11] and Zhang et al.[47] observed that sonication did not affect the sorption of naphthalene and phenanthrene to non-CNTs. Our results showed that pores are inaccessible to large sorbates for CNTs with and without functionalization unless they were enlarged by sonication. Small compounds may have access to the relatively looser structure of

functionalized CNTs but may not have access to the dense structure of non-CNTs. Further research investigating the effect of sonication for compounds with different molecular size is needed to test this hypothesis.

Figure 5.7*. Sorption isotherms of pyrene to four types of CNTs pre-treated by sonication, in the absence of humic acids. The lines represent the fits by the Dubinin–Ashtakhov (DAM; ——) and Toth (TM; ·····) model.*

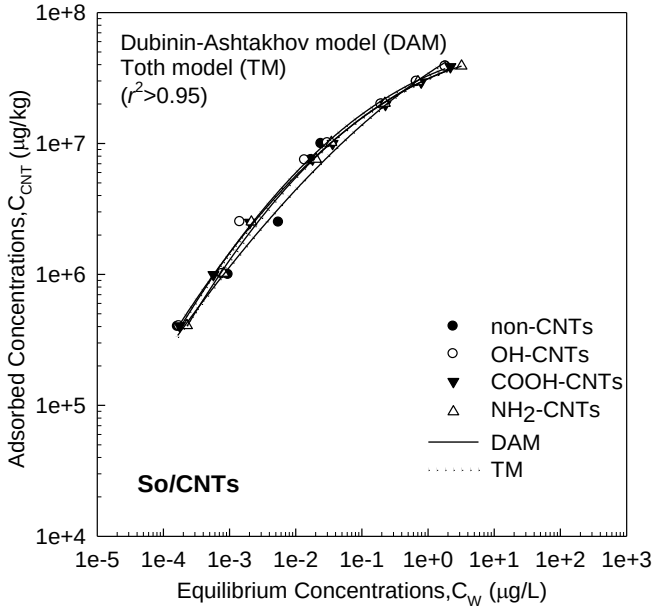

Table 5.3*. Fitting parameters ± standard error and r^2 for Ashtakhov and Toth models fitting the isotherms of pyrene on four types of CNTs pretreated by sonication.*

Sonication	DAM:				TM			
	log Q^0	E(kJ/mol)	b	r^2	log Q^0	*K*t (L/μg)	t	r^2
Non-CNTs	7.95±0.21	19.7±2.79	1.71e±0.35	0.96	8.55±0.81	1.92±0.67	0.18±0.09	0.95
OH-CNTs	7.73±0.28	23.6±3.68	2.28±0.81	0.98	7.88±0.21	3.49±1.04	0.30±0.71	0.98
COOH-CNTs	7.72±0.27	23.4±3.64	2.18±0.73	0.99	7.95±0.63	3.16±2.28	0.27±0.17	0.99
NH_2-CNTs	7.70±0.24	23.5±3.07	2.32±0.72	0.99	7.84±0.09	3.48±0.47	0.35±0.03	0.99

5.4.3.2 So/CNTs

Interestingly, after sonication, the sorption isotherms of the four types of CNTs became similar (Figure 5.7). Sonication may change the surface chemistry of CNTs by oxidization. FTIR suggested that sonication generated some hydroxyl groups (Figure 4.8 of Chapter 4). Yang et al. observed that 2% oxygen group was generated after sonication of CNTs in milli-Q water.[48] After sonication, the surface charges of all four types of sonicated CNTs significantly increased but remained in the same order as before sonication: non- < OH- < COOH- < NH_2-functionalized CNTs (Table 5.1). Similar sorption for all four types of CNTs implies that the effect of surface chemistry became negligible after sonication treatment.

For the four types of CNTs, the average size of So/CNTs aggregates was much smaller than that of Bulk/CNTs (Eyetech results, Figure 5.4). Even though reaggregation occurred during additional shaking, the pores of aggregates were enlarged for both non-CNT (as discussed in Chapter 4 (Figure 4.5–4.6) and for functionalized-CNTs (COOH-CNTs SEM images 5.2c). The enlarged pores of So/CNTs are more accessible for pyrene sorption than the narrow pores in Bulk/CNTs for all types of CNTs. It is possible that the initial functionalization was complemented by oxidation by sonication (i.e., 1–2%, EDX results). However, it seems that after sonication, the overall effect of functionalization was minor compared to that of pore enlargement.

With the aim to quantifying the importance of the pore enlargement, one can consider two extreme cases. In the first, sonication makes all the pores of the aggregates to become available for pyrene sorption. The available surface area for sorption can then be calculated based on the diameters, length and density of the CNTs (i.e., about 3000 m^2/g).[49, 50] In the second, only the external surface of the dense Bulk/CNTs aggregates is available for pyrene sorption. This area can be estimated based on the size distribution and the concentration of CNTs (i.e., about 100 m^2/g). Comparing those two values suggests that sonication can potentially increase the surface available for sorption by a factor of 30. Even though the effective effect of sonication is probably less than that suggested above, the reasoning illustrates how the effect of enlarged pores may become dominant over the effect of functional groups.

The determination of the effective surface area available for sorption is not straightforward, especially for So/CNTs. The BET-nitrogen adsorption method is subject to uncertainties due to unavoidable artifacts introduced during sample preparation (Chapter 4). On the other hand, the surface area derived from the size of the aggregates only reflects the external surface area

and certainly underestimates the surface available for sorption. This is particularly true for small sorbates that can access a larger portion of pores, relative to larger molecules. The results presented in Chapter 3 suggest (i) molecular sieving effect and (ii) flat sorption of PAHs at the surface of CNTs. We therefore suggest that PAHs may serve as useful probes to assess the surface area available for sorption in aqueous solutions.

5.4.4 Effects of HA

Figure 5.9 shows the effect of three HA concentration (i.e., 0, 5 and 40 mg/L) on sorption of pyrene to four types of CNTs pretreated with shaking and sonication. The presence of HA suppressed pyrene sorption in all cases. The linear equation was selected to derive numbers that allow a quantification of discrepancies between treatments. Note that the relationships between log K_{CNT} and 0–40 mg/L HA shown in Chapter 4 (Figure 4.11) were for non-CNTs and equilibrium concentration about one order of magnitude higher than that showed in Figure 5.8. The linear relationships obtained here are of a much lower quality than those presented in Chapter 4. This may be due to (i) larger data deviations in the low concentration range and (ii) differences in the sorption of HA to different types of CNTs. Sorption of HA to non-CNTs was reported to follow a Langmuir-like shape[51], indicating that sorption of HA by CNTs will increase with increasing HA concentration until saturation occur. Saturation may occur at different HA concentration range for non-CNTs and functionalized CNTs. Studies of HA sorption to functionalized CNTs are very limited and require further systematical investigation.

5.4.4.1 Bulk/CNTs

The slope of the regressions can be used to evaluate the extent to which sorption was suppressed by HA. For Bulk/CNTs, HA suppressed sorption following the order: non- < OH- < COOH- < NH_2- functionalized CNTs (Figure 5.8 a), meaning that HA had a greater effect for the smaller aggregates. In Chapter 4, we showed that the effect of HA was greater for dispersed CNTs than for CNTs aggregates. The present results are thus consistent with this trend and indicate a greater decrease in sorption by HA for the more dispersed functionalized CNTs relative to non-CNTs (Figure 5.2, Figure 5.3). The sorption of HA to smaller CNTs aggregates is expected to be greater than to large aggregates due to a larger number of sorption sites available (i.e, mainly on the outer surface of CNTs aggregates due to the large molecular size of HA).

Figure 5.8*. Logarithmic CNT-water distribution coefficients (log K_{CNT}) for pyrene as a function of humic acid concentration for four types of CNTs, following two pretreatments: (a) shaking by hand and (b) 2 h sonication. Solid lines are linear fits for CNTs in the 0–40 mg/L range.*

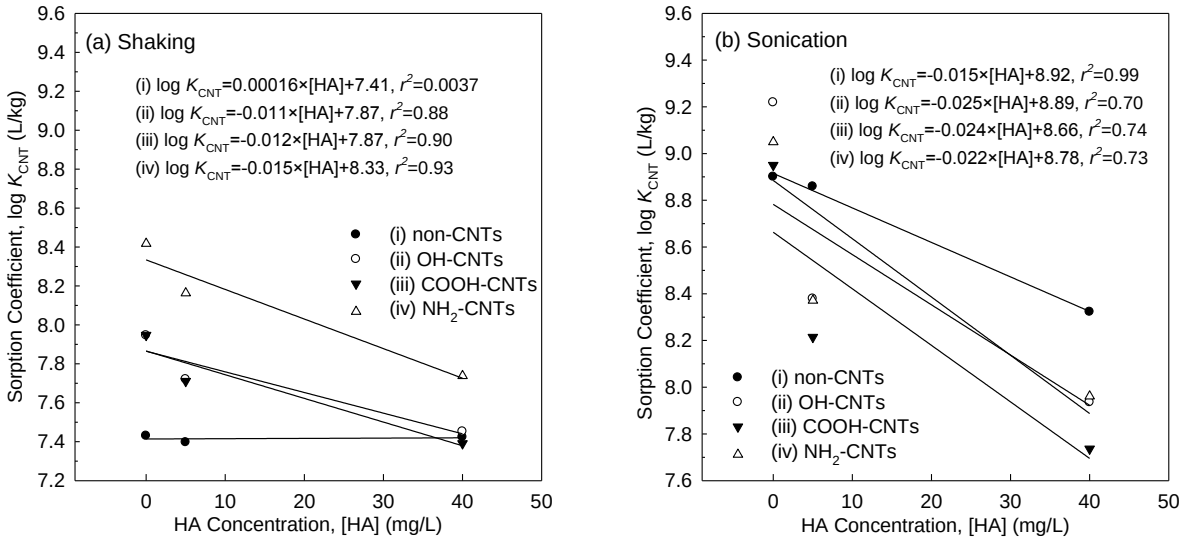

5.4.4.2 So/CNTs

HA had a greater effect on the sorption of So/CNTs than that of Bulk/CNTs with four types (Figure 5.8b). Again, the greater suppression by HA may be due to the greater sorption of HA to CNTs pretreated by sonication than by shaking. In the absence of HA, sorption was similar for the four types of So/CNTs (Figure 5.7). The presence of HA affected sorption differently according to the type of functional groups. In section 5.4.3, we suggested that the effect of surface chemistry was weaker than that of sonication. The results presented in Figure 5.8 further support the trend. The effect of HA followed the order: non- < NH_2- < OH- ≈ COOH-functionalized CNTs (based on the slope values, Figure 5.8). In the presence of HA, log K_{CNT} was in the order: non- > NH_2- ≈ OH- > COOH- functionalized CNTs. (Figure 5.8). The greater effect of HA on the sorption of functionalized CNTs may be explained by a greater sorption of HA, through the formation of covalent bonds with the functional groups at the surface of CNTs. The majority of functional groups in HA are OH- and COOH groups (Table 4.1, Chapter 4). Those groups in HA may form stronger bonds with the oxygen containing groups (i.e., COOH- and OH-) than with NH_2 groups on CNTs. These differences in interactions could explain the greater suppression of sorption of pyrene observed for OH and

COOH functionalised CNTs. The values of absorbance in the presence of HA followed the order: non < NH_2 < COOH ≈ OH and therefore further support this hypothesis.

There is a very limited knowledge about the sorption of NOM to CNTs, and to functionalized CNTs in particular. Zhou et al.[23] studied the colloidal behavior of CNTs in peat HA solution.

The authors reported that the sorbed amount of peat HA to CNTs pretreated by shaking was twice more than to sonicated CNT but there was no significant effect of sonication in the sorbed amount of HA to between non-CNTs and COOH-CNTs. However, the authors did not measure sorption isotherms for CNTs. Results suggested that sonication decreased the sorbed amount of peat HA to CNTs but that there was no significant difference between non-CNTs and COOH-CNTs. However, those results have to be taken with care as no sorption isotherms were measured. Investigating the sorption of HA to CNTs under sonication treatment is a challenging task that should carefully integrate the influence of the HA:CNT:water ratio, sonication power and time. The use of a robust method to separate the solid and liquid phase is also of utmost importance. Further research in this direction would be extremely useful to support the conclusions made in the present Chapter.

5.5 Literature Cited

(1) Sinnott, S. B.; Andrews, R. Carbon nanotubes: Synthesis, properties, and applications. *Crit. Rev. Solid State Mater. Sci.* **2001**, *26*, (3), 145-249.

(2) Lan, Y. C.; Wang, Y.; Ren, Z. F. Physics and applications of aligned carbon nanotubes. *Adv Phys* **2011**, *60*, (4), 553-678.

(3) Injang, U.; Noyrod, P.; Siangproh, W.; Dungchai, W.; Motomizu, S.; Chailapakul, O. Determination of trace heavy metals in herbs by sequential injection analysis-anodic stripping voltammetry using screen-printed carbon nanotubes electrodes. *Anal. Chim. Acta* **2010**, *668*, (1), 54-60.

(4) Singhal, S. K.; Pasricha, R.; Jangra, M.; Chahal, R.; Teotia, S.; Mathur, R. B. Carbon nanotubes: Amino functionalization and its application in the fabrication of Al-matrix composites. *Powder Technol.* **2012**, *215-16*, 254-263.

(5) Sun, Y. P.; Fu, K. F.; Lin, Y.; Huang, W. J. Functionalized carbon nanotubes: Properties and applications. *Acc. Chem. Res.* **2002**, *35*, (12), 1096-1104.

(6) Fakhari, A. R.; Ahmar, H. A new method based on headspace adsorptive accumulation using a carboxylated multi-walled carbon nanotubes modified electrode: application for trace determination of nitrobenzene and nitrotoluene in water and wastewater. *Anal Methods-Uk* **2011**, *3*, (11), 2593-2598.

(7) Zhou, Q. X.; Xiao, J. P.; Wang, W. D. Trace analysis of triasulfuron and bensulfuron-methyl in water samples using a carbon nanotubes packed cartridge in combination with high-performance liquid chromatography. *Microchim Acta* **2007**, *157*, (1-2), 93-98.

(8) Leghrib, R.; Llobet, E. Quantitative trace analysis of benzene using an array of plasma-treated metal-decorated carbon nanotubes and fuzzy adaptive resonant theory techniques. *Anal. Chim. Acta* **2011**, *708*, (1-2), 19-27.

(9) Petersen, E. J.; Zhang, L. W.; Mattison, N. T.; O'Carroll, D. M.; Whelton, A. J.; Uddin, N.; Nguyen, T.; Huang, Q. G.; Henry, T. B.; Holbrook, R. D.; Chen, K. L. Potential Release Pathways, Environmental Fate, And Ecological Risks of Carbon Nanotubes. *Environ. Sci. Technol.* **2011**, *45*, (23), 9837-9856.

(10) Yang, K.; Xing, B. S. Adsorption of organic compounds by carbon nanomaterials in aqueous phase: Polanyi theory and its application. *Chem. Rev.* **2010**, *110*, (10), 5989-6008.

(11) Cho, H. H.; Smith, B. A.; Wnuk, J. D.; Fairbrother, D. H.; Ball, W. P. Influence of surface oxides on the adsorption of naphthalene onto multiwalled carbon nanotubes. *Environ. Sci. Technol.* **2008**, *42*, (8), 2899-2905.

(12) Zhang, S. J.; Shao, T.; Bekaroglu, S. S. K.; Karanfil, T. Adsorption of synthetic organic chemicals by carbon nanotubes: Effects of background solution chemistry. *Water Res.* **2010**, *44*, (6), 2067-2074.

(13) Gotovac, S.; Yang, C. M.; Hattori, Y.; Takahashi, K.; Kanoh, H.; Kaneko, K. Adsorption of polyaromatic hydrocarbons on single wall carbon nanotubes of different functionalities and diameters. *J. Colloid Interface Sci.* **2007**, *314*, (1), 18-24.

(14) Lu, C.; Su, F.; Hu, S. Surface modification of carbon nanotubes for enhancing BTEX adsorption from aqueous solutions. *Appl. Surf. Sci.* **2008**, *254*, (21), 7035-7041.

(15) Chen, J. L.; Chen, Q. H.; Ma, Q. Influence of surface functionalization via chemical oxidation on the properties of carbon nanotubes. *J. Colloid Interface Sci.* **2012**, *370*, 32-38.

(16) Wepasnick, K. A.; Smith, B. A.; Schrote, K. E.; Wilson, H. K.; Diegelmann, S. R.; Fairbrother, D. H. Surface and structural characterization of multi-walled carbon nanotubes following different oxidative treatments. *Carbon* **2011**, *49*, (1), 24-36.

(17) Smith, B.; Wepasnick, K.; Schrote, K. E.; Cho, H. H.; Ball, W. P.; Fairbrother, D. H. Influence of surface oxides on the colloidal stability of multi-walled carbon nanotubes: A structure-property relationship. *Langmuir* **2009**, *25*, (17), 9767-9776.

(18) Scaffaro, R.; Maio, A.; Agnello, S.; Glisenti, A. Plasma functionalization of multiwalled carbon nanotubes and their use in the preparation of nylon 6-based nanohybrids. *Plasma Process Polym* **2012**, *9*, (5), 503-512.

(19) Meyyappan, M. A review of plasma enhanced chemical vapour deposition of carbon nanotubes. *J Phys D Appl Phys* **2009**, *42*, (21).

(20) Chen, C. L.; Liang, B.; Lu, D.; Ogino, A.; Wang, X. K.; Nagatsu, M. Amino group introduction onto multiwall carbon nanotubes by NH_3/Ar plasma treatment. *Carbon* **2010**, *48*, (4), 939-948.

(21) Dongil, A. B.; Bachiller-Baeza, B.; Guerrero-Ruiz, A.; Rodriguez-Ramos, I.; Martinez-Alonso, A.; Tascon, J. M. D. Surface chemical modifications induced on high surface area graphite and carbon nanofibers using different oxidation and functionalization treatments. *J. Colloid Interface Sci.* **2011**, *355*, (1), 179-189.

(22) Schwyzer, I.; Kaegi, R.; Sigg, L.; Magrez, A.; Nowack, B. Influence of the initial state of carbon nanotubes on their colloidal stability under natural conditions. *Environ. Pollut.* **2011**, *159*, (6), 1641-1648.

(23) Zhou, X. Z.; Shu, L.; Zhao, H. B.; Guo, X. Y.; Wang, X. L.; Tao, S.; Xing, B. S. Suspending multi-walled carbon nanotubes by humic acids from a peat soil. *Environ. Sci. Technol.* **2012**, *46*, (7), 3891-3897.

(24) Xin, X.; Xu, G. Y.; Zhao, T. T.; Zhu, Y. Y.; Shi, X. F.; Gong, H. J.; Zhang, Z. Q. Dispersing carbon nanotubes in aqueous solutions by a starlike block copolymer. *J. Phy. Chem. C.* **2008**, *112*, (42), 16377-16384.

(25) Lee, J. U.; Huh, J.; Kim, K. H.; Park, C.; Jo, W. H. Aqueous suspension of carbon nanotubes via non-covalent functionalization with oligothiophene-terminated poly(ethylene glycol). *Carbon* **2007**, *45*, (5), 1051-1057.

(26) Matarredona, O.; Rhoads, H.; Li, Z. R.; Harwell, J. H.; Balzano, L.; Resasco, D. E. Dispersion of single-walled carbon nanotubes in aqueous solutions of the anionic surfactant NaDDBS. *J. Phys. Chem. B* **2003**, *107*, (48), 13357-13367.

(27) Tummala, N. R.; Morrow, B. H.; Resasco, D. E.; Striolo, A. Stabilization of aqueous carbon nanotube dispersions using surfactants: Insights from molecular dynamics simulations. *Acs Nano* **2010**, *4*, (12), 7193-7204.

(28) Hyung, H.; Fortner, J. D.; Hughes, J. B.; Kim, J. H. Natural organic matter stabilizes carbon nanotubes in the aqueous phase. *Environ. Sci. Technol.* **2007**, *41*, (1), 179-184.

(29) Zhang, X. R.; Kah, M.; Jonker, M. T. O.; Hofmann, T. Dispersion state and humic acids concentration-dependent sorption of pyrene to carbon nanotubes. *Environ. Sci. Technol.* **2012**, *46*, (13), 7166–7173.

(30) Kah, M.; Zhang, X. R.; Jonker, M. T. O.; Hofmann, T. Measuring and modelling adsorption of PAHs to carbon nanotubes over a six order of magnitude wide concentration range. *Environ. Sci. Technol.* **2011**, *45*, (14), 6011-6017.

(31) Zhao, J.; Wang, Z. Y.; Mashayekhi, H.; Mayer, P.; Chefetz, B.; Xing, B. S. Pulmonary surfactant suppressed phenanthrene adsorption on carbon nanotubes through solubilization and competition as examined by passive dosing technique. *Environ Sci Technol* **2012**, *46*, (10), 5369-5377.

(32) Cheng, Q. H.; Debnath, S.; Gregan, E.; Byrne, H. J. Ultrasound-assisted SWNTs dispersion: Effects of sonication parameters and solvent properties. *Journal of Physical Chemistry C* **2010**, *114*, (19), 8821-8827.

(33) Grossiord, N.; Regev, O.; Loos, J.; Meuldijk, J.; Koning, C. E. Time-dependent study of the exfoliation process of carbon nanotubes in aqueous dispersions by using UV-visible spectroscopy. *Anal. Chem.* **2005**, *77*, (16), 5135-5139.

(34) Saleh, N. B.; Pfefferle, L. D.; Elimelech, M. Aggregation kinetics of multiwalled carbon nanotubes in aquatic systems: Measurements and environmental implications. *Environ. Sci. Technol.* **2008**, *42*, (21), 7963-7969.

(35) Sun, Z.; Nicolosi, V.; Rickard, D.; Bergin, S. D.; Aherne, D.; Coleman, J. N. Quantitative evaluation of surfactant-stabilized single-walled carbon nanotubes: Dispersion quality and its correlation with zeta potential. *J. Phy. Chem. C.* **2008**, *112*, (29), 10692-10699.

(36) Wu, W. H.; Chen, W.; Lin, D. H.; Yang, K. Influence of surface oxidation of multiwalled carbon nanotubes on the adsorption affinity and capacity of polar and nonpolar organic compounds in aqueous phase. *Environ. Sci. Technol.* **2012**, *46*, (10), 5446-5454.

(37) Wisniewski, M.; Furmaniak, S.; Kowalczyk, P.; Werengowska, K. M.; Rychlicki, G. Thermodynamics of benzene adsorption on oxidized carbon nanotubes - experimental and simulation studies. *Chem. Phys. Lett.* **2012**, *538*, 93-98.

(38) Zhang, S. J.; Shao, T.; Bekaroglu, S. S. K.; Karanfil, T. The Impacts of aggregation and surface chemistry of carbon nanotubes on the adsorption of synthetic organic compounds. *Environ. Sci. Technol.* **2009**, *43*, (15), 5719-5725.

(39) Wang, X. L.; Liu, Y.; Tao, S.; Xing, B. S. Relative importance of multiple mechanisms in sorption of organic compounds by multiwalled carbon nanotubes. *Carbon* **2010**, *48*, (13), 3721-3728.

(40) Liao, Q.; Sun, J.; Gao, L. The adsorption of resorcinol from water using multi-walled carbon nanotubes. *Colloids and Surfaces a-Physicochemical and Engineering Aspects* **2008**, *312*, (2-3), 160-165.

(41) Chen, W.; Duan, L.; Wang, L. L.; Zhu, D. Q. Adsorption of hydroxyl- and amino-substituted aromatics to carbon manotubes. *Environ. Sci. Technol.* **2008**, *42*, (18), 6862-6868.

(42) Kubicki, J. D. Molecular simulations of benzene and PAH interactions with soot. *Environ. Sci. Technol.* **2006**, *40*, (7), 2298-2303.

(43) Wu, W. H.; Chen, W.; Lin, D. H.; Yang, K. Influence of Surface Oxidation of Multiwalled Carbon Nanotubes on the Adsorption Affinity and Capacity of Polar and Nonpolar Organic Compounds in Aqueous Phase. *Environ. Sci. Technol.* **2012**, *46*, (10), 5446-5454.

(44) Nguyen, T. H.; Goss, K. U.; Ball, W. P. Polyparameter linear free energy relationships for estimating the equilibrium partition of organic compounds between water and the natural organic matter in soils and sediments. *Environ. Sci. Technol.* **2005**, *39*, (4), 913-924.

(45) Lu, C. S.; Chung, Y. L.; Chang, K. F. Adsorption of trihalomethanes from water with carbon nanotubes. *Water Res.* **2005**, *39*, (6), 1183-1189.

(46) Chen, G. C.; Shan, X. Q.; Wang, Y. S.; Pei, Z. G.; Shen, X. E.; Wen, B.; Owens, G. Effects of Copper, Lead, and Cadmium on the Sorption and Desorption of Atrazine onto and from Carbon Nanotubes. *Environ. Sci. Technol.* **2008**, *42*, (22), 8297-8302.

(47) Zhang, S. J.; Shao, T.; Kose, H. S.; Karanfil, T. Adsorption kinetics of aromatic compounds on carbon nanotubes and activated carbons. *Environ. Toxicol. Chem.* **2012**, *31*, (1), 79-85.

(48) Yang, D. Q.; Rochette, J. F.; Sacher, E. Functionalization of multiwalled carbon nanotubes by mild aqueous sonication. *J. Phys. Chem. B* **2005**, *109*, (16), 7788-7794.

(49) Takagi, H.; Hatori, H.; Soneda, Y.; Yoshizawa, N.; Yamada, Y. Adsorptive hydrogen storage in carbon and porous materials. *Mat. Sci. Eng. B-Solid* **2004**, *108*, (1-2), 143-147.

(50) Peigney, A.; Laurent, C.; Flahaut, E.; Bacsa, R. R.; Rousset, A. Specific surface area of carbon nanotubes and bundles of carbon nanotubes. *Carbon* **2001**, *39*, (4), 507-514.

(51) Wang, X. L.; Shu, L.; Wang, Y. Q.; Xu, B. B.; Bai, Y. C.; Tao, S.; Xing, B. S. Sorption of Peat Humic Acids to Multi-Walled Carbon Nanotubes. *Environ. Sci. Technol.* **2011**, *45*, (21), 9276-9283.

6. Conclusions and Outlook

Understanding the interactions between organic contaminants and engineered nanoparticles (ENPs) is essential for evaluating the materials' potential environmental risk as well as the potential efficiency for remediation applications. We applied a passive sampling method to examine the effect of sorbate concentration, dispersion and surface chemistry of carbonaceous ENPs (CNPs) on sorption. PAHs were selected as model sorbates and their sorption to CNTs was studied over a range of conditions that were never investigated before. For the first time, sorption data and extensive characterization of the CNTs systems were combined in order to support mechanistic interpretations of the results. The main results of this project are summarized below:

i) Conversely to previous studies carried out at unrealistic high concentration ranges, sorption isotherms in the low concentration range (pg–ng/L) indicate that sorption can be described using single sorption coefficients.
ii) Isotherm fits over a six order of magnitude wide concentration range showed that (a) monolayer sorption models described the data very well, and (b) sorption capacity was directly related to the surface area of CNTs.
iii) Sorption coefficients for 13 PAHs (11 of which have never been reported before) showed that no competition occurred in the low concentration range and sorption affinity was directly related to the solubility of the subcooled liquid of the compounds.
iv) Dispersion greatly affected the maximum sorption capacity, affinity, and heterogeneity of the CNT surface.
v) Both the nature (e.g., sonication or presence of dispersants) and the chronological sequence of the dispersion events are essential in determining the extent and irreversibility of the effects on sorption behavior of CNTs.
vi) The influence of CNT surface chemistry on sorption greatly depends on the dispersion status. For instance, the effect of surface chemistry was negligible for CNTs dispersed by sonication.
vii) The suppression of sorption by natural dispersants greatly depends on the CNT surface chemistry.
Overall, our results show that the effects of concentration, dispersion and surface chemistry cannot be neglected when studying interactions between organic contaminants and CNPs (i.e. discrepancies of orders of magnitude were observed in some cases). The most exciting achievement is that sorption of CNPs can be studied in a dispersed system through adaptation

of classical experimental setup. This study opens up a way to study sorption for a wider range of compounds and ENPs, and over a wider range of conditions, including complex dispersion status. Several aspects identified as requiring further research are described below:

1). Wider range of sorbates and sorbents

The present study focused on PAHs and CNTs and research covering a wider range of compounds (including polar and nonpolar compounds) to ENPs in dispersed systems is required. The coexistence of organic pollutants is an important issue when dealing with wastewater. Therefore, sorption behavior of coexisting organic compounds needs to be studied in future work. Competition between coexisting sorbates is likely to occur in the high concentration range[1] and should be considered in future work. Experimental design covering wide concentration ranges are important to capture the sorption behavior likely to occur in both natural and wastewater conditions. Aggregation and dispersion are expected to affect the sorption behavior of other CNPs (e.g., C60) and metal-based ENPs (e.g., Zero-valent iron, TiO_2). Research including a wider range of ENPs is also needed to evaluate the applicability of the conclusions made in the present thesis to other systems.

2). Mechanical treatments and parameter evaluation

Our study shows that sonicated CNTs exhibit much greater sorption potential relative to non-sonicated CNTs. Besides sonication, ENPs can be dispersed using other mechanical treatments as summarized in Chapter 2. Different mechanical treatments as well as their settings can influence the dispersion efficiency of ENPs. For example, different sonication power and time can result in different levels of CNT dispersion which are expected to affect their sorption behavior.[2, 3] To apply the selected ENPs in wastewater treatment, it may be necessary to pre-disperse ENPs using mechanical treatment. Therefore, further research is required in order to select the most adequate mechanical treatment combined with optimized setting parameters for remediation purposes.

3). Variability of dispersants

In the present study, we examined the effect of one type of natural dispersant (i.e., humic acids, HA). It would be worth examining the effects of more dispersants including natural and engineered surfactants and polymers since they widely exist in the environment or are produced in the industry, respectively. One challenge when using passive sampling, is to find an material that does not interact with the selected dispersant in order to measure the truly dissolved sorbate concentration. More passive samplers materials should therefore be

evaluated prior to being applied to sample the sorbate of interest. Interactions between sorbates and dispersant also require further examination. For example, the formation of surfactant micelles can influence the solubility of the sorbate (e.g., PAHs)[4] which may in turn influence ENP sorption of the sorbate, besides the dispersion effect caused by surfactant. A system comprising sorbate, dispersant, sampler and nanosorbent is rather complicated. It is therefore essential that interactions between each phases are well understood, prior to examining sorption in the complex dispersed system.

4). Sorption of NOM to ENPs

We have shown that HA exert a great suppression effect on sorption of CNTs when combined with sonication pretreatment. Extensive characterization data points towards a great sorption between HA and CNTs. However, the sorption between HA and CNTs was not directly examined in this study. Although dispersion of ENPs by NOM has been widely reported (e.g., ref 5 and 6), the sorption of NOM to ENPs was only rarely reported, probably because it is extremely challenging to study using traditional sorption experiment design. We demonstrated that sorption of organic compounds to ENPs can be measured using passive sampling method. However, the method cannot be applied to the large NOM molecules due to limited diffusion. Therefore, an alternative method should be developed and validated. This could include techniques such as ultracentrifugation, ultrafiltration or dialysis to separate suspended NOM and the aqueous phase. Finally, it is often assumed that the portion of adsorbed NOM on ENPs behaves the same as the dissolved NOM.[7, 8] However, some results indicate that sorption of NOM on ENPs may experience fractionation, with important consequences in terms of sorption behavior and environmental impact. Adequate separation and characterization techniques (e.g., nuclear magnetic resonance) should be applied to investigate this aspect.

5). Development of characterization methods

The majority of studies published so far on sorption, presented a fairly limited characterization of the nano-sorbent system. The present thesis illustrates the importance of a extensive characterization to support the occurrence of sorption mechanisms. We believe that future work should include such data. However, each characterization techniques has limitations (listed in Chapter 2). For example, the BET-nitrogen adsorption method is widely used to determine CNT surface area.[9-12] However, our results show that this method may not be suitable to characterize CNTs dispersed by sonication. This may be linked to the sample preparation step during which amorphous carbon may block the pores during the drying

procedure.[13] Sample preparation can irreversibly affect the physical and chemicals states of samples. Particular attention should be paid to develop sample preparation methods with a minimum impact on the samples so that measurement reflects the initial conditions. The drying step cannot be avoided when using the BET-nitrogen adsorption method. Our results suggest that PAHs could serve as an alternative model sorbate to assess the surface and pores available for sorption in an aqueous media due to the flat sorption on the CNT surfaces.

There are still many research questions to be elucidated to further understand the sorption behavior of ENPs. A potential exciting application of CNTs is the development of new water remediation strategies. Conversely to other commonly used carbonaceous sorbents (e.g., activated carbon and biochars), which can be applied directly in water remediation, additional efforts are necessary to explore the potentiality of CNTs due to their colloidal behavior. The present study makes a step forward to design nano sorbents to a wide range of compounds for specific purposes.

Literature Cited

(1) Yang, K.; Wang, X. L.; Zhu, L. Z.; Xing, B. S. Competitive sorption of pyrene, phenanthrene, and naphthalene on multiwalled carbon nanotubes. *Environ. Sci. Technol.* **2006**, *40*, (18), 5804-5810.

(2) Vichchulada, P.; Cauble, M. A.; Abdi, E. A.; Obi, E. I.; Zhang, Q. H.; Lay, M. D. Sonication power for length control of single-walled carbon nanotubes in aqueous suspensions used for 2-dimensional network Formation. *J. Phy. Chem. C.* **2010**, *114*, (29), 12490-12495.

(3) Cheng, Q. H.; Debnath, S.; Gregan, E.; Byrne, H. J. Ultrasound-assisted SWNTs dispersion: Effects of sonication parameters and solvent properties. *J. Phy. Chem. C.* **2010**, *114*, (19), 8821-8827.

(4) Edwards, D. A.; Luthy, R. G.; Liu, Z. B. Solubilization of polycyclic aromatic-hydrocarbons in micellar nonionic surfactant solutions. *Environ. Sci. Technol.* **1991**, *25*, (1), 127-133.

(5) Dickson, D.; Liu, G. L.; Li, C. Z.; Tachiev, G.; Cai, Y. Dispersion and stability of bare hematite nanoparticles: Effect of dispersion tools, nanoparticle concentration, humic acid and ionic strength. *Sci. Total Environ.* **2012**, *419*, 170-177.

(6) Lin, D. H.; Xing, B. S. Tannic acid adsorption and its role for stabilizing carbon nanotube suspensions. *Environ. Sci. Technol.* **2008**, *42*, (16), 5917-5923.

(7) Wang, S. G.; Liu, X. W.; Gong, W. X.; Nie, W.; Gao, B. Y.; Yue, Q. Y. Adsorption of fulvic acids from aqueous solutions by carbon nanotubes. *J. Chem. Technol. Biotechnol.* **2007**, *82*, (8), 698-704.

(8) Wang, X. L.; Shu, L.; Wang, Y. Q.; Xu, B. B.; Bai, Y. C.; Tao, S.; Xing, B. S. Sorption of peat humic acids to multi-walled carbon nanotubes. *Environ. Sci. Technol.* **2011**, *45*, (21), 9276-9283.

(9) Wang, H. J.; Zhou, A. L.; Peng, F.; Yu, H.; Chen, L. F. Adsorption characteristic of acidified carbon nanotubes for heavy metal Pb(II) in aqueous solution. *Materials Science and Engineering a-Structural Materials Properties Microstructure and Processing* **2007**, *466*, (1-2), 201-206.

(10) Cho, H. H.; Wepasnick, K.; Smith, B. A.; Bangash, F. K.; Fairbrother, D. H.; Ball, W. P. Sorption of aqueous Zn[II] and Cd[II] by multiwall carbon nanotubes: the relative roles of oxygen-containing functional groups and graphenic carbon. *Langmuir* **2010**, *26*, (2), 967-981.

(11) Zhang, S. J.; Shao, T.; Bekaroglu, S. S. K.; Karanfil, T. Adsorption of synthetic organic chemicals by carbon nanotubes: Effects of background solution chemistry. *Water Res.* **2010**, *44*, (6), 2067-2074.

(12) Chen, W.; Duan, L.; Wang, L. L.; Zhu, D. Q. Adsorption of hydroxyl- and amino-substituted aromatics to carbon manotubes. *Environ. Sci. Technol.* **2008**, *42*, (18), 6862-6868.

(13) Zhang, X. R.; Kah, M.; Jonker, M. T. O.; Hofmann, T. Dispersion state and humic acids concentration-dependent sorption of pyrene to carbon nanotubes. *Environ. Sci. Technol.* **2012**, *46*, (13), 7166–7173.

Appendix

List of Tables

(Short titles)

List of Figures

(Short titles)

Contributions

Study Ⅰ

Measuring and Modeling Adsorption of PAHs to Carbon Nanotubes Over a Six Order of Magnitude Wide Concentration Range

Melanie Kah, Xiaoran Zhang, Michiel T. O. Jonker, Thilo Hofmann*

Environmental Science & Technology. 2011, volume 45, issue 14, pages 6011–6017

Melanie Kah	35%	Concept, results discussion, data interpretation, manuscript preparation
Xiaoran Zhang	35%	Concept, lab work, results discussion, data interpretation, manuscript preparation
Michiel T. O. Jonker	20%	Concept, lab work, results discussion, data interpretation, proof reading
Thilo Hofmann	10%	Concept, results discussion, proof reading

Study Ⅱ

Dispersion State and Humic Acids Concentration-Dependent Sorption of Pyrene to Carbon Nanotubes

Xiaoran Zhang, Melanie Kah*, Michiel T. O. Jonker, Thilo Hofmann*

Environmental Science & Technology. 2012, volume 46, issue 13, pages 7166–7173

Xiaoran Zhang	50%	Concept, lab work, results discussion, data interpretation, manuscript preparation
Melanie Kah	35%	Concept, results discussion, data interpretation, manuscript preparation
Michiel T. O. Jonker	5%	Results discussion, proof reading
Thilo Hofmann	10%	Concept, results discussion, proof reading

Study Ⅲ

Influence of Surface Chemistry on Sorption of Pyrene to Carbon Nanotubes

Xiaoran Zhang, Melanie Kah, Thilo Hofmann

To be submitted to *Environmental Science & Technology*

Xiaoran Zhang	60%	Concept, lab work, results discussion, data interpretation, manuscript preparation
Melanie Kah	30%	Concept, results discussion, data interpretation, manuscript preparation
Thilo Hofmann	10%	Concept, results discussion, proof reading

Curriculum Vitae

Xiaoran Zhang

Email: xiaoran_zhang@yahoo.cn; xiaoran.zhang@univie.ac.at

Education

03.2009-present	Ph.D candidate. Department of Environmental Geosciences, University of Vienna, Austria. Major: Environmental Geosciences
09.2006-01.2009	Master. School of Water Resources and Environment, China University of Geosciences (Beijing). Major: Environmental Sciences
09.2002-07.2006	Bachelor. School of Environmental Engineering and Science, Hebei University of Science and Technology. Major: Environmental Engineering

Presentation at conferences

Oral

05.2012	2012 Annual meeting of the German Water Chemical Society - Division of the Society of German Chemists. Ulm, Germany.
09.2011	23rd International Symposium on Polycyclic Aromatic Compounds (ISPAC 23). Munster, Germany.
09.2010	5th Late Summer Workshop "Nanoparticles and Nanomaterials in Aquatic Systems". Maurach, Gemany.

Poster

05.2012	Setac Europe 22nd Anual Metting. Berlin, Germany.
08.2011	Goldschmidt 2011. Prague, Czech Republic
05.2010	Setac Europe 20th Annual Meeting. Sevilla, Spain

IT skills

Sigmaplot, Core Draw, Adobe Photoshop, Originlab

Awards

11.2007	Outstanding student leader award of China University of Geosciences (Beijing)
06.2006	Outstanding undergraduate award of Hebei University of Science and Technology